INVESTIGATION OF WASTE PAPER-DERIVED CARBON AEROGEL/ELASTOMER SYSTEM AS A CARDIAC PATCH

ATIK KAĞITTAN TÜRETİLMİŞ KARBON AEROJEL-ELASTOMER SİSTEMİNİN KARDİYAK DOKU YAMASI OLARAK İNCELENMESİ

ABDULRAHEEM MOHAMMED NAJI ATYA

PROF. DR. HALiL MURAT AYDIN

Supervisor

Submitted to
Graduate School of Science and Engineering of Hacettepe University
as a Partial Fulfillment to the Requirements
for the Award of the Degree Master of Science
in Bioengineering.

2019

This work titled **"Investigation of Waste Paper-Derived Carbon Aerogel/Elastomer System as a Cardiac Patch"** by **Abdulraheem Mohammed Naji Atya** has been approved as a thesis for the Degree of **MASTER OF SCIENCE IN BIONEGINEERING** by the below mentioned Examining Committee Members.

Prof. Dr. İbrahim Vargel
Head ..... 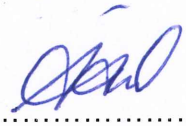

Prof. Dr. Halil Murat Aydın
Supervisor ..... 

Assoc. Prof. Dr. Sedat Odabaş
Member ..... 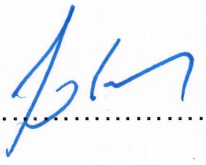

Assoc. Prof. Dr. İ.Çağatay Karaaslan
Member ..... 

Assist. Prof. Dr. Dinçer Gökcen
Member ..... 

This thesis has been approved as a thesis for the degree of **Master Of Science In Bionegineering** by Board of Directors of the institute of Graduate School of Science and Engineering on ...../ ..... / .....

Prof. Dr. Menemşe Gümüşderelioğlu
Director of the Institute of
Graduate School of Science and Engineering

To my precious family…

ETHICS

In this thesis study, prepared in accordance with the spelling rules of Institute of Graduate School of Science and Engineering of Hacettepe University,

I declare that

- all the information and documents have been obtained in the base of the academic rules
- all audio-visual and written information and results have been presented according to the rules of scientific ethics
- in case of using other Works, related studies have been cited in accordance with the scientific standards
- all cited studies have been fully referenced
- I did not do any distortion in the data set
- and any part of this thesis has not been presented as another thesis study at this or any other university.

20/09/2019

Abdulraheem Mohammed Naji ATYA

YAYIMLAMA VE FİKRİ MÜLKİYET HAKLARI BEYANI

Enstitü tarafından onaylanan lisansüstü tezimin/raporumun tamamını veya herhangi bir kısmını, basılı (kağıt) ve elektronik formatta arşivleme ve aşağıda verilen koşullarla kullanıma açma iznini Hacettepe Üniversitesine verdiğimi bildiririm. Bu izinle Üniversiteye verilen kullanım hakları dışındaki tüm fikri mülkiyet haklarım bende kalacak, tezimin tamamının ya da bir bölümünün gelecekteki çalışmalarda (makale, kitap, lisans ve patent vb.) kullanım hakları bana ait olacaktır.

Tezin kendi orijinal çalışmam olduğunu, başkalarının haklarını ihlal etmediğimi ve tezimin tek yetkili sahibi olduğumu beyan ve taahhüt ederim. Tezimde yer alan telif hakkı bulunan ve sahiplerinden yazılı izin alınarak kullanması zorunlu metinlerin yazılı izin alarak kullandığımı ve istenildiğinde suretlerini Üniversiteye teslim etmeyi taahhüt ederim.

Yükseköğretim Kurulu tarafından yayınlanan ***"Lisansüstü Tezlerin Elektronik Ortamda Toplanması, Düzenlenmesi ve Erişime Açılmasına İlişkin Yönerge"*** kapsamında tezim aşağıda belirtilen koşullar haricince YÖK Ulusal Tez Merkezi/H.Ü. Kütüphaneleri Açık Erişim Sisteminde erişime açılır.

☐ Enstitü / Fakülte yönetim kurulu kararı ile tezimin erişime açılması mezuniyet tarihimden itibaren 2 yıl ertelenmiştir.

☐ Enstitü / Fakülte yönetim kurulu gerekçeli kararı ile tezimin erişime açılması mezuniyet tarihimden itibaren .... ay ertelenmiştir.

☐ Tezim ile ilgili gizlilik kararı verilmiştir.

20/09/2019

ABDULRAHEEM MOHAMMED NAJI ATYA

ÖZET

ATIK KAĞITTAN TÜRETİLMİŞ KARBON AEROJEL- ELASTOMER SİSTEMİNİN KARDİYAK DOKU YAMASI OLARAK İNCELENMESİ

Abdulraheem Mohammed Naji ATYA

Yüksek Lisans, Biyomühendislik Bölümü

Tez Danışmanı: Prof. Dr. Halil Murat AYDIN

Eylül 2019, 76 sayfa

Kardiyovasküler hastalıklar, dünya genelinde ciddi sayıda ölümün sorumlusu olarak gösterilmektedir. Bu hastalıklar arasında yer alan miyokard enfarktüsü, koroner arterlerden birinde kan akışı bloke olduğunda meydana gelmekte ve tıkanmaya maruz kalan miyokard alanındaki kardiyomiyositleri, besin ve oksijenden mahrum bırakmaktadır. Perfüzyonun kısa süre içinde onarılmaması halinde, kardiyomiyositlerde kronik hasar meydana gelmekte ve bunun sonucunda, miyokard içerisinde önemli düzeyde kardiyomiyosit kaybı yaşanmaktadır. Kardiyomiyositlerde herhangi bir kendini kopyalama mekanizması bulunmadığı için, bu tip bir hasar sonrasında düzelmeleri mümkün olmamaktadır. Dolayısıyla, akut miyokard enfarktüsünü sağ atlatanlarda, sol ventrikülün büyüdüğü ve sol ventrikül duvarının inceldiği bir kalp yetmezliği durumu baş göstermektedir. Nihayetinde, kalp tarafından vücudun farklı bölümlerine yeterli miktarda kan pompalanması olanaksız hale gelmekte ve son olarak hasta kaybedilmektedir.

Akut miyokard sonrası gelişen kalp yetmezliğine dönük mevcut tedavi stratejileri, sözünü ettiğimiz son evrenin ortaya çıkış sürecini yavaşlatmakla sınırlıdır.

Günümüzde yeni yeni gelişen Miyokardiyal Doku Mühendisliği yaklaşımında, sağlıklı kardiyak hücreler ile yapay kardiyak yamanın birleştirilmesi sayesinde, enfarktüs geçirmiş miyokardın kendini yenilemesini sağlayacak mükemmel bir tedavi stratejisinin ortaya çıkması umulmaktadır. Bununla birlikte, başarılı bir kardiyak yama meydana getirecek en uygun kültür substratı henüz bulunabilmiş değildir. Dolayısıyla, bu çalışmada, yeni iletken elastomer esaslı kompozitin sentezlenmesi ve miyokardiyal doku mühendisliğinde kardiyak yama olarak kullanımına dönük potansiyelin değerlendirilmesi amaçlanmıştır.

Özellikle, Karbon Aerojel-Poli (Gliserol Sebakat) (CA-PGS) sisteminde elektriksel açıdan iletken bir kompozitin sentezlenmesi ilk olarak bu çalışmada açıklanmaktadır. Çalışmada, atık kâğıttan elde edilen uygun maliyetli bir karbon kaynağı niteliğini taşıyan ve kardiyak doku mühendisliği uygulamalarında kullanımı bugüne dek incelenmemiş olan, elektrik iletkenliğine sahip Karbo Aerojel, biyolojik olarak ayrışabilen PGS matrisi ile birleştirilmiş, bu şekilde optimal özelliklere sahip bir kardiyak yapının elde edilmesi hedeflenmiştir. Sonuçta ortaya çıkan kompozit, Taramalı Elektron Mikroskopu (SEM), Fuorier Dönüşüm Kızılötesi (FTIR) Spektroskopisi, X-ışını Difraksiyonu (XRD) ve Temas Açısı Ölçümleri ile incelenmiştir. Ek olarak, geliştirilen sistemin mekanik ve elektriksel özellikleri, ayrıca hücre-materyal etkileşimleri de bu yeni elastomerik kompozitin, miyokardiyal doku mühendisliğinde bir kardiyak yama olarak kullanım potansiyelini değerlendirmek üzere masaya yatırılmıştır.

Sonuçlar, polimerik matrise Karbon Aerojel Mikrokemerlerin (CAMs) dahil edilmesi sayesinde, geliştirilen yapılarda elastisite modülü ve şekil değiştirme yeteneğinin kayda değer ölçüde yükseldiğini, böylece ortaya çıkan yapının, asıl kardiyak dokuya mekanik özellikler açısından uyum sağladığını göstermiştir. Bunun yanında, Karbon Aerojel Mikrokemerlerin eklenmesi, geliştirilen yapıya elektriksel iletkenlik kazandırmış ve iletkenlik değeri, insan miyokardı için bildirilen aralık içinde kalmıştır. Hücre-matris etkileşimi açısından, MTT (3-(4,5-dimetiltiazol-2-il)-2,5-difeniltetrazolium Bromür) analizinin ortaya koyduğu sonuçlar, CA-PGS kompozitinin, L929 fare fibroblast hücrelerinde herhangi bir *in vitro* sitotoksik etki geliştirmediğini göstermiştir. Ek olarak, H9C2 sıçan kardiyak miyoblast hücrelerinin kompozite yapıştığı ve orada çoğaldığı gösterilmiş, yine bu da kompozitin biyolojik uyumluluk sergilediğini ortaya koymuştur. Bulgular bir arada değerlendirildiğinde, geliştirilen sistemin, kardiyak onarıma yönelik miyokardiyal doku mühendisliği açısından ümit verici bir aday olduğu sonucuna ulaşılmıştır.

Anahtar Kelimeler: Miyokardiyal Doku Mühendisliği, Biyomateryaller, Poli(gliserol sebakat) (PGS), Atık Kâğıt, Karbon Katkı Maddeleri, Karbon Aerojel, Kardiyak Yama.

ABSTRACT

INVESTIGATION OF WASTE PAPER-DERIVED CARBON AEROGEL/ELASTOMER SYSTEM AS A CARDIAC PATCH

Abdulraheem Mohammed Naji ATYA

Master of Science, Department of Bioengineering

Supervisor: Prof. Dr. Halil Murat AYDIN

September 2019, 76 pages

Cardiovascular diseases (CVDs) are blamed for the major number of deaths around the world. Among of these is Myocardial Infarction (MI) which occurs when the flow of the blood through one of the coronary arteries is blocked, depriving the cardiomyocytes in the myocardial area under the occlusion from the nutrients and oxygen. If the perfusion does not be restored rapidly, the cardiomyocytes are exposed to chronic damages resulting in a significant cardiomyocyte loss within the myocardium. Since cardiomyocytes lack a self-replication mechanism, they cannot regenerate after such an injury. Therefore, the survivals from the acute MI end up with Heart Failure; where the left ventricle expands and the left ventricle wall becomes thinner. Ultimately, the heart becomes unable to pump a sufficient amount of blood to the different parts of the body, leading finally to the death of the patient.

The current therapeutic strategies of heart failure following MI are confined to slowing the progression of the end-state condition. Myocardial Tissue Engineering (MTE) is a newly emerging field in which a combination of healthy cardiac cells

and engineered cardiac patch is expected to be an excellent therapeutic strategy to regenerate the infarcted myocardium. However, finding the optimal culture substrate to be a successful cardiac patch is still an open question. Therefore, this study aimed at synthesizing novel conductive elastomer-based composite and evaluate its potential as a cardiac patch for myocardial tissue engineering.

In particular, we describe, for the first time, the synthesis of an electrically conductive composite of Carbon Aerogel-embedded poly (glycerol sebacate) (CA-PGS) system. In this work, electrically conductive Carbon Aerogel, which is a waste-derived and cost-effective carbon source that its utilization in cardiac tissue engineering applications has not been explored to date, was combined to the biodegradable PGS matrix to obtain a cardiac construct with optimal properties. The resulting composite was characterized by Scanning Electron Microscopy (SEM), Fourier Transform Infrared (FTIR) Spectroscopy, X-ray Diffraction (XRD), and Contact Angle Measurements. Furthermore, the mechanical and electrical properties of the developed system as well as the cell-material interactions were also assessed to evaluate the potential of using this novel elastomeric composite as a cardiac patch for myocardial tissue engineering.

The results showed that incorporating Carbon Aerogel Microbelts (CAMs) to the polymeric matrix notably enhanced the elastic modulus and the deformability of the developed constructs, making the resulting construct matching the native cardiac tissue in terms of mechanical properties. Moreover, the addition of CAMs made the developed construct electrically conductive with a conductivity value falling within the range of that reported for the human myocardium. In the cell-matrix interaction context, the results of MTT (3-(4,5-dimethylthiazol-2-yl)-2,5-diphenyltetrazolium Bromide) assay demonstrated that CA-PGS composite showed no cytotoxic effects for the L929 mouse fibroblast cells *in vitro*. In addition, it was shown that H9C2 rat cardiac myoblast cells attached and proliferated on the composite, which gave further confirmation of composite biocompatibility and its suitability for MTE application. Taking together, it is concluded that our developed system is a promising candidate for myocardial tissue engineering for cardiac repair.

Keywords: Myocardial Tissue Engineering, Biomaterials, Poly (glycerol sebacate) (PGS), Waste Paper, Carbon additives, Carbon Aerogel, Cardiac Patch.

ACKNOWLEDGEMENTS

First and foremost, I would like to thank Allah Almighty; my one and only Lord, for guiding and helping me not only throughout my study, but during my entire life. I always know that He is there for me throughout guiding, helping, and protecting me, even compensating me for the hardships and difficulties I have been through. All praise is due to Him in this life and the hereafter, and His is the judgment, and to Him I shall be brought back. Truly, my life and my death all for Him.

I would like to express my deep gratitude and appreciation to my thesis supervisor Prof. Dr. Halil Murat AYDIN who had spared no effort to support me since the very first moment of my involvement in his laboratory. Adopting me as one of his lab members and making all the potentials in his laboratory available for me are sincerely appreciated. For sure, his encouragement, kindness, and understanding kept me motivated and brought out the best in me.

I am extremely indebted to my family; my father Asst. Prof. Mohammed ATIYAH, my mother Ms. Faiza Hindad, my wife Ms. Hanan ALYAFIE, my little princess Noor ATYA, my little prince Yousef ATYA, my brothers Gassan ATYA, Ebrahim ATYA, and Saleh ATYA, my sister Rayhana ATYA and her husband Mohsen AL-MAHBASHI, and all the others for their believing in me, and for their endless love, support and patience. Indeed, this thesis was not possible without their support and sacrifices they have been making throughout my graduate career.

Dr. Atakan TEVLEK is gratefully acknowledged for helping me getting started in our laboratory, conducting *in vitro* studies as well as co-writing the relevant sections.

I would also like to send my special thanks to my lab partner; Mohannad ALMEMAR, for all his assistance with my experiments, for his advice and partnership, and for sharing the same stress during the time we shared in our lab.

Also, I want to thank all my other lab mates for their support and assistance throughout all stages of this study, for the lovely atmosphere they have been creating, and for their precious friendship. I would especially thank Bengisu TOPUZ for her help in my hour of need and for conducting the mechanical testing for my samples, Gülçin Günal KARATAŞ for her kindness and for all the assistance she has been providing, Selcen GÜLER for her constant caring about my experiments and for her valuable advice and observations.

My sincere acknowledgements go to Assist. Prof. Dr. Dinçer GÖKCEN for conducting the electrical conductivity test for my samples.

I owe my special thanks to my thesis committee members, Prof. Dr. İbrahim VARGEL, Assoc. Prof. Dr. Sedat ODABAŞ, Assoc. Prof. Dr. İ.Çağatay KARAASLAN, and Assist. Prof. Dr. Dinçer GÖKCEN for their invaluable reviews and feedbacks.

I would also like to thank my dear friend Mr. Ahmed AL-MALMI for proofreading my thesis and correcting my grammar and spelling errors.

I would like to thank the Presidency for Turks Aboard and Related Communities (YTB) for being the most important factor for pursuing my graduate career in Turkey through its Turkish Scholarships Program. YTB is greatly appreciated that they facilitated all the necessary procedures relevant to my movement to Turkey including securing the university admission, getting me the visa, providing me with all the initial financial support to establish my master’s career in Turkey.

Last but not least, I owe my exceptional thanks to BMT Calsis Co. for equipment and material support that made the conduction of the different experiments and tests of this study possible.

CONTENTS

Page

LIST OF FIGURES

Page

LIST OF TABLES

Page

SYMBOLS AND ABBREVIATIONS

Symbols

α	Alpha
β	Beta
ε	Epsilon
θ	Theta
p-value (p)	Probability value in t-test
°C	Degree Celsius
Au	Gold
Pd	Palladium
Cu	Copper
λ	Wavelength
Å	Angstrom (10^{-10} m)
N	Newton ($kg \cdot m \cdot s^{-2}$)
ρ	Electrical resistivity
V	Voltage
I	Current
A	Area
d	Distance
σ	Electrical conductivity
Pa	Pascal ($kg \cdot m^{-1} \cdot s^{-2}$)
M	Mega (10^6)
m	Meter
S	Siemens ($kg^{-1} \cdot m^{-2} \cdot s^3 \cdot A^2$)
gr	Gram (10^{-3} kg)

Abbreviations

CAMs	Carbon Aerogel Microbelts
CA	Carbon Aerogel
PGS	Poly (glycerol sebacate)

PGS-CAMs	Poly (glycerol sebacate)-Carbon Aerogel's Microbelts
CA-PGS	Carbon Aerogel-embedded PGS
CVDs	Cardiovascular diseases
MI	Myocardial Infarction
HF	Heart Failure
LV	Left ventricle
CMs	Cardiomyocytes
ECM	Extra Cellular Matrix
ATP	Adenosine Triphosphate
ACE	Angiotensin Converting Enzyme
ICD	Implantable Cardioverter Defibrillator
CRT	Cardiac Resynchronization Therapy
VADs	Ventricular Assist Devices
LVADs	Left Ventricular Mechanical Assist Devices
FDA	Food and Drug Administration
CAV	Cardiac Allograft Vasculopathy
OPTN	Organ Procurement and Transplantation Network
MTE	Myocardial Tissue Engineering
ESc	Embryonic stem cells
iPSCs	Induced pluripotent stem cells
EHT	Engineered Heart Tissue
PLA	Polylactic acid
PLLA	Poly-L-lactic acid
PGA	Polyglycolic acid
PLGA	Poly (lactic acid-co-glycolic acid)
PCL	Poly (ε-caprolactone)
PEG	Poly (ethylene glycol)
PU	Polyurethanes
PIPAAm	Poly (N-isopropylacrylamide)
PGCL	Poly-glycolide-co-caprolactone
PLCL	Poly (lactide-co-ε-caprolactone)
POCS	Poly [1,8-octanediol-co-(citric acid)-co-(sebacic acid)]
POMaC	Poly (octamethylene maleate (anhydride) citrate
TMC	Trimethylene carbonate

CNTs	Carbon nanotubes
CNFs	Carbon nanofibers
CNHs	Carbon nanohorns
SEM	Scanning Electron Microscopy
FTIR	Fourier Transform Infrared
XRD	X-ray Diffraction
S.D.	Standard Deviation
MTT	3-(4,5-Dimethylthiazol-2-yl)-2,5-diphenyltetrazolium bromide
ISO	International Organization for Standardization
PBS	Phosphate-buffered saline
DMEM	Dulbecco’s modified eagle medium
FBS	Fetal bovine serum
DMSO	Dimethyl sulfoxide
OD	Optical density
ECAAC	European Collection of Cell Cultures
THF	Tetrahydrofuran
DMF	Dimethylformamide
DCB	1,2-Dichlorobenzene
3D	Three-dimensional
PANI	Polyaniline
PED	Poly (ethyleneterephathalate)
wt	Weight
TCPS	Tissue culture polystyrene

1. INTRODUCTION

1.1. Objectives of Study

The primary objective of this thesis is to develop a new, simple and inexpensive composite, and investigate its feasibility to be used as a cardiac muscle repair material for post-MI heart failure disease. In this work, a novel carbon additive, which is Carbon Aerogel Microbelts (CAMs), is going to be used as a doping material to develop a conductive PGS-based composite. This novel system is expected to be cost-effective, biocompatible, and cell culture supportive, with mechanical and electrical properties matching those of the native cardiac tissue.

1.2. Significance of Study

To develop material to regenerate the myocardial tissue, a composition of PGS elastomer with waste paper-derived carbon material will be reported for the first time. In this thesis, instead of using the already-exist carbon sources which have several drawbacks including the high cost of some of which and the potential cytotoxicity of the others, it is planned to use the waste papers as a natural carbon source which, to the best of our knowledge, is not reported in any cardiac tissue engineering literature.

1.3. Literature Review

1.3.1. Architecture of Cardiac Muscle

The heart contracts continually pumping the blood which is the reach of oxygen and nutrients along with other substances through the circulatory system. This vital contraction mechanism depends entirely on cardiac muscle (myocardium).

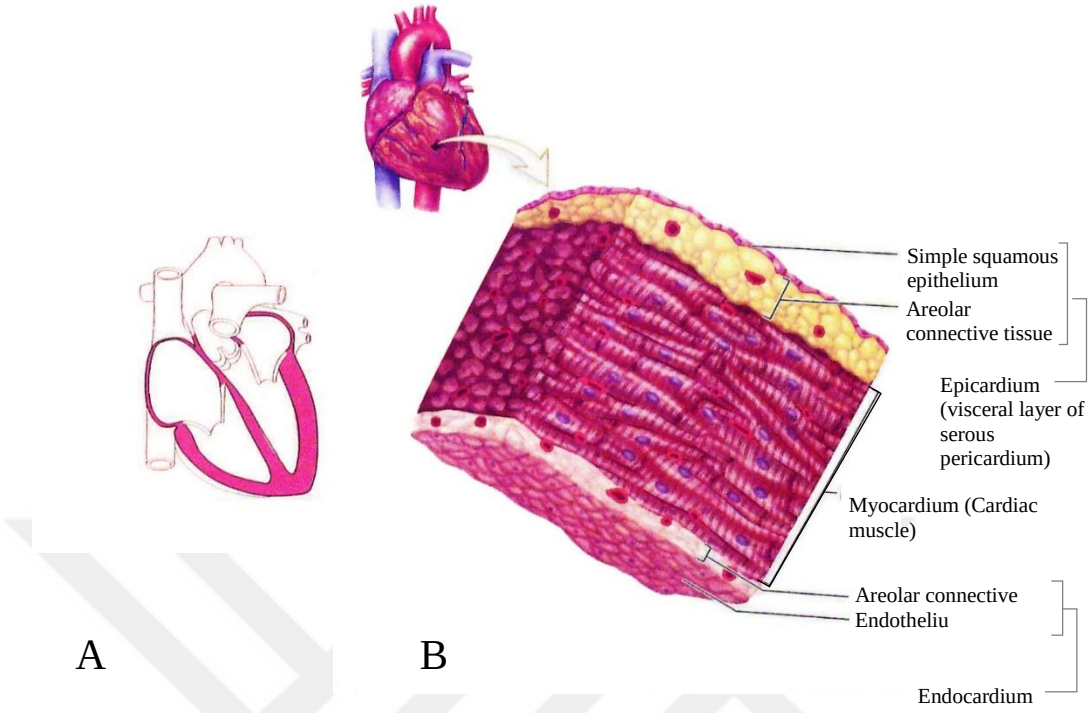

Figure 1.1. (A) Walls of the heart [1]. (B) Myocardium within the heart wall [2].

The myocardium is the tissue of the heart wall between the pericardium and endocardium [3] representing the bulk of the heart and is mainly composed of cardiac muscle [4] (Figure1). The function of cardiac muscle is to push the blood through the blood vessels to all the body [1]. Cardiac muscle is composed of a branching chain of cardiac myocytes (or cardiomyocytes) [5] which are able to contract squeezing the blood through the heart in certain directions [3]. Cardiac muscle cells arranged in a certain way to form thick bundles within the wall of the heart [2].

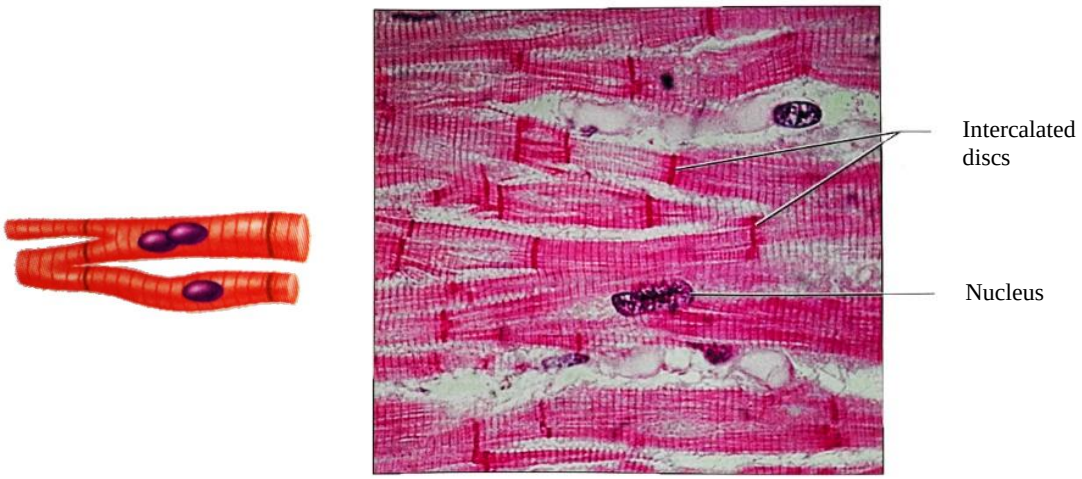

Figure 1.2. (A) Cardiac cells shapes [5]. (B) Cardiac muscle photomicrograph [1]

Like skeletal muscles, cardiac muscle fibers are striated [2, 4, 5] and contracted by sliding filament mechanism [4]. However, unlike the skeletal muscle fibers which are voluntary [5], long (100 µm – 30 cm) [2], cylindrical-shaped [4] and multinucleate [4, 5], the cardiac muscle fibers are involuntary[5], short (50 -100 µm) [2] , branched, interconnected [2, 4] and uni- or binucleate [2, 5] (Figure 2). Additionally, cardiac muscle has myofibrils composed of sarcomeres but the myofibrils have different thickness [5]. Contrary to skeletal muscle fibers which are separated from each other structurally and functionally, cardiac muscle cells are interlaced at specialized junctions termed Intercalated Discs [4]. These discs are composed of desmosomes and gap junctions [2, 4] (Figure 3). While the desmosomes join the adjacent cells preventing them from separating during the contraction, the gap junctions permit the ions to move from cell to cell [4] and hence permit for the communication between cells [3] and also allow the electrical stimulus to spread through the entire heart [4]. Importantly, cardiac muscle cells have a large number of mitochondria which is necessary for producing Adenosine Triphosphate (ATP) required for their ceaseless beating [2] (see Figure 3-A).

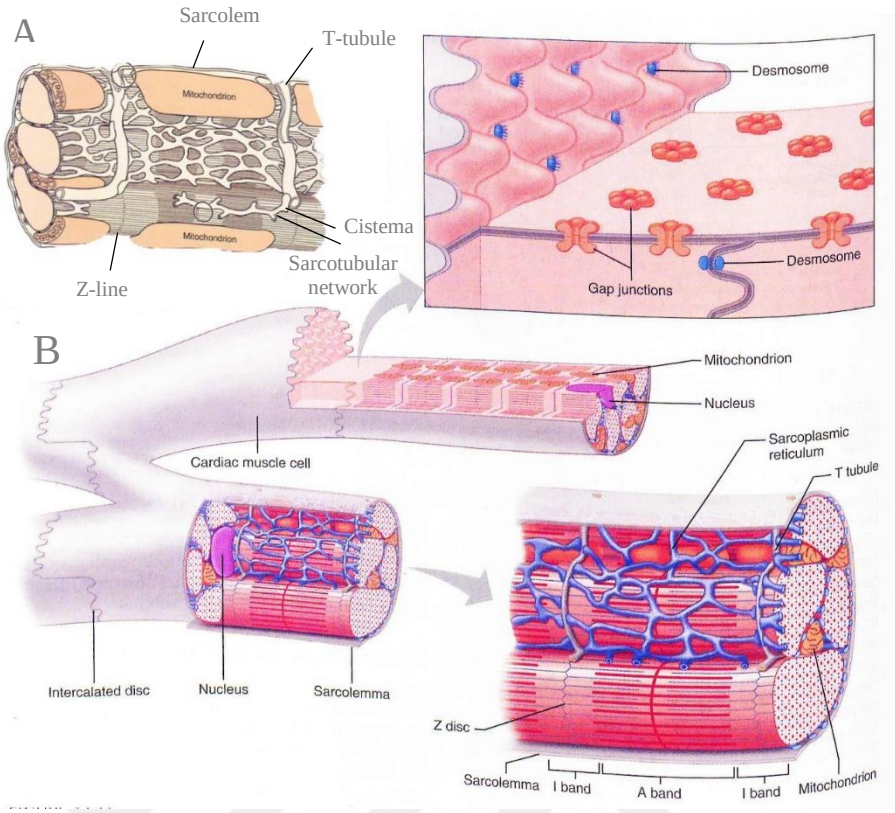

Figure 1.3. (A) Structure of cardiac cells [6]. (B) Microscopic anatomy of cardiac muscle [4].

The extracellular matrix of the myocardium is a connective tissue matrix called endomysium which is composed of collagen and elastin fibers [4]. These fibers work on the myocardium reinforcement and the cardiac muscle fibers anchoring by which the cardiac muscle cells are tied to each other to form spiral and circular muscle bundles along the heart. These interwoven bundles efficaciously bind all the heart parts together [4] (Figure 4).

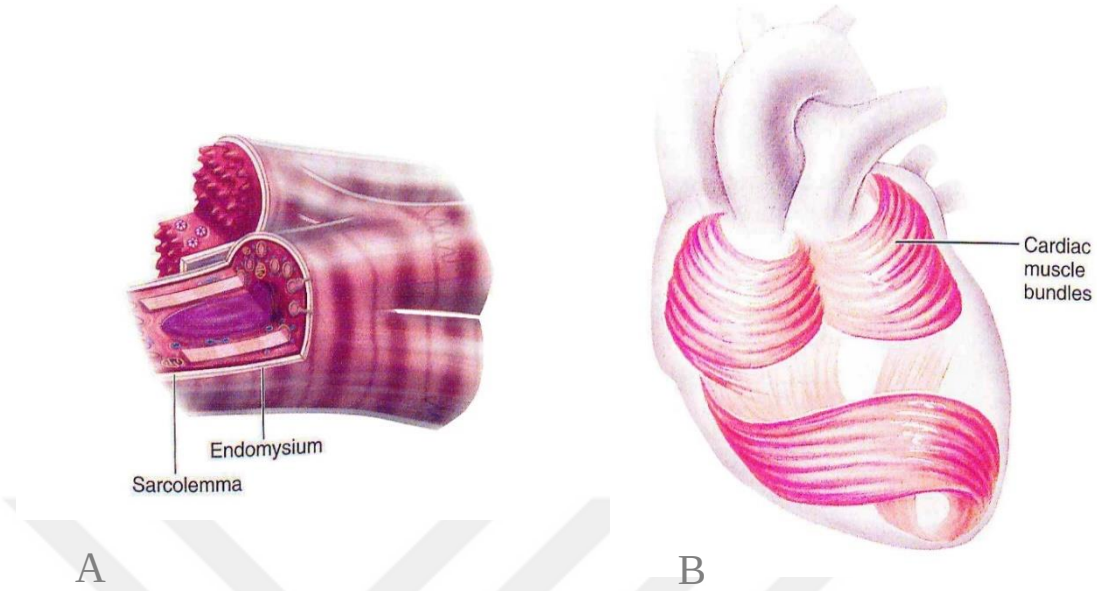

Figure 1.4. (A) The connective tissue of the myocardium (endomysium) [2] (B) The circular and spiral arrangement of cardiac muscle bundles [4].

1.3.2. Heart Failure

Cardiovascular disease (CVD) is the leading cause of total deaths worldwide, accounting for 31% of total mortality in 2015 with an estimated 17.7 million deaths, of which 7.4 million people died from coronary heart disease [7]. The global burden of ischemic heart disease experiences an increasing trend where it is estimated to increase from 47 million in 1990 to reach 82 million disability-adjusted life years (DALYs) in 2020 [8]. Patients with CVDs die mostly because of Myocardial Infarction (MI) (or so-called heart attack). The survivals of the acute event of MI usually develop heart failure syndrome due to the loss of cardiomyocytes within the left ventricle.

In order to function properly, heart relies, among other factors, on sufficient cardiac cell counts with normal contraction-relaxation mechanism, enough myocardial perfusion, proper structure and composition of myocardial extra cellular matrix (ECM) and normal metabolic activity of the ECM and the myocardium. Any disorder, consequently, in one of the aforementioned factors may lead to heart failure [9].

Heart failure (HF) is a clinical syndrome in which the heart becomes too weak to pump sufficient blood to meet metabolic body demands. HF constitutes the end state clinical condition of many forms of heart disease [10].

HF constitutes a huge global burden as it is still the only cardiovascular disease (CVD) syndrome whose prevalence experiences increasing trends throughout the world [9]. In USA alone, the HF prevalence among adults is estimated to be 6.5 million with 960,000 new cases every year. This figure is predicted to witness an increase of 46% between 2012 and 2030 to reach 8 million. The estimated direct and indirect cost of HF registered about $30.7 billion in 2012. By 2030, it is anticipated to rise by 127% to $69.7 billion [11]. Despite large advancements that have been achieved over the past few decades in CVD treatments, HF 5-year survival rates remain low by 25% for men and 38% for women [10]. Importantly, our distinct comprehension of the underlying progressive mechanisms of HF is of paramount importance to come up with new treatment strategies [12].

1.3.3. Pathophysiologic Event Series Leading to HF

In general, HF is the end-state condition for many heart diseases, and its pathophysiology results from many factors (Figure 5). Such factors include ischemia, stimulation of neurohormones, alterations in the blood pumping forces, ventricular remodeling, inflammation, and genetic disorders [13]. Generally, the clinical course of HF begins with an ischemia or overload.

Heart failure is usually trigged by a myocardial ischemic injury, represented by its common form; myocardial infarction (MI) [14]. MI results from atherosclerosis in which an accumulation of fatty acids deposits on an inner wall of one of the coronary arteries responsible for supplying the heart muscle with blood. Overtime, a thrombus may form which completely blocks the blood inflow resulting in depriving the cardiac muscle under that artery of oxygen and nutrients necessary for vital metabolism activity [15] (Figure 6). If the perfusion does not be restored rapidly, the cardiac muscle is exposed to chronic damages resulting in cardiac functional impairment and adverse structural alterations.

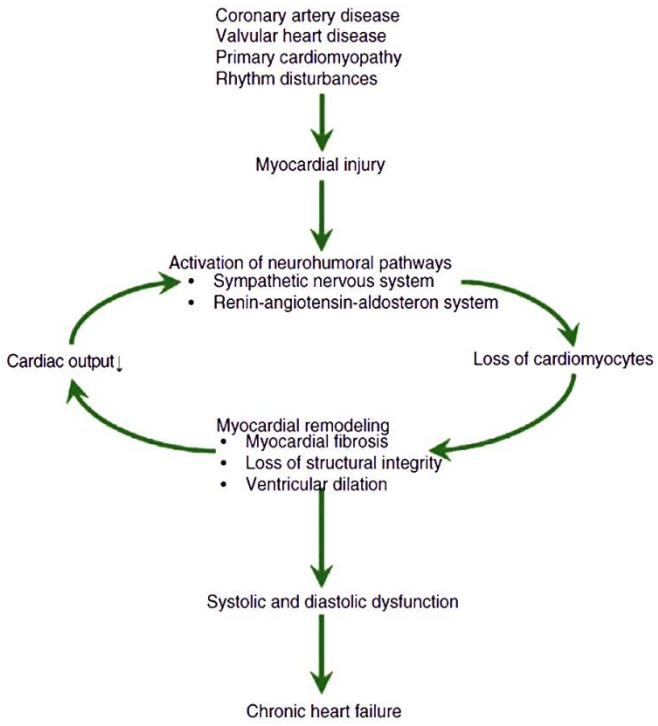

Figure 1.5. Pathophysiologic event series leading to HF [16].

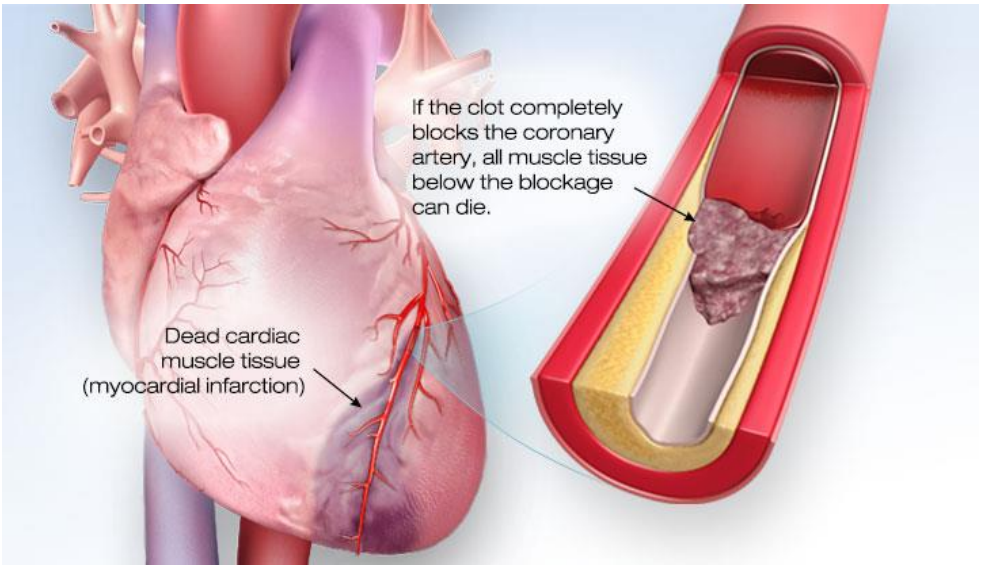

Figure 1.6. The death of cardiac muscle located under a coronary artery undergone a blockage formation [17].

In an effort to compensate for the decreased cardiac output, the injured heart undergoes series of complex, structural and functional changes that begin with cardiac hypertrophy and end with heart failure [14].

1.3.3.1. Neurohormonal Activation

In a complex process called neurohormonal activation, the sympathetic nervous system is activated due to severe pain and reduced output of the heart accompanying the MI event. In this process, at a molecular level, a set of vasoconstrictor hormones such as angiotensin II, norepinephrine, epinephrine, aldosterone, and the endothelin family of peptides are released stimulating vasoconstrictor β-adrenergic and α-adrenergic receptors. This mechanism works on improving the contractile function of the non-infarcted part of the myocardium and increasing blood pressure as an attempt to compensate for the reduction in the cardiac output.

Although this compensatory mechanism seems to be beneficial and effective in restoring the momentum of pumping in the short term, the activation of neurohormones takes the primarily responsibility for the subsequent deterioration of the situation as it derives a series of chronic changes in the structure and function of the heart leading eventually to progressive adverse effects on survival [14]. In addition, neurohormonal activation makes the cardiac ischemia even worse through expanding the infarct area by rising the non-infarcted myocardium's demand for oxygen of which the myocardium actually deprived [14].

1.3.3.2. Cardiac Hypertrophy

At the cellular level, the cardiac myocytes experience an enlargement (hypertrophy) with a view to increasing their function [14]. This cellular response occurs due to the fact that the released neurohormones are actually growth factors which activate upregulations of altered proteins that resulted in an enlargement of the healthy cardiomyocytes [13].

Cardiac hypertrophy, nevertheless, is not a well enough process to compensate for the function of the lost myocardium neither quantitatively nor qualitatively [14]. Quite the contrary, this process leads to irreversible functional and structural disintegration [13] which eventually develops to an HF syndrome [14].

1.3.3.3. Death of Cardiac Myocytes

Death of healthy cardiac myocytes and their replacement by fibrotic tissue is one mechanistic characteristic of failing heart [14]. Myocyte loss is a crucial factor for the transition from cardiac hypertrophy to end-stage heart failure. While the mediators of hypertrophy are considered as growth factors in normal conditions, they become death factors as they cause cardiac cell death [18]. Necrosis, autophagy, and apoptosis are the cardiac myocyte loss pathways carried out due to post-infarct remodeling [14].

Necrosis of myocytes results from the starvation of myocytes when the mitochondria become ischemic. The increasing of myocytes diameter due to hypertrophy increases the diffusion barrier making it so hard for the oxygen to diffuse from the adjacent capillary to the mitochondria which result in the death of cardiomyocytes [14].

Autophagy, on the other hand, is a myocyte death pathway that is activated and contributed to the myocyte dropout. The presence of phagosome-like cytoplasmic inclusions is a common observation within the hypertrophied cardiac muscle. The proteasome system responsible for the degradation of intracellular proteins becomes, presumably, overwhelmed and be unable to keep up with the abnormal activity of hypertrophied myocytes. Consequently, the accumulation of proteins needed to be eliminated contributes to myocyte death [14].

After the cardiovascular event, cardiac myocytes also undergo incidence of apoptosis which considered a programmed cell death in which necrosis with karyorrhexis and cell shrinkage take place in a cell [18]. Apoptotic myocyte death happens in the myocardium as a response of myocardial infarction [19, 20] and heart failure [21]. Given the quite limited myocardial regenerative capability, apoptosis rarely takes place among cardiac cells in the normal conditions, reported to be about 1/10,000 apoptosis incidence to 100,000 cardiac myocytes. In the ischemic cardiomyopathies, however, the apoptosis genes expressions are noticed to be upregulated and the apoptotic bodies count rises by order of magnitude within the ischemic myocardium [14].

1.3.3.4. Ventricular Remodelling

The left ventricle (LV) responses to the dropout of cardiac myocytes and the excessive volume and pressure loads by undergoing a remodeling process in its shape, size, and function. In this process, LV chamber dilates, as a response to the volume load, and LV wall experiences thinning in response to the pressure load [22].

Left ventricular remodeling symptoms may begin to arise once the ischemic event takes place. Over the following months and years, the symptoms gradually become more evident. Such symptoms include increasing in end-diastolic and end-systolic volumes, ventricular cavity, systolic bulging, as well as a thinning in the ventricular wall [8].

Among the factors that contribute to the ventricular post-infarct remodeling is the changes occur to the shape and dimensions of cardiac cells after a cardiovascular event due to their spatial arrangement within the ventricular wall. Myocyte length accounts for the ventricular cavity size while its diameter contributes to the wall thickness. Therefore, any alteration in the myocyte length-to-width ratio, which is estimated to be 7:1 in healthy cardiac myocytes, contributes to the changes happens to the ventricle geometry [10].

Eventually, this functional and structural compensatory strategy involves long-term adverse effects on heart failure survival where, at this point, affliction with HF becomes more evident [23] (Figure 7).

The remodeling is also observed in the myocardial extracellular matrix (ECM) [9, 22]. After cardiovascular events, collagen is caused to be over-synthesized within the myocardium. Consequently, the collagen accumulation results in fibrous non-contractile scar tissue formation [22]. This loss of cardiac myocytes and its replacement by a fibrotic tissue is a significant indication for HF [14].

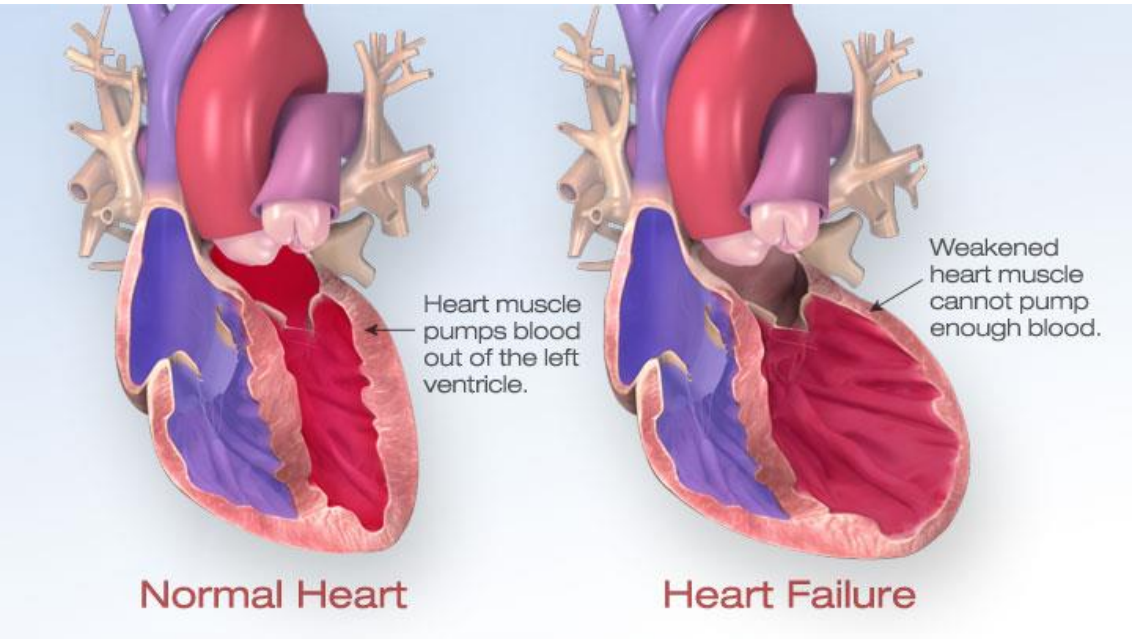

Figure 1.7. LV dilation and wall thinning in post-infarction heart failure [24].

1.3.4. Current HF Management Therapies

Pharmacological, device, and surgical therapies are the current main treatment paradigms that post-MI patients receive [24] (Figure 8). However, the goal of these current treatment strategies is merely to relieve HF symptoms and prolong survival [24]; as a result, they cannot prevent the progression to the terminal state and, consequently, death. In addition, not all patient subgroups benefit from the current therapeutic approaches. The following paragraphs will discuss each therapy in brief.

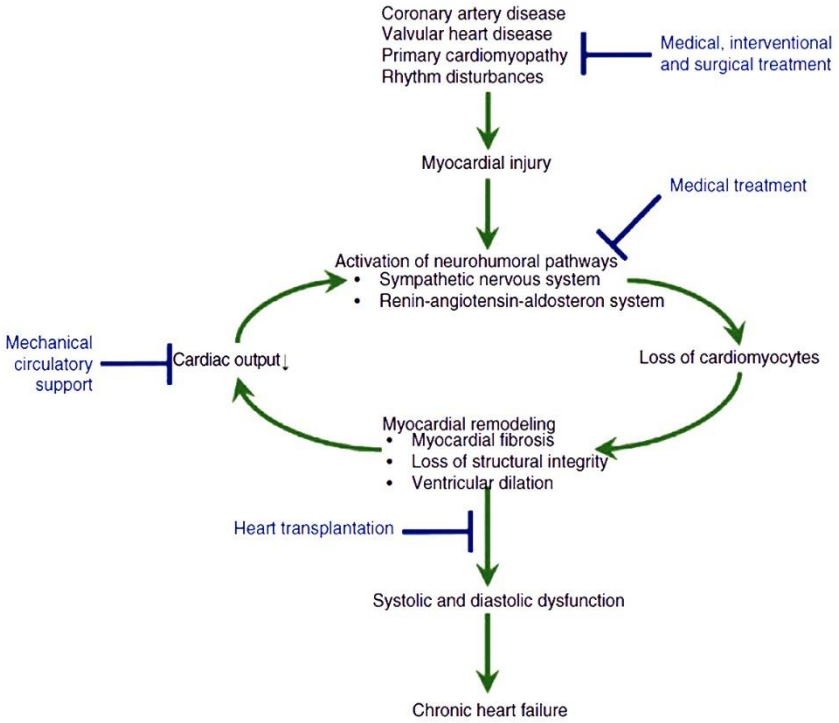

Figure 1.8. Current state-of-the-art therapy for chronic heart failure (blue). Figure adapted from [16].

1.3.4.1. Pharmacological Therapy

The advancements in our understanding of HF progression mechanisms have led to new therapeutic agents rising which results in a significant reduction in morbidity and mortality rates. Pharmacotherapy becomes the standard therapy to which HF patients may be subjected for a long time. Such therapeutic agents include angiotensin-converting enzyme (ACE) inhibitors, beta-adrenergic blockade (beta-blockers), and aldosterone antagonists (aldosterone receptor blockers) [13].

ACE inhibitors, like benazepril, zofenopril and captopril, are the standard medications for those who have chronic HF or systolic myocardial infarction, as they reduce morbidity and improve survival by reducing the size of the heart and slowing the progression towards HF [25-27]. ACE inhibitors, nevertheless, are detrimental to those who have hypotension, renal dysfunction [24], angioedema, or renal or aortic artery stenosis. These inhibitors should also be avoided in pregnancy [13]. In

addition, the outcomes of ACE inhibitors in patients with diastolic cardiac dysfunction are questionable [24].

Beta-blockers, include bisoprolol, metoprolol succinate, and carvedilol, are indicated for patients who do not endure ACE inhibitors with mild to severe HF and symptomatic HF as well as those who have LV dysfunction. Beta-blockers are showed to enhance the function of the heart, soothe the symptoms of symptomatic HF as well as improve the outcomes on patients with MI and LV dysfunction. These agents work on blocking the sympathetic nervous system activation, improving ventricular function and mechanics, and lowering the risk of abrupt death [13]. Nonetheless, beta-blockers have adverse effects on a sub-group of patients with decompensated heart failure and tachycardia. Like ACE inhibitors, Beta-blockers are also detrimental for patients with hypotension [24]. Besides, beta-blockers result in symptoms deterioration if the therapy is initiated at high doses [13].

Aldosterones (spironolactone, Eplerenone and Placebo) are usually indicated along with standard pharmacotherapy for patients who have systolic dysfunction and severe HF after MI as they enhance the clinical results [13, 24]. Hyperkalemia is one drawback of Aldosterones, though [13]. In addition, it has been shown that Eplerenone and Placebo are lethal to systolic heart failure patients with mild symptoms [28].

Therefore, it can be obviously noticed that the pharmacological therapy is limited to addressing the symptoms of HF and it may have negative consequences on survival [24]. Combining two or more above-mentioned medical agents is also inadvisable as doing so increases the risk of having hyperkalemia or renal dysfunction [13].

1.3.4.2. Device Therapy

1.3.4.2.1. Implantable Cardioverter Defibrillator (ICD)

ICD is used, alongside medical agents, to lower mortality rate by preventing the abrupt death of the heart in post-MI ventricular dysfunction patients as well as those with mild or moderate HF who are predisposed to heartbeat instability, fibrillation of the ventricle, or tachycardia in which blood pumping forces are not stable [13]. The shortcomings of ICD is that it does not have significant positive effects on clinical outcomes for more than 12 months [29]. Moreover, ICD is not effective for patients

with good chances to survive and proper functional performance exceeding 1 year [13].

1.3.4.2.2. Cardiac Pacing

The main objectives of the cardiac pacing therapy, which also called Cardiac Resynchronization Therapy (CRT), are to improve symptoms and, in some cases, survival as well as to enhance living conditions. Cardiac pacing therapy is indicated for a specific subgroup of patients who suffer from disturbances in the cardiac electrical conduction system (cardiac dyssynchrony), which is a comparatively frequent MI complication [30]. In this case, an artificial pacemaker takes place the abnormal intrinsic heart pacemaker activity in providing the electrical pacing. Nonetheless, CRT is inadvisable for patients presenting no or mild HF symptom [31]. If the necrosis occurs on a large scale, furthermore, the cardiac pacing therapy does not significantly contribute to the prognosis, and in some instances, the pacing therapy may be harmful [30]. In addition, pacing therapy must not be indicated for patients with tachycardia in which the QRS complex is shorter than 120ms. The effectiveness of pacing therapy on mild-to-moderate HF has to be more investigated too [30].

1.3.4.2.3. Ventricular Assist Devices (VADs)

VADs are mostly used as a bridge to cardiac transplantation. VADs may also be utilized as durable therapy for refractory cases where symptoms and survival improvement are not achieved when the pharmacological therapy is administered [13, 24]. Moreover, FDA approved certain VAD models as an alternative therapy for selected patients who are ineligible for heart transplantation [13]. The function of the VAD is to reduce the load on the diseased left ventricle (LV) by pumping the blood coming to the LV to all over the body [32] (Figure 9). It has been shown that Left Ventricular Mechanical Assist Devices (LVADs) reduce the risk of death, increase the rate of survival, and improve the quality of life [32]. Although tremendous efforts have been exerted to significantly reduce adverse events associated with VADs such as infection possibility, bleeding, neurologic dysfunction and device failure [13, 33], many central issues remain controversial; that are, the extent of long-term patient survival achievement, selecting patients based on recovery possibility, device long-term endurance, and accessibility of the device due to its high-cost [24].

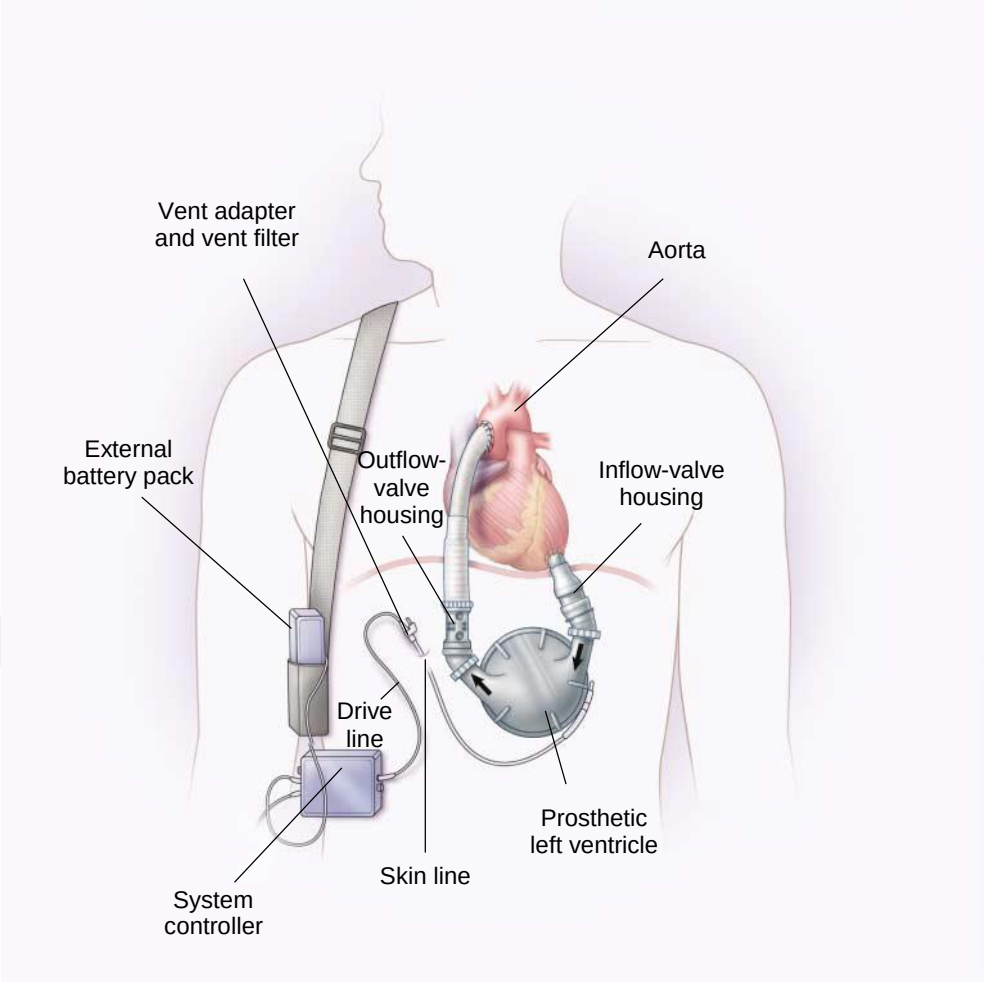

Figure 1.9. Parts of Left ventricular mechanical assist device [33].

1.3.4.3. Cardiac Transplantation

To date, the only evidence-based destination therapy for the terminal HF is the cardiac transplantation [13, 34]. The annual transplantation count experiences a consistently increasing trend over the last years reaching its peak figure of 5,074 transplants in 2015. However, limited transplant eligibility, shortage of donors, and post-transplant morbidity are common drawbacks to the cardiac transplantation.

The median long-term post-transplant survival is 10.7 years, and the long-term survival is limited by Cardiac Allograft Vasculopathy (CAV) which is a common disease after transplantation. Other common post-transplant diseases include, among others, renal function, diabetes, and malignancy. Eventually, such morbidities significantly contribute to the mortality of cardiac transplant patients [35].

Another major problem associated with cardiac transplantation is the limitation of optimal donor hearts [13]. The figures for cardiac transplantation surgeries show an increasing trend, and between 2004 and 2012, the number of transplantation candidates registered an increase of 25% [36]. For example, based on OPTN data as of August 26, 2019, there are 3,734 candidates on the US national waiting list [37]. As a result, the demand for non-standard hearts marks a steady increase to be used for patients at high risk and those of severe illness [13].

Thus, even though many significant HF-related breakthroughs have been achieved successfully during the last three decades which have an important impact on the clinical results, the figures for morbidity and mortality among patients with HF are still high [13]. Therefore, the only way to repair the diseased heart and thus reduce the global HF burden is to adopt new treatment strategies that involve introducing new contracting muscle to the injured myocardium which cannot be achieved by the current treatment paradigms [38].

1.3.5. Currently-Investigated Cardiac Repair Approaches

For just about a century, considerable scientific efforts have been devoted to coming up with a piece of tissue that mimics the functional properties of the myocardium [39]. The currently found commercial cardiac patches (ventricular restraints) are not designed to address the loss of cardiomyocytes. They just act as physical restraints whose functions are limited to alleviate the symptoms and delay the progression towards the HF [40]. Developing an artificial elastomeric scaffold or cardiac patch that can not only serve as a constraint, but also introduce healthy cells in order to regenerate the injured myocardium has been a dream for the humanity for a long time [40]. However, renewing one billion cardiomyocytes post MI appears to be a real challenge [41]. Consequently, a significant breakthrough has not been achieved yet despite the huge scientific efforts that have been reported in this context [39].

Providing the contractile mechanism, cardiomyocytes represent the natural key for the myocardium repopulation [42]. Driven by the shortage of heart donors and the essential presumption saying that the dysfunction of the ventricular is attributed in large part to the enormous drop in cardiac cells number, regeneration of the injured area through delivering new beating cells might be a probable modality to reverse the dysfunction curing the diseased heart and recovering function [43, 44]. In the

later years, many techniques to heal or replace the injured myocardium have been reported with a view to provide a pulsatile cardiac muscle that can couple to the native myocardium electrically and mechanically and to enforce the affected heart function [41]. One of these promising approaches is the Myocardial Tissue Engineering (MTE) approach which should be seen in the foundation of fruitful endeavors to regenerate the cardiac muscle through direct injection of the cells intramyocardially [45].

1.3.5.1. Cell Therapy

The easiest method to repair the damaged heart is through the direct intramyocardial injection of stem cells or cardiomyocytes [41] which could most likely be accomplished percutaneously [45]. The aim of cell injection is to repair and replace the infarcted myocardium [40].

The cell therapy based on the regeneration of damaged cardiac muscle is thought to demand a solid transplantation of nearly one billion myocardial cells [46]. Several clinical trials have been performed using an injection of different cell types to the infarcted zone, including bone marrow stem cells, embryonic stem cells, skeletal myoblasts, peripheral blood-derived cells and cardiac progenitor cells (cardiac stem cells) [43, 47]. However, although some of which have demonstrated a modest improvement, at best, in contractile function [47, 48], various issues related to the poor cell transplantation efficiency have arisen. Cell death and substantial cell washing out within the next few hours post transplantation is the most severe of which [48, 49]. In particular, cell death happens during the first days of injection owing to the harsh conditions within the injured zone. Such conditions include anoikis (cell death due to the absence of the matrix), hypoxia, ischemia and acute inflammation and immunology actions [44, 50, 51].

In general, over half of the cells undergo death during the first week after injection [51], and the seeding efficiency could be reported to be only from 5% to 10% [44]. One of the major cell death pathways is mediated by anoikis which is a programmed cell death (apoptosis) due to the absence of the extracellular matrix [52]. Basically, the integrins and other receptors attach the cardiomyocytes to the ECM in which they are embedded sending survival signals. The disruption of these signal releases cytochrome c and activates caspases which degrade the proteins in the cytoplasm

and nucleus resulting in cell death [51, 52]. Besides, the low injection efficiency of 10% requires a transplantation of 10 billion cells which is not practical due to the high cost [41]. There can be no doubt that the remuscularization of the infarcted heart needs more than the simple injection of the correct cells in the desired zone [53]. The shreds of evidence suggest that the first step toward treating the injured cardiac muscle is to enhance the introduced cell survival and retention [44].

1.3.5.2. Myocardial Tissue Engineering

Driven by the cell therapy downside of low cells retention and the fact that not only the cardiomyocytes but also the native ECM undergo damage and modification after MI [44], a second generation of cell-therapy have emerged, namely, Myocardial Tissue Engineering (MTE) which is regarded as a promising strategy to overcome the drawbacks of the direct cell injection and the serious lack of the donor hearts. This technique involves developing either scaffolds to create an artificial cardiac tissues *in vitro* or cardiac patches to engraft healthy cells for repair the injured myocardium [40] (Figure 10).

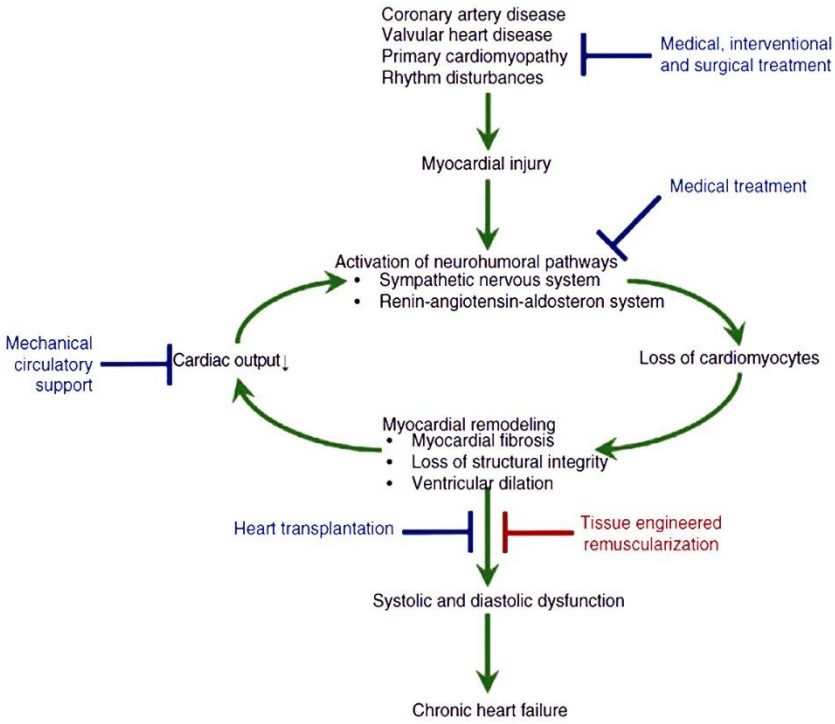

Figure 1.10. The position of the myocardial tissue engineering strategy (red) compared to the current therapy for chronic heart failure (blue) within the pathophysiological event chain resulting in HF. Figure adapted from [16].

The approach of replacing the infarcted tissue with a cardiac wall substitute (or so-called cardiac patch) is anticipated to be a promising alternative therapeutic solution for heart disease [54]. With a view to creating a functional cardiac patch, the MTE is based on the concept that support and regeneration of the damaged myocardium demand not just a source of cells but also a biodegradable biomaterial that acts as a cell scaffolding [55]. Hereby, the biomaterial serves as an alternative ECM in/on which cardiac cells can be seeded providing the necessary support for the cells to grow and proliferate until a new ECM is formed by the seeded cells [43, 49]. After a cell growth in a thin layer on the matrix [56], the cardiac patch is transplanted onto the scarred cardiac muscle followed by its integration and coupling with the host tissue electrically and mechanically with a high cell retention rate (Figure 11). As such, it is anticipated that the affected myocardium will restore its original density, contraction and cardiac role [43, 49]. Ultimately, the seeded cells would aggregate to form a structural and functional anisotropic cardiac muscle that is well-integrated with the host one [42].

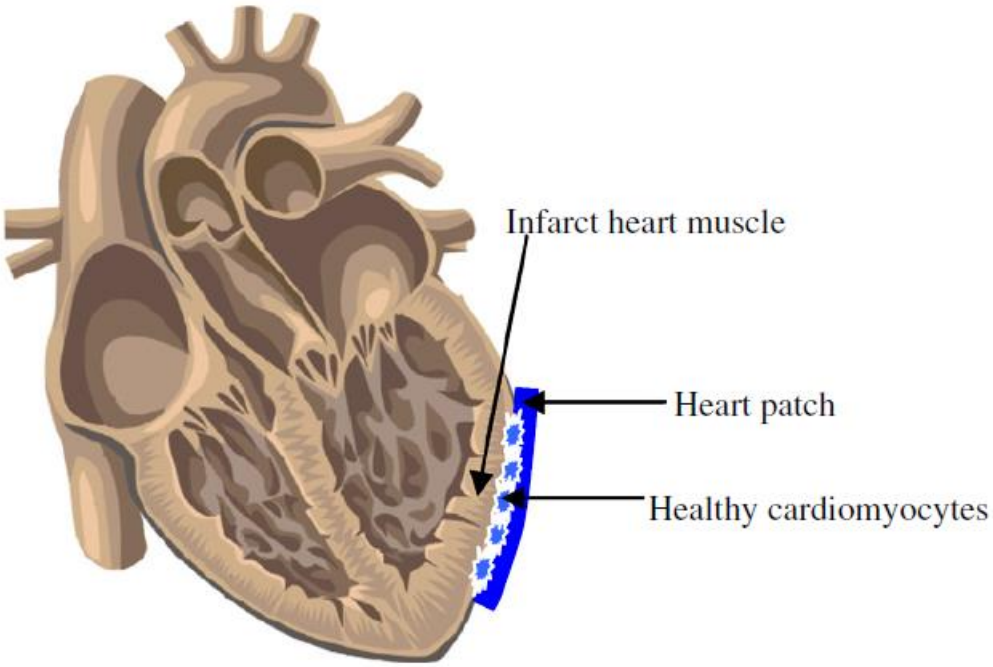

Figure 1.11. Cardiac patch approach. The cardiac patch is grafted to the infarcted area to perform two functions; delivering healthy cardiac cells and serving as a restraint to support the scar [57].

The two main aims of the cardiac patches are to deliver healthy cardiomyocytes or stem cells to the damaged area and to serve as a restraint to support the left ventricle [40]. The advantage of cardiac patches over the direct cell-therapy is that the biomaterial transplanted with the cells creates a suitable environment for the seeded cells securing them against hostile conditions that cost them death. Mechanical support is another advantage of suturing a biomaterial to the damaged cardiac muscle along with cells. The matrix is expected to act as a physical constraint reducing the wall stress and preventing the scar tissue from further extension and the left ventricle from further deterioration and dilation [44, 56].

For the sake of developing a successful cardiac patch whose properties as similar to those of host tissue as possible, a number of factors have to be taken into consideration including the biomaterial matrix and the cell source [44, 58]. In this context, various cell sources and matrices have been studied and evaluated for MTE in recent years which will be highlighted in the following discussion.

1.3.5.2.1. Cell Sources Utilized in MTE

Cell source is a critical element for the success of the engineered construct. In the context of MTE, cardiomyocytes were used to be the potential cell source for myocardium regeneration [44] owing to their intrinsic electrophysiological, pulsatile, and structural characteristics [58]. However, human cardiomyocytes sources are unavailable up to date due to their lack of proliferation which imposes limits upon using them clinically [44, 59]. As a consequence, many researchers turn to investigate other cell sources. Various cell types have been proposed for myocardial regeneration within the scope of MTE (Table 1). Fetal and neonatal cardiomyocytes have been utilized to approve the proof of concept of heart regeneration therapy based on engineered tissue [50]. Recently, driven by the advancements in stem cell biology, there have been growing interests in stem cells as promising cell sources that possess the potential to regenerate the injured cardiac muscle. Stem cells are defined as cells with intrinsic renewal and plastic capability that show the ability to differentiate into multiple lineages including functional cardiomyocytes [58, 60]. Stem cells are recognized as a favorable alternative cell source especially for patients with advanced end-stage heart failure whose autologous cells lack the ability to replicate [61].

Table 1.1. Different Potential Cell Sources Utilized in Myocardial Tissue Engineering

Cell type	**Ref.**
Non-stem (mature) cells	
1. Fetal rat cardiomyocytes	[62-65]
2. Skeletal myoblasts	[66-72]
3. Smooth muscle Cells	[64, 73]
4. Fibroblasts	[64, 74-77]
5. Neonatal rat cardiomyocytes	[78-85]
Stem Cells	
6. Mesenchymal stem cells	[86-99]
7. Adipose-derived stem cells	[100-108]
8. Endothelial progenitor cells	[109]
9. Crude bone marrow (bone marrow stem cells)	[110]
10. Umbilical cord cells	[111, 112]
11. Embryonic stem cells (ESc)	[113-126]
12. Induced pluripotent stem cells (iPSCs)	[127-130]
13. Cardiac stem cells	[131-133]
14. Cardiac progenitor cells	[134]

Each of the cell source candidates that mentioned in the table has its advantages and disadvantages. Ideally, with a view to obtain a suitable engineered tissue, cell source must be easy to harvest, do not produce an immunogenic response, and able to proliferate and differentiate into the desired terminal cells [53, 58, 61]. But unfortunately, such a cell source does not exist up to now [58]. The issue of lacking the ideal cell source limits the efforts of creating a successful cardiac patch significantly. Therefore, MTE approaches have been counted on using cell types like neonatal rat cardiomyocytes and fetal cardiomyocytes that are potent, yet

clinically irrelevant [39]. Accordingly, the ideal cell source for myocardial regeneration is yet to be determined [41].

1.3.5.2.2. Biomaterials Utilized in MTE

MTE ultimately aims at creating myocardium that is biocompatible and non-immunogenic which has the same properties as of the native cardiac muscle in terms of function and morphology [135]. In the context of tissue engineering, most of the utilized cells isolated from any source are anchorage-dependent so that they count on a matrix to support their growth [61]. To this end, biomaterials play a vital role in MTE techniques. Biomaterial scaffolds are designed as carriers that match the structure and function of the native ECM with a view of providing protection, a physical stability, and a suitable microenvironment to the transplanted cells until they produce their own ECM [39, 48, 61]. In addition, scaffolding biomaterials guide and organize the activity and function of the cells as well as provide space of cell attachment, replication, migration, and differentiation by promoting cell-material interaction and cell-cell communication [53, 58, 61]. Basically, the biomaterial must have the capacity of interacting with the cell at the molecular level as well as integrating to the natural interaction between cells and the host environment in a proper and controlled way [58]. Furthermore, biomaterials facilitate the remodeling and the formation of neural tissue and vascularization (neovascularization) while allow the nutrient and growth factors to be transported and wastes to be removed in an efficient manner [61].

However, producing an ideal tissue-like biomaterial scaffold with morphology and properties matching those of the native ECM remains one of the main challenges in the field of MTE, which yet to be found [38], owing to the different functions, complicated structure and the dynamic nature of the native ECM [61].

Generally, an ideal biomaterial has to meet several criteria; that are:

- **Biodegradability**: Biomaterials are biodegradable matrices that are composed of biocompatible polymers [55]. After transplantation, biomaterials should gradually decompose in vivo into its products in a relatively short period but long enough until the cells produce their own ECM. In other words, the degradation rate of the biomaterial must be consistent with the

regeneration rate of the recently produced ECM [38, 136]. The degradation is achieved by intravital enzymatic decomposition, hydrolysis, or dissolution mechanisms [55, 137]. The degradation property of the matrix is of crucial importance in MTE as the stress and function must be transferred from the patch to the newly formed tissue over time [40].

- **Biocompatibility**: The biomaterial and its degradation products must be non-toxic so that it promotes the extent of biological interactions, such as cell adhesion, proliferation, viability, and differentiation, on which the new tissue formation extremely depends [39].
- **Non-immunogenicity**: The biomaterial must be not provoking any immunogenic response by the host [44].
- **Possessing desired mechanical properties**: Developing a biomaterial construct with proper mechanical properties is of paramount importance. In general, the mechanical properties of the biomaterial such as elasticity and mechanical strength should be practically identical to those of the host tissue [61]. For MTE application, the cardiac construct should have suitable mechanical properties to be able not only to withstand the systole/diastole process of the heart, but also to provide mechanical support for the heart pumping function post transplantation. The mechanical support provided by the cardiac patch is also important for the seeded cells to be able to attach and produce their own ECM [38]. Moreover, there is a close relationship between mechanical properties of the biomaterial and cell differentiation [137].

Besides the aforementioned requirements, engineering the heart tissue requires additional biomaterial criteria, that is, the biomaterial should maintain and contribute to cardiac electrophysiological function by providing an electrical support to the heart [44, 137].

Various polymeric materials, natural, synthetic and composites, have been utilized or under investigation for MTE applications especially as cardiac patches. Table 2 provides an overview of biomaterials utilized in MTE.

Table 1.2. An overview of biomaterials used in MTE

Biomaterial	Physical State	Ref.
Natural Polymers		
• Collagen type I	Liquid/Gel	[99, 125, 138-143]
	Solid	[112, 144-146]
• Gelatin	Solid	[62, 147, 148]
• Alginate	Solid	[63, 65, 149, 150]
• Hyaluronan	Solid	[151]
• Collagen-Matrigel (EHT)	Liquid/Gel	[85, 138, 141, 143, 152]
• Fibrin	Gel	[110, 126, 138, 153, 154]
• Peptide nanofibers	Gel	[155, 156]
• Elastin	Solid	[157]
• Agarose	Gel	[108]
Synthetic Polymers		
• PLLA	Solid	[158]
• Polylactic acid (PLA)	Solid	[159]
• Polyglycolic acid (PGA)	Solid	[77, 160]
• Poly (lactic acid-co-glycolic acid) [PLGA]	Solid	[74, 147, 159, 161]
• Poly (glycerol sebacate) [PGS]	Solid	[57, 124, 148, 162-166]
• Poly (ε-caprolactone) (PCL)	Solid	[158, 167, 168]
• Polyurethanes (PU)	Solid	[68-72, 169, 170]
• Poly (N-isopropylacrylamide) [PIPAAm]	Solid	[171]
• Poly-glycolide-co-caprolactone (PGCL)	Solid	[172]

• Poly (lactide-co-ε-caprolactone) (PLCL)	Solid	[73, 97]
• Poly (L-lactide-co-trimethylene carbonate)	Solid	[173]
• Poly [1,8-octanediol-co-(citric acid)-co-(sebacic acid)] (POCS)	Solid	[174]
• Poly (octamethylene maleate (anhydride) citrate) (POMaC)	Solid	[175]
• Poly (octamethylene maleate (anhydride) 1,2,4-butanetricarboxylate) (124 polymer)	Solid	[176]

Natural biomaterials, which can be obtained from natural tissues, have been utilized as implant materials for a long time. The advantages of natural biomaterials over their synthetic counterparts include biological degradation, favorable biological characteristics, and cellular responses similar to those noted in natural tissues [137]. Natural biomaterials promote viability, replication and differentiation of the transplanted cells [44] and have the ability to control different cell behavior thanks to their binding motifs which provide a suitable cell-material interaction. Nevertheless, the over interaction of these materials with the cells seems to provoke an immunogenic response against them which is one of many factors that hinder their application as promising myocardial patches. The other drawbacks of natural biomaterials include poor and variable physical properties, mechanical properties as well as low stability and reproducibility [137].

Unsurprisingly, many investigators have recently turned to synthetic polymers, elastomers in particular, owing to their repeatable properties [38]. Synthetic biomaterials are biocompatible, can be synthesized in huge quantities [137], and their mechanical and chemical properties as well as degradation rates can be tuned in an easy manner according to the specific tissue engineering application [44]. Synthetic biomaterials are generally non-immunogenic as their unequivocal chemical composition eliminates the likelihood of contamination with germs like that expected to be observed in the natural biomaterials obtained from animal tissues [39]. However, synthetic biomaterials are not free from downsides; that is, they lack

interaction with cells and may cause inflammatory response following engraftment [137].

Polyesters, which are of synthetic ones, are polymeric macromolecules whose monomers are connected by ester bonds. The latter is a covalent bond which is formed between hydroxyl groups (-OH) and carboxyl groups (-COOH) when an alcohol reacts with a carboxylic acid. Polyesters are usually hydrophobic materials with tunable physical and mechanical properties. Many polyesters show good elastic properties, so they have the ability to recover their original shape after deformation. These elastomeric materials are viscoelastic with weak intermolecular forces, low Young's modulus and high failure strain. Polyester elastomers are intrinsically biodegradable. In the biological environment, ester bonds decompose by either hydrolysis or esterase that found naturally in the body. While the conventional elastomeric polyester such as PLLA, PGA and PCL go through bulk degradation mechanism during degradation, losing their geometry and integrity disastrously and changeably, some new ones such as PGS and trimethylene carbonate (TMC) undergo degradation by surface erosion. This implies that they preserve their geometry and integrity during decomposition as the degradation procedures happen just at the surface of the embedded material, and mass loss and dimensional reduction are corresponding to the water-accessible surface area. Biodegradable polyester elastomers are strong therapeutic myocardial patch candidates as they have the ability to endure the periodic mechanical strain of the contractile heart, provide mechanical constraint to the fibrous non-contractile scar tissue, and deliver cardiac cells contributing to regenerate the myocardial infarct [40].

One of the major promising elastomeric polyesters is Poly (glycerol sebacate) or (PGS) which represents the next generation of the biomaterials used as myocardial patches. PGS is inexpensive, non-toxic and biocompatible. The monomers of PGS are glycerol, which is a sugar alcohol containing multiple hydroxyl groups, and sebacic acid, which is a dicarboxylic acid. These monomers bind together by ester bonds which is hydrolysable (figure 12). This means that PGS is catalyzed in vivo by the process of hydrolysis in which biological enzymes play the catalysis part [38]. Glycerol and sebacic acid are human endogenous metabolites which can be found naturally in human metabolism; therefore, the in vivo degradation of PGS bares no

risks to the human body. What also makes PGS preferable for tissue engineering applications is that no solvents, catalysts or added substances are required during its preparation. Moreover, its mechanical properties can be tailored according to the specific application by tuning the polycondensation of glycerol and sebacic acid and/or curing parameters. In particular, different curing temperature and time conditions give different crosslinking density which can be adjusted to give a Young's modulus that is compatible with that of soft tissues. In addition to the proper Young's modulus, PGS possesses a high tensile strain that makes it withstand the heart contraction cycles [40].

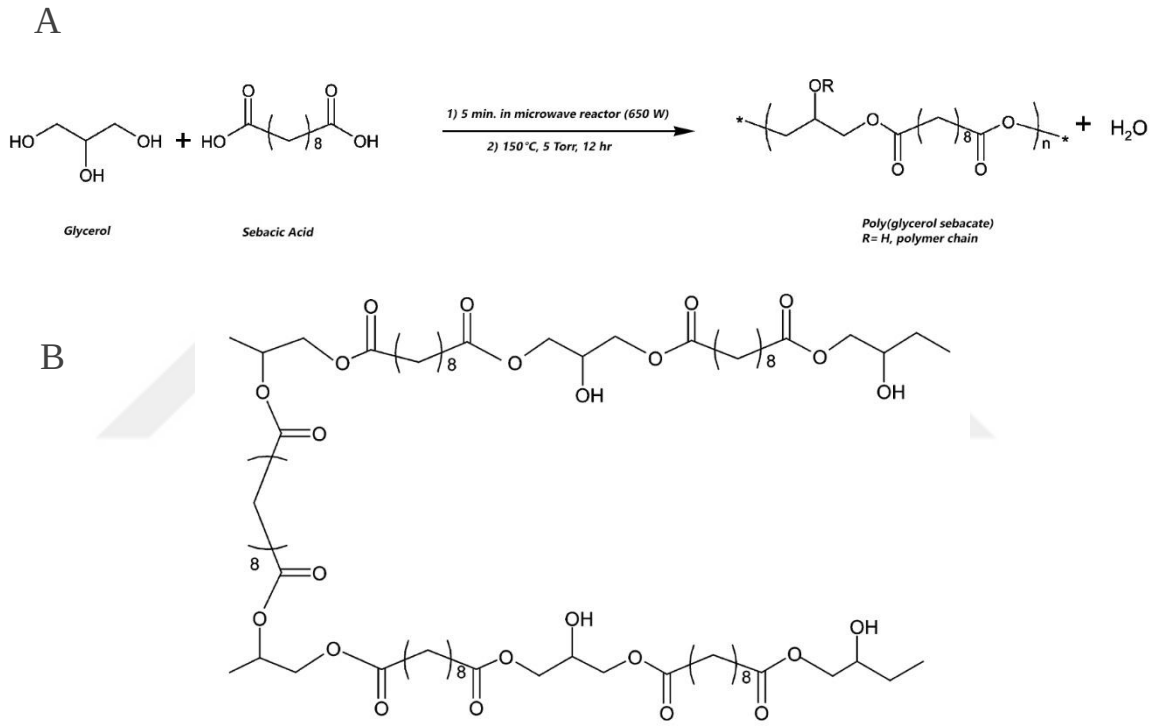

Figure 1.12. (A) reaction scheme of PGS condensation. PGS is synthesized through two steps: 1- Prepolymerization which is a polycondensation of Glycerol and sebacic acid. 2- Crosslinking reaction. (B) Crosslinking scheme for two PGS polymer chains [177].

Unlike polyester-based thermosetting polymers which show a plastic deformation when they undergo a cyclic strain, PGS shows a unique elastic property thanks to the covalent crosslinking between the polymer network and hydrogen bonds between its polymer chains. The PGS degradation mechanism is another cause behind its popularity as a good tissue engineering matrix. As mentioned earlier, PGS

degrades in vivo through surface erosion which allows the matrix to maintain its mechanical strength and shape. The process of degradation takes place slowly (can be months or even years) in which the PGS mechanical strength drops significantly before the mass loss. This slow degradation is preferable as it matches the recovery rate of the damaged area [40].

1.3.5.2.2.1. Electroactive Biomaterials

Another major determinant in building a cardiac construct for heart repair is the electrical conductivity which is an important property of the heart [178]. The cardiac conduction system is a key factor in allowing a simultaneous contraction of cardiomyocytes within the myocardium which is vital for the heart to pump the blood harmoniously from the atria to the ventricles before pumping it to the other organs of the body [40].

In the context of characteristics biomaterials should have, biomaterials for MTE must be electroactive, that is, they are able to transmit electrical stimulus throughout their geometry so as not to contribute to the irregular beating of the cardiac muscle and hence not to provide space for arrhythmia and other conditions to be developed [179]. Furthermore, an ideal electroactive matrix should enhance the transplanted cells attachment and their biological performance (like coordinated beating for cardiomyocytes or differentiation mechanism for stem cells) in an efficient way. Additionally, electrically conductive scaffolds not only promote cardiomyocyte-specific marker expressions, such as cTnT/cTnI and connexin 43, resulting in better cardiac cell functions, but also stimulate spontaneous simultaneous pulsation of the engineered tissue [178].

Since conventional polymeric biomaterials like PGS are not electroactive matrices, conductive stuff or fillers include carbon-based materials like graphene [180] carbon nanotubes (CNTs) [78-80, 83, 181], carbon nanofibers (CNFs) [81, 182-184], carbon nanohorns (CNHs) [84] and gold nanoparticles [185] were incorporated to those polymeric biomaterials with a view to come up with electrically active matrices that can beat synchronically with the native myocardium. Nevertheless, there is as yet a limitation associated with the use of conductive biomaterials in order to appropriately match the host cardiac tissue. In addition, the potential toxicity effects and high costs of the above-mentioned fillers remain drawbacks.

2. MATERIALS AND METHODS

2.1. Preparation of Carbon Aerogel-embedded PGS Cardiac Patch

Figure 13 illustrates the fabrication process of Carbon Aerogel-embedded PGS (CA-PGS) cardiac patch. Typically, CA-PGS composites were synthesized by a three-step process, namely, Carbon Aerogel synthesis, PGS synthesis, and the composite synthesis.

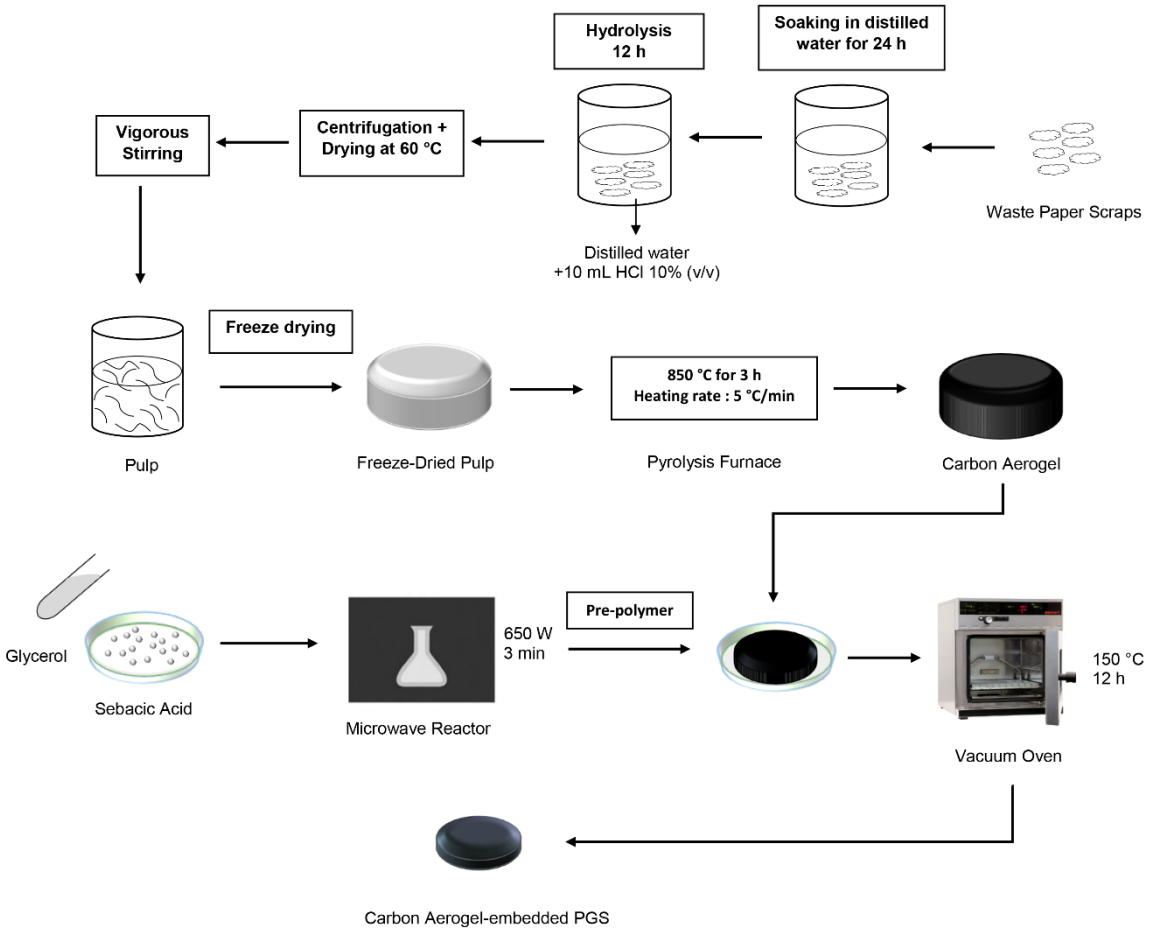

Figure 2.1. Preparation steps of Carbon Aerogel-embedded PGS cardiac patch.

2.1.1. Carbon Aerogel Synthesis

The Carbon Aerogels were obtained as previously described with a slight variation [186]. Briefly, 240 mg of waste office paper scraps were soaked in distilled water for 24 h. For hydrolysis, 40 ml of HCl (10% v/v) was added to the paper-water mixture

and kept for 12 h. Afterwards, paper scraps were completely purified from chloride ions by undergoing centrifugation with distilled water for several times and subsequently dried in an oven at 60 °C for 24 h. After that, 80 ml of distilled water was added to the paper scraps and the mixture was subjected to magnetic stirring followed by vigorous stirring until a paper pulp of cellulose strands was obtained. Freeze-drying was carried out for the pulp for 2 days at -80 °C under vacuum with a Labconoco Freezone 6 Plus freeze dryer system (USA) after pre-freezing the sample at -80 °C for 24 h. The freeze-dried pulp (pulp aerogel) was then carbonized at 850 °C for 3 h under vacuum and argon atmosphere with a heating rate of 5 °C/min to give the waste paper-derived lightweight Carbon Aerogel.

2.1.2. PGS synthesis

Pure PGS films and PGS pre-polymer solutions were produced based on microwave-assisted approach [187]. Briefly, PGS synthesis involves a two-step process: poly-condensation/esterification of monomers and thermal crosslinking reaction. For the esterification step, equimolar ratios of glycerol and sebacic acid were prepared and reacted in the microwave at 650 W for 5 min. Every minute of esterification duration was separated by an interval of 10 seconds in order to allow the removal of the water vapor. At the end of this step, PGS pre-polymer solution was attained. To obtain the elastomeric pure PGS films, the pre-polymer solution was thermally cured under vacuum at 150 °C for 8 h.

2.1.3. CA-PGS Composite Synthesis

In order to obtain the CA-PGS composite, following PGS pre-polymerization step, the Carbon Aerogel was immersed in the pre-polymer solution and the combination is put in the vacuum oven to be thermally cured under vacuum at 150 °C for 12 h. The composites were named as CA-PGS system.

2.2. Characterization of Carbon Aerogel-embedded PGS Cardiac Patch

2.2.1. Scanning Electron Microscopy (SEM) Characterization

The surface morphologies of pure PGS, Carbon Aerogel, and CA-PGS composite were studied under a scanning electron microscope (QUANTA 400F Field Emission SEM, Thermo Fisher Scientific, USA). Before the examination, all the samples were mounted on a metal stubs and sputter-coated with a thin layer of Au-Pd alloy under vacuum. The samples were then examined at an acceleration voltage of 30 kV to

acquire high-resolution images for the surface of the specimens at 500x and 1000x magnification. The fiber and pore diameter were measured by utilizing the image analysis of the obtained SEM images of CA using ImageJ software (NIH, Bethesda, MD).

2.2.2. Fourier Transform Infrared (FTIR) Spectroscopy

The chemical and structural investigation of pulp aerogel, pure PGS, Carbon Aerogel, and CA-PGS composite was carried out using Fourier Transform Infrared (FTIR) spectroscopic analysis on Nicolet is50 spectrometer (Thermo Fisher, Germany). FTIR spectral images of pulp aerogel, pure PGS, Carbon Aerogel, and Carbon Aerogel-PGS composite were recorded and collected in the mid infrared region (4000-650 cm^{-1} wavenumber range) with a resolution of 0.5 cm^{-1}. The vibrational spectra were gathered by touching the FTIR objective on the samples and recording the spectra generated from the samples.

2.2.3. X-ray Diffraction (XRD)

The phase formation of Carbon Aerogel, pure PGS and CA-PGS composite were further studied by X-ray diffraction (XRD) technique. X-ray diffraction patterns for the samples of interests were collected using an x-ray diffraction instrument (Rigaku Ultima-IV, Japan) with graphite-monochromated Cu-Kα Radiation (λ =1.5406 Å) at 40 kV and 30 mA. The scattering ranges were from 5° to 75° in the step of 2θ = 0.02°.

2.2.4. Contact Angle Measurements

The surface hydrophobicity of pulp aerogel, pure PGS, Carbon Aerogel, and CA-PGS composite was determined by evaluating contact angles of water droplets on the surface of the samples. In particular, using Attension® Theta contact angle instrument (Biolin Scientific, Sweden), a droplet of sessile water (nearly 3 µL) was placed onto the surface of each substrate of interests. By collecting optical images, the water-in-air contact angle between the substrate surface and the droplet was calculated using the image processing software of the instrument. The test was repeated for at least three times for each group, and the data was shown as mean ± standard deviation. Differences between means were assessed by running one-way ANOVA analysis followed by Turkey's multiple comparison using GraphPad Prism software (V 7.00). A P-*value* of <0.0001 was considered significant.

2.2.5. Mechanical Properties Characterization

For the analysis of mechanical properties, pure PGS films and CA-PGS composites were cut into cylindrical pieces with a diameter and a thickness of 10 mm and 4 mm, respectively. Their mechanical properties were measured using compression test method on tabletop compression tester (Univert Mechanical Test System, Cell Scale, Canada) with a load of 50 N. The test was carried out in room temperature with a strain rate of 5 mm min^{-1}. The stress-strain curves were obtained, and from which Young's modulus, ultimate compressive strength, and maximum strain were extracted. The linear section of the initial slope of the stress-strain curve was deployed to calculate the elastic modulus. The test was conducted four times for each group, and the results were demonstrated as mean values ± standard deviation (S.D.).

2.2.6. Electrical Conductivity Measurements

In order to evaluate the electrical properties of our CA-PGS system, Four-point probe technique (Keithley 2450 Sourcemeter, USA) was utilized. In this method, the electrical conductivity for the samples is measured using four electrodes instead of two to eliminate the effect of probe resistance which makes the results more accurate. The outer pair of electrodes are used to conduct the electrical current across the samples while the other pair of electrodes was used to measure the voltage drop across the equipment.

Using the values of voltage, current, and thickness of the sample, the electrical resistivity could be obtained according to the following equation,

$$\rho = \left(\frac{V}{I}\right)\left(\frac{A}{\mathrm{d}}\right) \qquad \text{…. Eq. (2.1)}$$

Where ρ is the electrical resistivity of the sample, V is the voltage across the inner pair of probes, I is the current transmitting through the sample, A is the area of the cross section of the sample, and d is the distance between the inner pair of the setup.

The electrical conductivity could then be calculated according to the following formula,

$$\sigma = 1/\rho \qquad \text{…. Eq. (2.2)}$$

Where σ is the electrical conductivity.

The measurements were carried out in room temperature, and the conductivity value for each group was averaged over four measurements of electrical conductivity. The data was shown as mean ± S.D.

2.3. *In Vitro* Studies

2.3.1. *In Vitro* Cytotoxicity Assessment of the Carbon Aerogel Embedded-PGS Cardiac Patch

MTT (3-(4,5-dimethylthiazol-2-yl)-2,5-diphenyltetrazolium Bromide) assay was utilized to evaluate the possible cytotoxic effect of the CA-PGS composite on mouse fibroblast cells.

MTT assay is a colorimetric assay used to assess cell cytotoxicity. The rationale of this assay is that the cellular tetrazolium reduction is proportional to the cell viability rate. At cellular level, the water-soluble tetrazolium compound, which is a yellow dye, is reduced by metabolically active cells to purple formazan precipitates which are insoluble in water. This process takes place in the mitochondria of viable, but not dead cells, where dehydrogenase enzymes take over the reduction reaction. If the formazan crystals are solubilized by a suitable detergent, the optical intensity of the crystals can be measured by spectrophotometric means allowing the number of living cells within the culture to be quantified.

In this study, the assay was carried out by performing an indirect cell culture test using L929 mouse fibroblast cell line (Passage 45) (NCTC clone 929, ATTC, USA) according to the standard cytotoxicity assessment (ISO 10993-5) set by International Organization for Standardization. For this purpose, 4 gr of CA-PGS composite was sterilized by 70% (v/v) ethanol for 3h. After several washing processes with phosphate-buffered saline (PBS), the composite was soaked in 8 mL Dulbecco's modified eagle medium-high glucose (DMEM, Sigma-Aldrich, USA) and incubated at 37 °C and 5% CO_2 for 24 h to prepare the extraction medium. The extract was prepared according to ISO10993- 12:2007; i.e. 200 mg of sample per

1mL of DMEM. Subsequently, the extract was supplemented with 10% (v/v) fetal bovine serum (FBS, HI-12A, Capricorn, Germany), 1% (v/v) L-glutamin (Lonza, USA) and 1% (v/v) penicillin and streptomycin (Gibco, Thermo Fisher Scientific, USA).

In parallel, L929 cells were cultured into a 24-well tissue culture plate at a density of 20-25x10^3 cells per well. The cells were additionally cultured in complete growth medium composed of DMEM with high glucose, 10% fetal bovine serum, 1% L-glutamin and 1% penicillin and streptomycin (v/v) for 24h in an incubator under 5% CO_2 at 37 °C. At the end of the incubation period, the culture medium was removed from the wells and the cells were exposed to various concentrations of the extraction medium (100%, 50% and %25 (v/v)) in order to observe a dose-dependent change for 24 hours. At this point, a complete medium was used as the positive control. At the end of the incubation period, both culture medium and the extraction medium was discarded from the wells and 600 µL plain DMEM high glucose containing 60 µL MTT (Sigma Aldrich, USA) solution (5mg/mL in PBS) was added instead. The culture plate covered with aluminium foil was kept in the incubator set to 37 °C with 5% CO_2 for 3 h allowing the tetrazolium to be reduced to Formazan by live cells. For dissolving the Formazan crystals, the MTT solution was finally replaced by 600 µL DMSO. In order to measure the optical density of the cultured cells, the contents of each well were transferred to a new 96-well plate as 3 parallel and were read at 570 nm by using a spectrophotometer (Epoch BioTek, USA). To calculate the percentage of viable cells in each well, the following equation was used:

$$\text{Cell viability (\%)} = (OD_{sample} / OD_{control}) \times 100 \quad \text{…. Eq. (2.3)}$$

For each group, three replicates were tested and the results were expressed in mean ± standard deviation (S.D). Differences between means were assessed by running a one-way ANOVA analysis followed by Turkey's multiple comparisons using GraphPad Prism software (V 7.00). A P-*value* of <0.05 was considered significant.

2.3.2. H9C2 Cell Culture and Maintenance

H9C2 rat cardiac myoblast cells were obtained from the European Collection of Cell Cultures (ECAAC, Germany) and were expanded in Dulbecco's Modified Eagle's

Medium-high glucose (DMEM, Sigma-Aldrich, USA) supplemented with 10% (v/v) fetal bovine serum (FBS, HI-12A, Capricorn, Germany), 2 mM L-Glutamine (Lonza, USA) and 1% (v/v) antibiotic-antimycotic (Gibco, Thermo Fisher Scientific, USA). Cells were cultured till they reach %70-80 confluency in an incubator set to 37 °C, 95% humidity and 5% CO_2. Upon reaching the confluency they were split in a 1:4 ratios. The cells already passage 7 were used in this study.

2.3.3. Cell Seeding to Carbon Aerogel Embedded PGS Cardiac Patches

In order to evaluate the *in vitro* performance of the resulting materials, they were shaped in a cylindrical form which has 10 mm diameter and 4 mm thickness. The materials were first sterilized with 70% (v/v) ethanol for 2 hours and then washed 3 times with sterile phosphate-buffered saline (PBS) to remove ethanol completely. $5x10^5$ H9C2 cells suspended in 25 µL medium were inoculated to each tissue scaffold and they were incubated for 4 hours to allow the cells to attach the material surface. Subsequently, 2.5 mL of the culture medium was added to cover the cell seeded scaffolds and the materials continued to be cultured in a 24-well culture plate.

2.3.4. Cell Viability on the Material Surface

The cell viability on the materials was tested by AlamarBlue analysis (Thermo Fisher Scientific, USA) on the 1st, 4th, 7th and 10th day of the culture. Briefly, the culture medium was changed with the equivalent volume of the test solution consisting of a combination of culture medium and up to 10% (v/v) AlamarBlue solution on the analysis day (n=3). Then, the culture plates were covered with aluminum foil and placed in the incubator used for the cell culture for 3 hours. At the end of the incubation period, 200 µL of the test solution was exemplified to a 96 well-plate as 5 parallel and was read at 570/600 nm by using a microplate reader (BioTek, UK). The equal amount of cells was seeded to TCPS (n=3) and was used as a control group. For each group, three replicates were tested and results were expressed in mean ± standard deviation (S.D). Differences between means were assessed by running a two-way ANOVA analysis followed by Sidak's multiple comparisons using GraphPad Prism software (V 7.00). A P-value of <0.05 was considered significant.

2.3.5. Cell-Material Interactions Analysis

The cell attachment and cell behavior on the material surface were examined by using SEM (Supra 50VP, Germany). For these purposes, cell seeded materials were fixed with 4% (v/v) paraformaldehyde (Sigma Aldrich, Germany) on the 1st, 4th and 7th day of the culture. Following the materials were exposed to increasing alcohol series. Lastly, Hexamethyldisilazane (Sigma Aldrich, Germany) was used to dry the samples. The materials were coated with gold-palladium alloy before imaging and all images were obtained under the same magnifications.

3. RESULTS AND DISCUSSION

3.1. CA-PGS Cardiac Patch Preparation

The adult left ventricle is evaluated to contain a sum of 5 billion cardiomyocytes. After the ischemic event, the left ventricle experiences a loss of about one billion cardiomyocytes [59]. Basically, the heart muscle lacks the regeneration ability [43] as adult cardiomyocytes are unable to renew themselves [58]; therefore, the injured muscle cannot be regenerated after an ischemic event. Instead, a formation of a scar tissue occurs to replace the diseased cardiac muscle. Since the latter lack the elasticity, it ends up extended over time owing to the pressure of the ventricle [40]. Accordingly, the loss of cardiomyocytes after the heart attack and their replacement by a fibrous tissue finally results in congestive heart failure [43].

Myocardial Tissue Engineering holds the future of the cardiac repair after MI event. One of the MTE strategies is the cardiac patch approach. In this strategy, the cardiac patch aims at regenerating an infarcted heart by delivering healthy cardiomyocytes to the affected region while providing a mechanical support to the left ventricle [188]. There are specific properties a biomaterial must possess in order to be a suitable cardiac patch candidate. Such properties include suitable flexibility; so that it can withstand the cyclic contraction of the cardiac muscle, and a convenient electrical conductivity; that would not hinder the propagation of action potentials. However, an ideal cardiac patch is yet to be developed. To date, various elastomer-filler composite biomaterials have been developed to this end.

Generally speaking, synthetic elastomeric polymers have attracted a considerable amount of attention in MTE due to their flexibility, biocompatibility and biodegradability. Among such elastomers; PGS, which is a commonly used nonconducting polymer, has become a prime focus of research owing to its biocompatibility, soft and flexible mechanical properties, low-cost, and superior physical properties [163]. The potential of using PGS in mechanically dynamic environments such as the cardiac muscle has already shown [57, 166, 189], thanks to its natural pliability that makes it withstand deformation and hence enables it to restore its original shape upon being subjected to the deformation [188]. Importantly, PGS follows surface erosion degradation mechanism which is a linear mass

decomposition pattern so that the construct preserves its geometry and mechanical strength while keeps its surface intact [190]. Such characteristics make PGS a convenient substrate as a cell carrier and a mechanical support device in MTE.

On the other side, waste paper accounts for the major part of organic wastes and is recognized as the main municipal waste [191]. Since the demand for finding applications for the waste paper waste increases, the present work paves the ways for a novel and an unexpected application for the waste paper as it was used in this study as the carbon source for the Carbon Aerogel which served as a carbon filler. Waste paper is mainly composed of organic matter like cellulose, hemicellulose and lignin making it a perfect carbon source [192]. In the context of tissue engineering, carbon materials have gained an increasing interest as additives to enhance the mechanical and/or the electrical properties of the developed biomaterials for various subareas such as cardiac, nerve, and bone tissue engineering. However, the so far investigated carbon fillers are restricted to laboratory-scaled production due to their precursors' high cost and complex equipment that is involved in their synthesis process which finally limits their production on a large scale. To the best of our knowledge, this is the first work on incorporating the Carbon Aerogel into elastomeric matrices to serve as a reinforcement component which might be considered as the cheapest alternative among all reported carbon-derived fillers. Relative to other carbon-based fillers, the fabrication of Carbon Aerogel from waste biomass, which is a cheap and abundant resource, is the most practical approach with many advantages like low-cost, high-yield and less pollution to the environment while the manufacturing of CA neither necessitates complex equipment nor takes place under radical conditions.

As PGS and CA have complementary properties, combining these two constituents to form a cardiac construct for cardiac tissue regeneration would be an ideal framework. In the present study, an elastic and electrically conductive CA-PGS cardiac patch system was synthesized by curing PGS entrapped within Carbon Aerogel in which the latter functioned as a filler and a skeleton for the construct. Following the PGS pre-polymerization step and the Carbon Aerogel immersing to the pre-polymer solution, it was observed that the former rapidly impregnated into

the porous network of the aerogel replacing the entrapped air within the aerogel thanks to the high oil absorption capacity of the aerogel.

It is envisioned that the developed cardiac patch would be the most cost-effective cardiac patch which makes it a practical biomaterial that can be produced on a massive scale which would bring the cardiac patch strategy from the laboratory into the market.

To confirm how well the carbon fibers were distributed within the PGS, a thin slice of the composite was cut and its cross-section was studied under the light microscope as shown in Figure 14. The optical image of the cross-section clearly demonstrates a branched distribution and a random orientation of the carbon microbelts within the polymeric matrix. It is expected that this branched and random orientation of the carbon microbelts would result in a unique as well as a uniform mechanical performance for the construct.

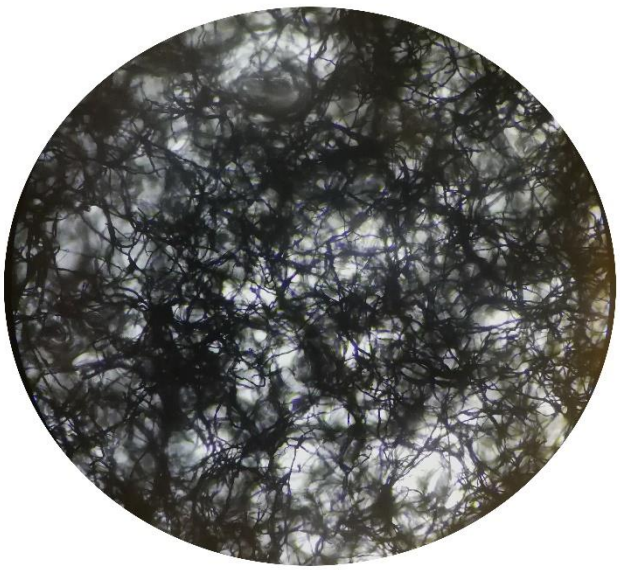

Figure 3.1. An optical image under the light microscope for a thin slice from the cross-section of CA-PGS composite.

The aggregation and the nonuniform dispersion of carbon fillers within the base polymers is a common issue that leads to a poor integration of the filler into the polymeric matrix and consequently impairs their contribution in enhancing the

mechanical and electrical properties of the construct in an effective manner. Additionally, the tendency of carbon fillers to aggregation results in heterogeneous properties [91] and decreased cell viability [181]. Although using harsh organic solvents and surfactants, such as Tetrahydrofuran (THF), Dimethylformamide (DMF), and 1,2-Dichlorobenzene (DCB), in synthesis of tissue-engineered constructs are not preferable for their potential toxicity for the cells, they are commonly used to prevent the carbon fillers aggregation within the polymeric matrix [91]. In the case of Carbon Aerogel, however, the aggregation problem was not evident as the aerogel forms a three-dimensional web-like structure that consists of uniformly and homogenously distributed microscale fibers.

3.2. Scanning Electron Microscopy (SEM) Characterization

The morphologies of CA, pure PGS sheet, and CA-PGS composite were visualized using scanning electron microscopy (SEM) as shown in Figure 15.

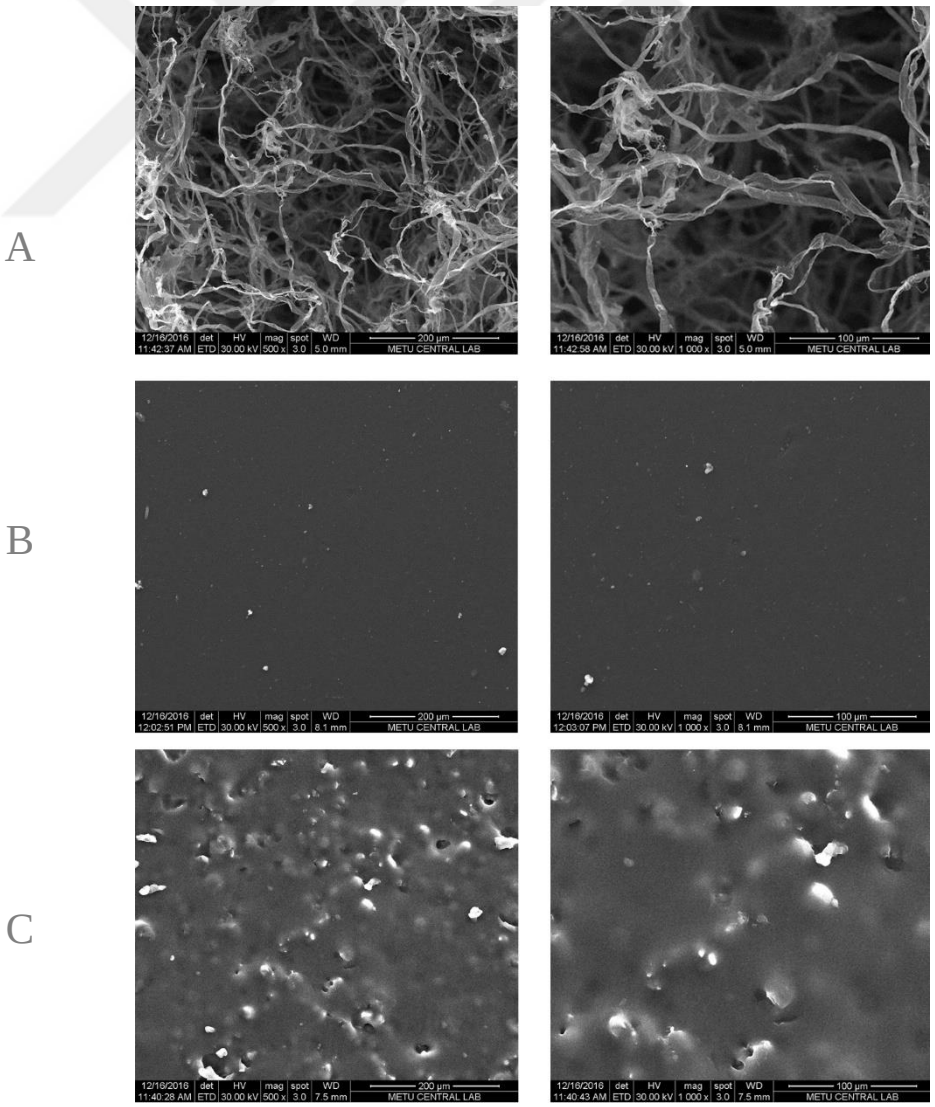

Figure 3.2. Scanning Electron Microscopy (SEM) images of (A) Carbon Aerogel, (B) pure PGS, and (C) CA-embedded PGS system.

Figure 15 (A) shows the structure of CA which is a highly porous, interconnected 3-D network. CA consists of randomly-oriented pure and solid carbon fibers with a diameter of 5.79 ± 1.86 μm which are curled and fused together at multiple junctions. The low-dense Carbon Aerogel resulted from its unique framework which consists of up to 99.98% air by volume [193].

Furthermore, SEM images in Figure 15 (B)-(C) revealed the alterations in the morphology of the pure PGS and the CA-PGS composite due to the CA incorporation into the PGS phase. While SEM images, Figure 15 (B), revealed that the pure PGS sheet presented smooth and dense surface, Figure 15 (C) clearly indicated that the composite has a rough surface with a random network of dots and interconnected macropores. The presence of macropores on the surface and within the construct was likely formed by glycerol vapor generated during the crosslinking step [194]. It is well known that the material biocompatibility and the cell adhesion and proliferation on a biomaterial are greatly correlated to the material topography (porosity and roughness) [195, 196]. Consequently, this rough, dotted and interconnected macropore-containing topography that the composite shows through the SEM images is anticipated to have a positive effect on the cell–biomaterial interaction [57].

3.3. Fourier Transform Infrared (FTIR) Spectroscopy

Chemical structure of prior-pyrolysis aerogel (pulp aerogel), Carbon Aerogel, pure PGS, and CA-PGS system were obtained by Fourier Transform Infrared Spectroscopy (FTIR) as shown in Figure 16.

FTIR absorbance spectra of the prior pyrolysis aerogel and Carbon Aerogel (i.e: after pyrolysis) were measured to assess the efficiency of pyrolysis process that has been carried out according to the aforementioned conditions. FTIR spectrum for the prior-pyrolysis pulp showed a pattern similar to those reported for cellulose-composed materials [197]. Unsurprisingly, there is a strong correlation between the

intensity of different peaks through the pulp spectrum and the presence of a high amount of oxygen and hydrogen elements intended to be subsequently eliminated through the pyrolysis process. The spectrum of pyrolyzed Carbon Aerogel, however, featured no absorption peaks, demonstrating that the pyrolysis conditions were optimized enough to achieve an efficient carbonization process and confirming the complete removal of oxygen and hydrogen contents. This result is in accord with the literature [186]. Therefore, given that the rise in the carbon content leads to a reduction in the intensity of oxygen and hydrogen-relative absorption peaks [198], the data shows that the obtained Carbon Aerogel has an increased amount of carbon content at the expense of oxygen and hydrogen elements. This is also evident in the CA-PGS composite spectrum where no peaks other than those denoted to the pure PGS were observed. Furthermore, the absence of any absorption peaks corresponding to hydrophilic functional groups such as -OH, C=O and C-O revealed that the obtained Carbon Aerogel is expected to have a super-hydrophobic property as discussed later on.

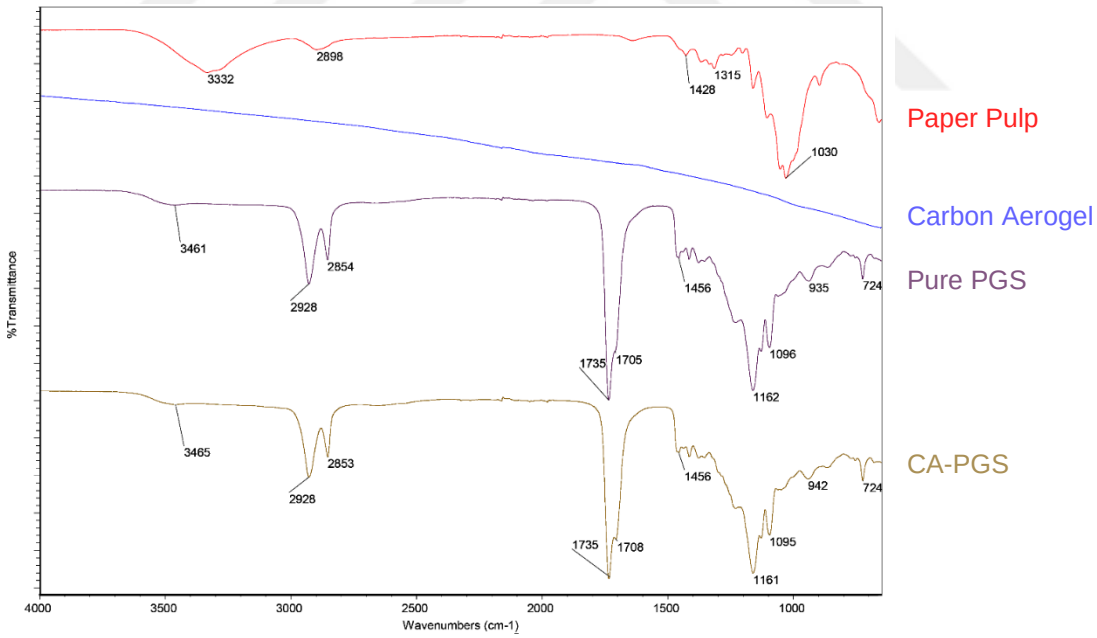

Figure 3.3. Fourier Transform Infrared (FTIR) spectral images of prior pyrolysis aerogel, Carbon Aerogel, pure PGS, and Carbon Aerogel-PGS composite.

The peak groups found in the FTIR spectrum of pure PGS were found to be in a convincing agreement with those in the well-known PGS pattern reported in the

literature [163, 187, 189, 199, 200]. In particular, the most intense absorption peak was observed at 1735 cm^{-1} which is attributed to C=O bond in ester groups [163, 187, 189, 199-201] confirming the efficiency of poly esterification using the quick microwave-assisted approach. Beside 1735 cm^{-1} absorption peak, the stretching mode of the C=O bond produced an absorption peak at 1705 cm^{-1} as well [201]. FTIR also exhibited a stretch of C-O found in ester groups as two main absorption bands at 1162 [199] and 1096 cm^{-1} where the former is broader and stronger [189, 200]. On the other hand, the absorption peaks at 2928, 2854, 1456 and 724 cm^{-1} are assigned to methylene groups (-CH2-) in the backbone of the PGS [189, 199, 202]. Specifically, the peaks at 2928 and 2854 cm^{-1} were due to asymmetric and symmetric C-H bonds stretching modes in methylene groups, respectively [202]. The absorption at 1456 cm^{-1} is, however, caused by methylene C-H bending while the characteristic absorption at 724 cm^{-1} occurs due to the C-H rocking of methylene groups as there are abundant of which in the backbone of the polymer [202].

Besides, absorption peaks at 935 cm^{-1} can be assigned to O-H stretching mode which we believe they might be, along with the absorption peak at 1705 cm^{-1}, indications of the degree of crosslinking within the construct. In particular, the reduced intensity of the peak at 1705 cm^{-1} compared to the intensity of that at 1735 cm^{-1}, which is relatively sharp herein, can be indicative of the increased density of cross-links [187]. Taking this along with the fact that there is a reduction in O-H bond-induced band at 3461 cm^{-1} due to hydroxyl groups (-OH) [189, 203], it might be argued that the carboxyl groups in sebacic acid further reacted with the hydroxyl groups in the backbone of the polymer resulting in further ester formation and significant degree of crosslinks within the pure PGS and the composite [204]. It is well known that the number of hydroxyl groups within the PGS is the determinant of the PGS hydrophilicity. Therefore, this result also indicates that the produced pure PGS and the composite are expected to be relatively hydrophobic as the curing time of 12 hours just leaves relatively few hydroxyl groups attached to the backbone of the polymer.

FTIR spectroscopy was also used to confirm the structure of the composite after Carbon Aerogel impregnating with PGS. As expected, the data revealed that the FTIR spectrum of CA-PGS composite was identical to that of pure PGS with slight

shifts in the absorption peaks at 3465, 2853, 1708, 1161, 1095 and 942 cm^{-1} assigned to O-H stretching, symmetric C-H stretching mode, C=O stretching mode, C-O stretching mode, and O-H bending mode, respectively. This congruence between the spectra of pure PGS and the CA-PGS composite signifies that having incorporated within the polyester structure, Carbon Aerogel added no additional function groups to the matrix.

3.4. X-ray Diffraction (XRD)

Figure 17 shows the XRD patterns of CA, pure PGS and CA-PGS composite. As it is clear from the figure, the CA diffraction pattern exhibits two broad diffraction peaks; the strongest attributes to (002) plane of graphite located at 2θ = 22.50° corresponding to a d-spacing of 3.79 Å, and the second is centered at 2θ = 43.76° due to (001) plane of graphene [205]. The broad and right-shifted d_{002} diffraction profile, compared with that of graphene (sharp peak at 2θ = 25.50°, d-spacing =3.4 Å), suggests that along with sp^2 sites and carbon-to-carbon π bonds which are responsible for the formation of graphitic structure, CA is also composed of many defects, folding structures, impurities and sp^1 and sp^3 hybridization structures [206], giving the CA an amorphous-like architecture with stacking aromatic layers that form crystalline units spread along the fibers of the aerogel. These graphitic crystallites are the components that give the aerogel its electrical conductivity nature. Overall, the CA's diffraction pattern is in accordance with the literature [207, 208].

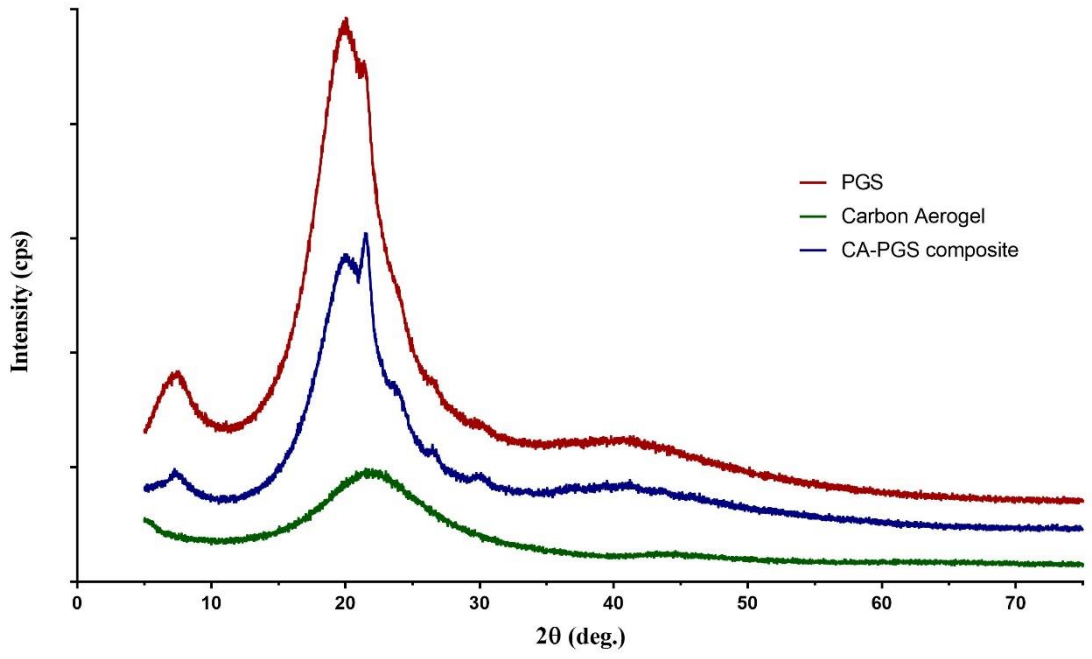

Figure 3.4 X-ray diffraction patterns for pure PGS, Carbon Aerogel, and CA-PGS composite.

Pure PGS presented a pattern with broad diffraction halos around 2θ = 20° confirming its amorphous phase in room temperature [57, 209, 210]. The composite demonstrated a pattern in which the CA's diffraction peaks were hidden owing to the presence of the intense Bragg peaks of the PGS.

3.5. Contact Angle Measurement

One of the major surface characterization methods is the contact angle measurement by which the degree of surface wettability is determined. Generally, surface wettability is correlated to the chemical and topographical patterning of the surface [211]. Concerning biomaterials especially cardiac patches, it is of predominant importance to characterize the surface properties of the cardiac patch as they dictate its potential success as a cardiac wall substitute. Having been transplanted in the affected area within the myocardium, a cardiac patch would interact with the surrounding environment through its surface [212]. In the present study, surface wettability of pure PGS, Carbon Aerogel, and CA-PGS composite were determined by utilizing water-in-air contact angle measurement as it is provided graphically in Figure 18.

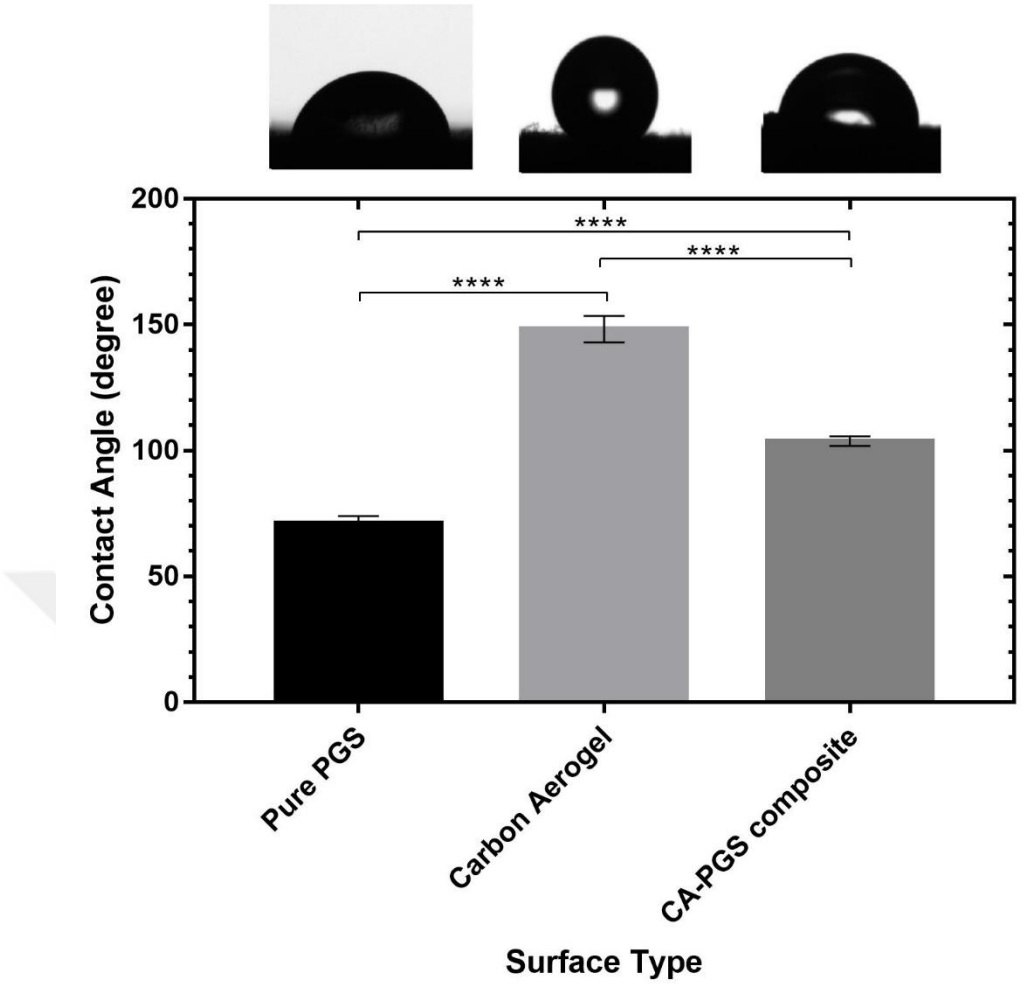

Figure 3.5. Water-in-air contact angles of pure PGS, Carbon Aerogel and CA-PGS composite. The data represented as mean ± standard deviation (****p< 0.0001, ANOVA with Tukey's multiple comparison test).

The water contact angle (WCA) of the pure PGS was observed to be 70.88° ± 3.15° which is similar to those of PGS previously reported in studies directed for soft tissue engineering; especially those directed for MTE. For example, Alpesh Patel et al. [213], Qi-Zhi Chen *et al.* [124], and Akhilesh K. Gaharwar *et al.* [214] reported pure PGS contact angles of 77.5°, 75° and 69.78°, respectively. The PGS surface hydrophilicity is greatly correlated to the number of hydroxyl groups on the backbone of the polymer. As a result, the relatively high crosslinking density, as it is the case in this study, leaves a limited number of hydroxyl groups on the backbone of the polymer which explains this value of WCA. However, even higher WCA values have already been reported for PGS directed for myocardial tissue applications. For instance, Taimoor H. Qazi *et al.* reported a PGS contact angle of 86° [189]. Even

though this high crosslinking density does not leave abundant hydroxyl groups attached to the PGS backbone, it turned out that this density is the ideal condition for synthesizing our CA-PGS system with desired mechanical properties suitable for myocardial tissue applications.

On the other hand, the water-in-air contact angle of Carbon Aerogel was observed to be 148.20° ± 5.27° which is considered super-hydrophobic. This super-hydrophobicity of the Carbon Aerogel resulted from the disappearance of any hydrophilic functional groups such as -OH, C=O and C-O after pyrolysis, as previously indicated by the FTIR measurement of Carbon Aerogel, with almost pure carbon contents that are naturally hydrophobic. The best advantage of this hydrophobicity was evident during the incorporation of Carbon Aerogel into PGS prepolymer. Generally speaking, the irregular dispersion of the other carbon fillers like carbon nanotubes (CNTs) within the polymeric construct is a common reported limitation in the literature owing to the strong π-π stacking interaction between CNTs that lowers the effective mechanical, chemical and biological reinforcing potential of such fillers once they are embedded into the polymeric matrices [214]. In the present experiments, however, such a problem disappeared and rather the super-hydrophobicity and lipophilicity of the Carbon Aerogel allow it to be impregnated with the prepolymer in an instant and effective way achieving a complete integration between the two components and forming a 3D compact construct with unique mechanical and electrical characteristics suitable for cardiac patching applications.

It is seen from the figure that the WCA for CA-PGS composite was 103.8° ± 1.93° which is regarded as relatively hydrophobic. This implies that the surface structure was altered upon the incorporation of CA, which is extremely hydrophobic, into the PGS matrix. This relative hydrophobicity of the composite might be preferable as part of the literature suggest that hydrophobic surfaces promote cell attachment and structural development of cardiomyocytes [159].

Generally speaking, the surface wettability is correlated to the adsorption of the adhesion proteins which in turn guides the cell adhesion [212]. In particular, as the first in vivo interaction following a biomaterial transplantation, cell adhesion-mediating proteins adsorb onto the biomaterial surface [212]. In the myocardium context, the proteins of interests are those that mediate the adhesion of

cardiomyocytes like laminin, fibronectin, and vitronectin [215]. Subsequently, cells bind to the surface-adsorbed adhesion proteins through their attachment receptors that exist within their membranes, anchoring themselves into the surface of the biomaterials [216].

Interestingly, hydrophobic surfaces were found to promote cell attachment. For instance, Silvestri *et al.* reported an elastomeric porous poly (ε-caprolactone) (PCL)-based polyurethane cardiac patch with a hydrophobic nature (137° contact angle). This construct was reported to support the viability and proliferation of cardiomyoblasts [217]. In a different research, Asiri *et al.* have demonstrated that the adsorption of laminin, fibronectin and vitronectin was promoted in CNFs-embedded hydrophobic surfaces which would necessarily lead to enhancing cardiomyocytes adhesion [215]. In another study, Bagdadi *et al.* reported fabrication of poly (3-hydroxyoctanoate) directed for cardiac tissue engineering applications. The construct was found to be hydrophobic and the cardiomyocyte responses, such as cell adhesion, viability and proliferation, were shown to be effectively achieved upon seeding the cells on the surface of the construct [216]. Also, magnetic nanoparticles-containing PLA films with a contact angle of 100° were found to promote the attachment and proliferation of cardiac-like rat myoblast (H9C2) cells [196]. In different work, Adipose-tissue derived stem cells and L929 mouse fibroblasts showed excellent adhesion and proliferation on poly (ethyl acrylate)-poly (ε-caprolactone) cardiac patches [218]. Taken together, embedding Carbon Aerogel within the PGS matrix is envisioned to promote cardiomyocyte attachment and proliferation behavior owing to its relative hydrophobic property.

In contrast to these findings, rat neonatal cardiomyocytes were shown that they do not attach well on Polyurethane films, which are hydrophobic, while they showed better attachment upon increasing their wettability by pre-coating the films with laminin [169]. In another study, Khang *et al.* have shown that hydrophilic surfaces promote the adsorption of fibronectin [219]. Some other studies reported that the maximal cell adhesion and proliferation occurs on moderate wettable surfaces and the extreme hydrophobic and hydrophilic surfaces do not support cell adhesion behavior [220]. For example, Arima and Iwata reported that the maximal cell

adhesion and proliferation occurs on relative hydrophilic surfaces with contact angles between 40° and 70° [221].

Taken aforementioned findings collectively, the adsorption of cell-adhesion proteins and consequently cell attachment appear to be too complex processes to only be guided by surface wettability. Alongside surface wettability, multiple factors are involved in regulating these processes. Such factors include cell type, surface topography, surface roughness, and surface energy [222]. Overall, the adsorption of cell-adhesion proteins and cell attachment on biomaterial surfaces are processes that are yet to be fully understood [196]. In any cases, CA-PGS surface can become more wettable, if needed, by exposing the composite to a serum-containing culture medium [169]. As such, serum proteins would instantly adsorb onto the hydrophobic surfaces driven by entropic forces [220]. This means that the cells can subsequently approach and attach to the biomaterial surface [223].

3.6. Mechanical Properties Characterization

The evaluation of mechanical and elastomeric properties is extremely essential for determining the possibility of deploying a culture substrate as a cardiac patch. The biomaterial that exhibits mechanical properties compatible with those of the native myocardium has a great potential to serve as a heart patch.

To identify the elastomeric properties of our CA-PGS system, a compression testing was conducted for both the pure PGS and CA-PGS system. The obtained stress-strain curve, compressive Young's modulus, ultimate compressive strength, and ultimate compressive strain are illustrated in Figure 19. The CA-PGS system displayed a compressive Young's modulus of 0.366 ± 0.080 MPa compared to that of the pure PGS which was observed to be 0.912 ± 0.220 MPa (Figure 19 B). The ultimate compressive strength and the ultimate compressive strain of CA-PGS system were measured to be 0.566 ± 0.150 MPa and 56.83 ± 11.67 % while those for the pure PGS were 0.792 ± 0.142 MPa and 39.38 ± 8.61 %, respectively (Figure 19 C and D).

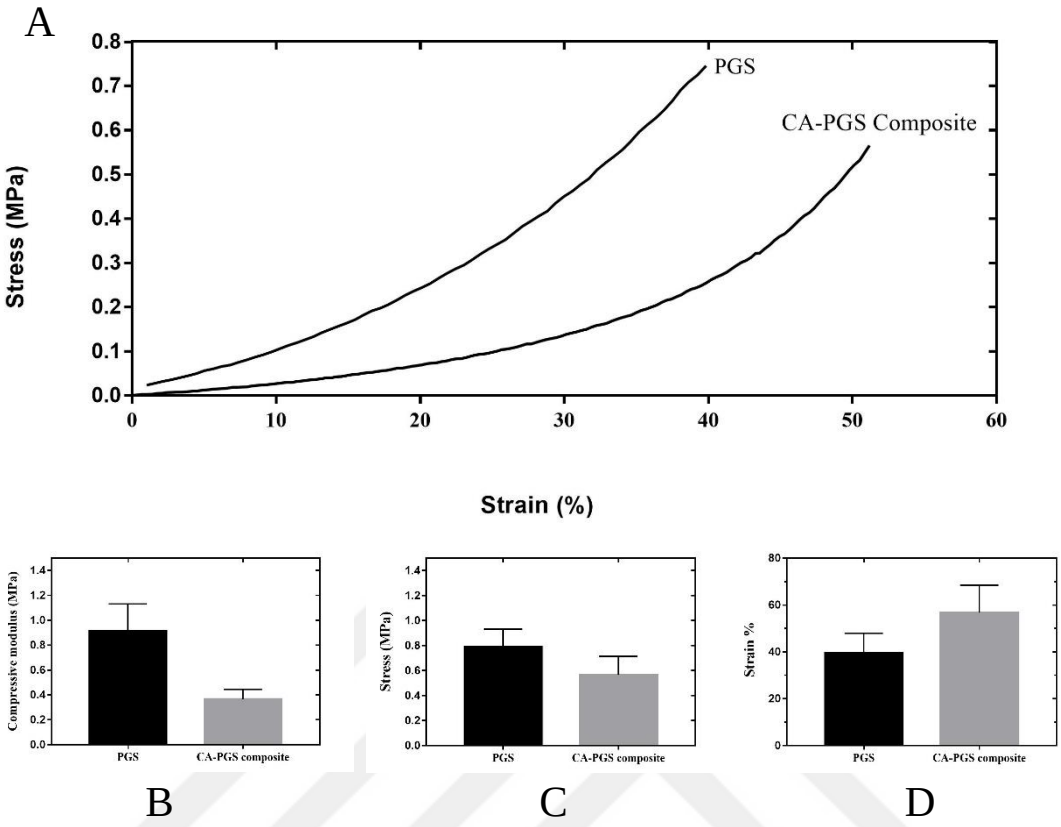

Figure 3.6. (A) Representative stress-strain curves of pure PGS and CA-PGS system acquired by compression testing, (B) Compressive Young's modulus, (C) Compressive strength, (D) Ultimate compressive strain. Data are shown as mean ± S.D.

The results of the compression testing revealed that the addition of carbon microbelt networks to the PGS matrix markedly altered its mechanical properties. In particular, the elasticity and the ultimate strain characteristics were enhanced for our developed system compared to those of the pure PGS, which make CA-PGS system super-elastic with improved deformation behavior and thus more suitable for cardiac patching applications. These enhanced mechanical properties (i.e. the elasticity and deformability) reflect the strong and unique physical interaction between the carbon microbelts of CA and PGS polymer. This synergy between CA and PGS is likely to be the underlying machinery behind the enhanced elasticity and deformability of the system where the carbon microbelt networks embedded within the polymer serve as a mechanical reinforcement component. Another probable cause for the improved mechanical characteristics in our system is the existence of

random macropores among the substrates that were formed during the synthesis procedures.

As a bulk, embedding additives (such as CNTs [91, 214], PANI [189], ethyl cellulose [224], and Graphene [225]) into an elastomer results in a decrease in the deformability as well as a decrease in the pliability of that elastomer that would shift the mechanical values away from those reported for the native cardiac tissue. In our system, however, incorporating carbon microbelts into the polymeric matrix was shown to reduce the Young's modulus (the stiffness) and improve the deformation behavior of the developed substrate giving the composite much more flexibility and deformability which can be recognized as a super advantage of carbon microbelt networks over the other traditional additives.

The strain of the human heart was reported to be 15-22% at the diastole [57], and its compressive modulus was evaluated to be 0.425 MPa at the systole [226]. The end-diastolic Young's modulus of the human cardiac tissue was estimated to range from 0.2 to 0.5 MPa [227]. An ideal cardiac patch must be pliable, possessing as same mechanical properties as those reported for the native myocardium such that it would imitate the mechanical behavior of the native one, would not impair the contractile activity of the heart and new-forming tissue, and would not fail under the continuous cardiac beating cycles [217, 228, 229]. Equally importantly, the scaffold pliability provides the cardiomyocytes with a suitable micromilieu for their contraction activities [79]. Moreover, the elastic scaffold fosters the attachment of the adjacent cardiac cells facilitating the formation of the new tissue [174]. In the present study, the mechanical results showed that the developed CA-PGS system better mimics the mechanical properties of the native myocardium which is consistent with other developed composites reported in the literature. For example, Kharaziha and co-workers developed a hybrid scaffold of PGS, gelatin and CNTs which was tough and elastic at the same time. Specifically, an addition of 1.5 wt.% CNTs was shown to enhance the toughness and pliability of the developed scaffold with a Young's modulus close to that of the human native myocardium [79].

By contrast, rigid culture substrates (their Young's modulus > 0.8 MPa) not only would fail during the contraction of the heart but also they would result in diastolic dysfunction if they were deployed as heart patches [57, 164]. Furthermore, stiff

materials were shown to impair the contractile and growth activities of the cardiac cells [230]. Across the literature, the bulk of synthetic cell culture platforms proposed as cardiac patch candidates exhibit mechanical properties with relatively high values compared to those of native myocardium which might affect the maturation and activity of the cardiac cells [164, 217, 224, 228, 231, 232]. As an example, Stuckey et al. have shown that the stiffness of PED-TiO_2, which is a thermoplastic elastomer composed of poly (ethyleneterephathalate)/dimer fatty acid reinforced with TiO_2 nanoparticles, with a Young's modulus of 26.7 MPa, caused a large-scale localized necrosis among the heart tissue around the transplanted graft by means of surface friction. In addition, it was shown that transplanting PED-TiO_2 scaffold resulted in more dilation of the left ventricle, further scar size expanding as well as a more decrease in the cardiac output [233].

Overall, the present study showed that our developed CA-PGS system has superior mechanical properties in terms of elasticity, mechanical strength and deformability that better matched the native myocardium. This is better than the other filler-based elastomeric constructs that have reported much higher mechanical values than the required ones.

3.7. Electrical Conductivity Measurements

One of the main aims of embedding Carbon Aerogel microbelt networks into the pure PGS was to increase the electrical conductivity of the construct. For measuring the value of electrical conductivity for the samples of interest, 4-point probe method was used.

The pure PGS showed no sign of conductivity with a value being out of Keithley 2450 device limits. Upon incorporating CA microbelt networks into the polymer matrix, however, the electrical conductivity increased to $65 \pm 14 \times 10^{-3}$ S · m^{-1} for the composite. These results clearly show that the conductivity of the CA-PGS system was due to the uniform distribution of the conductive carbon microbelts among the electrically insulating elastomer matrix. The integration of carbon microbelt networks within the elastomer provides the electrons with clear paths to relatively move freely throughout the substrate. Thus, as expected, the incorporation of CA microbelt network into the elastomer has a positive effect on improving the electrical properties of the developed construct.

The conductivity of the native myocardium was reported to be ranging from 5×10^{-3} S · m^{-1} transversely to 160×10^{-3} S · m^{-1} longitudinally [182], and the electrical conductivity value of our system falls in this range.

The native heart has a sophisticated structure such that any biomaterial intended to be transplanted as a cardiac patch should possess not only unique mechanical characteristics but also of electrical conductivity. It is widely recognized that the cardiac substrates have to be electrically conductive for many reasons. Generally speaking, the contractile activity of the CMs is largely governed by the transmission of electrical signals throughout the cardiac muscle [234]. This Electrical signaling represents the core of cell-cell communication which is essential for the regular and synchronous contraction-relaxation motion of the cardiac tissue in order to create enough forces to push the blood to the rest of the body [235]. After MI, the fibrotic tissue that replaced the CMs in the infarcted area possesses low or even no conductivity [236]. In this case, a conductive cardiac patch might ease the propagation of electric pulses over the diseased region, contributing to the simultaneous contraction of the heart. Moreover, the electrical conductivity of the transplanted construct may accelerate the tissue regeneration process through ensuring the smooth transmission of electrical signals and chemicals between the transplanted CMs which would facilitate their electrical and mechanical coupling to the host myocardium in an efficient manner [234]. In addition, electrically active scaffolds were shown to promote the electrical integration of the transplanted CMs with those of the host tissue. Another advantage of the cardiac patch being electrically conductive is that it fosters the maturation of stem cells-derived cardiomyocytes when the electrical field stimulation strategy is adopted for this purpose [45].

Various types of biomaterials have been suggested for MTE applications, and most of which are not electrically conductive which might not only compromise the transmission of the electrical signal across the new-forming tissue and therefore hinder the effective connection between CMs, but also might contribute to the arrhythmic beating in HF patients who suffer from arrhythmia [234]. With the aim of developing electroactive cardiac composites, many additives have been incorporated into the electrically insulating polymeric matrices. Such additives

include inherently conductive polymers, carbon-derived fillers, and nano-gold particles. In most cases, however, the addition of those fillers results in compromised mechanical properties. Therefore, the imbalance between the desired electrical properties in one side and mechanical properties on the other side was usually evident. To name few examples, Qazi and co-workers reported a maximum electrical conductivity of 1770 × 10^{-3} S · m^{-1} upon adding polyaniline (PANI) conductive polymer to the PGS matrix in a PANI ratio of 30 vol.%. The reported Young's modulus for this substrate was about 6 MPa compared to that of myocardium being 0.2-0.5 MPa [189]. In another work, adding 1 wt.% CNTs to PCL effectively increased the electrical conductivity of the developed composite to about 400 × 10^{-3} S · m^{-1}, but simultaneously increased the stiffness of the composite to about 17 MPa [91].

The CA-PGS system's electrical conductivity result is equivalent to, and in some cases more effective than those reported for traditional elastomer-carbon nanofiller based cardiac patches. Stout et al. [182, 237] synthesized PLGA-CNFs composite for myocardial tissue engineering applications. Despite the excessive weight ratio of CNFs in the construct (50 wt.%), the electrical conductivity of the patch was reported to be 0.7 × 10^{-3} S · m^{-1} which is lower than those of native myocardium. Later on, Asiri et al. [183] reported an increased value of electrical conductivity (75 × 10^{-3} S · m^{-1}) for the same composite (PLGA-CNFs), and yet the number of CNFs within the patch remained at the same high level (50 wt.%) which is still a concern in the light of the reports suggesting that CNFs are of high toxicity for the cells [238]. In the present work, similar electrical conductivity value was reached by embedding as low as 1 wt.% of carbon microbelts into the elastomeric matrix which is a great advantage of our system. Therefore, this study also provided evidence that incorporating Carbon Aerogel networks with fibers in microscale into elastomers represents an efficient and cheap alternative to increase the electrical conductivity of an elastomer, just like or better than carbon nanofillers, while keeping the carbon contents within the culture substrate at a minimum level.

3.8. *In Vitro* Cytotoxicity Assessment of the Carbon Aerogel Embedded PGS Cardiac Patch

In vitro evaluation of cell viability is of paramount importance as an initial assessment of the developed CA-PGS system's compatibility with the host tissue. Generally speaking, it is essential that the potential detrimental effects of by-products which might be released from the biomaterial during its degradation on the cells be evaluated [199].

To this end, MTT tetrazolium cytotoxicity assay was carried out as an indirect test in which the cultured cells were exposed to different concentrations of extract from CA-PGS system. Subsequently, tetrazolium salts were added which are transformed by metabolically active cells to formazan crystals. By dissolving the formazan crystals and read the optical density of which, the cell viability can be determined. According to the performed dose-dependent cytotoxicity analysis, the cytotoxic potential of the materials was evaluated and presented in Figure 20.

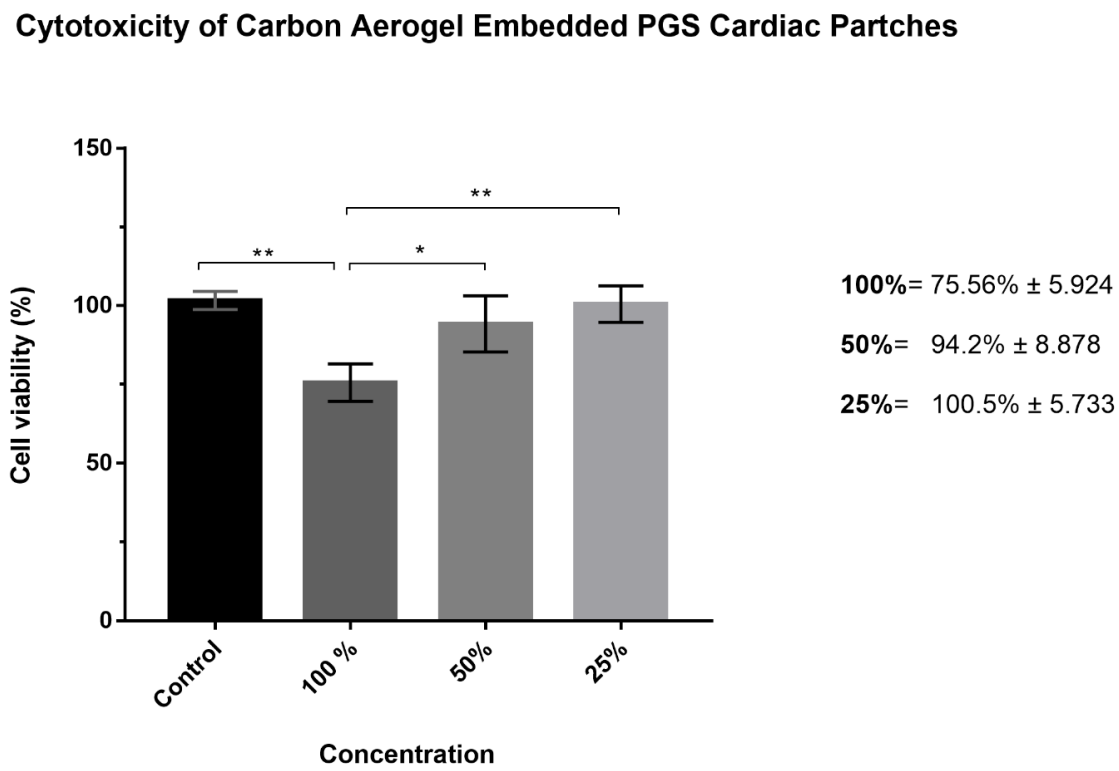

Figure 3.7. Cell viability of L929 cultured in different concentrations of CA-PGS system extract. The data represented as mean ± standard deviation; n=3 (*$p < 0.05$, **$p < 0.005$).

In comparison with the control group, the viabilities of L929 cultured in 50% (v/v) and 25% (v/v) extraction medium exhibited no significant differences ($p < 0.05$). Importantly, the cells exposed to a 100% extraction medium showed 75.6 ± 5.9% cell viability when compared with the control ($p<0.001$). According to ISO 10993-5:2009, a material is determined to have no cytotoxic potential if the cells cultured in the extract of the material exhibit cell viability of ≥ 70% compared to the control [239]. In this light, it can be concluded that CA-PGS system demonstrated no cytotoxic potential and showed sufficient cell viability for all extract concentrations.

One of the major concerns related to PGS is the acidic by-products that might be leached to the surrounding environment after incorporation into the human body. That being the case, the non-reacted carboxylic acid groups found among the non-crosslinked PGS monomers, are released to the surroundings decreasing the in situ pH level and causing the viable cells to die [166, 189]. The impact of PGS polymer on the cytotoxicity, however, could dramatically be limited by controlling the crosslinking density of the construct. The higher the crosslinking density, the less non-reacted carboxylic acid groups exist within the matrix and hence the less the construct affects the cells [166]. On the other hand, the highly-crosslinked PGS has a slower degradation kinetics that in turn would reduce the leaching of acidic products of degradation to the surrounding milieu which ultimately has a positive effect on the viability and proliferation of the seeded cells [240]. Also, it should be taken into account that an extreme crosslinking degree decreases the elastic properties of PGS elastomer. As a consequence, the balance between controlling the cytotoxicity and maintaining the desired flexibility is crucial at this point. Besides increasing the degree of crosslinking, some reports revealed that washing PGS with serial ethanol and water has a significant effect on reducing the remaining carboxyl groups within the PGS [229, 241]. For this purpose, the materials were initially washed with serial ethanol concentrations (100%, 70%, 50%, and 25% (v/v) for 1 h, 1 h, 15 min, and 15 min, respectively), followed by washing thrice with deionized water for 15 min each to get rid of the residual monomers in the materials [229]. In our study, the presented results confirmed nontoxic properties of the CA-PGS composite implying that the materials did not leach significant acidic by-products to the conditioned media thanks to the high degree of crosslinking achieved during thermally curing step and the washing process with a series of ethanol and water.

CA-PGS system composite has cytocompatibility performance equivalent to various elastomeric composites reported in the literature. Chen *et al.* performed a direct cytotoxicity experiment for pristine PGS cardiac patch using SNL mouse fibroblasts after conditioning the patch in a culture medium. The pre-conditioned PGS patch was found to support the viability of the fibroblast cells [124]. On the other hand, our cell viability results reveal that CA-PGS system has way better cytocompatibility results than those reported for several previously investigated cardiac patches across the literature. For instance, Silvestri *et al.* developed a porous poly (ester urethane) cardiac patch (PUR) from Poly (***ε***-caprolactone) (PCL) and Poly (ethylene glycol) (PEG) with suitable mechanical properties for myocardial repair. Cardiomyoblasts cultured on the patch, however, significantly exhibited a decreased viability as low as 60% relative to the control after 24 h of incubation time [217]. In another work, Tallawi and co-workers obtained PGS-poly (butylene succinate-butylene dilinoleate) (PBS/-DLA) electrospun fibrous scaffolds for cardiac patch applications. Despite of neither cell death nor morphological disorder was observed, myoblast cells cultured on all patches, which synthesized in different blend ratios of PGS and PBS/DLA, demonstrated cell viability of around 50% after 1 day of cell culture [231]. Also, Jawad *et al.* created a cell delivery construct, namely, poly (ethylene terephthalate)/dilinoleic thermoplastic elastomer (PET/DLA) which involves TiO_2 nanoparticles with a ratio of 0.2 wt.% as a filler in the matrix. The biocompatibility assessment, nevertheless, revealed that there was an increase in the cell death among the fibroblastic cells seeded on the developed nanocomposite compared to those in tissue culture plastic which served as a control [232].

Additionally, toxic chemicals and solvents were massively involved in the synthesis of the majority of the previously reported biomaterials intended to be candidates for cardiac patches across literature [79, 158, 164, 189, 217, 224, 231]. In carbon filler-based biomaterials, using solvents in composite scaffold fabrication provides a uniform distribution of carbon fillers in the polymeric fibers or matrices [91]. This is attributed in large part to the hydrophobic nature of carbon fillers which tend to aggregate upon embedding into the polymer as discussed previously. Such chemicals and solvents might leave residuals among the matrices which in turn may significantly have detrimental effects on the viability of the cells [231], hindering their potential to be suitable candidates for cell delivery applications. In order to obtain a

homogenous elastomer-carbon filler composite, using chemicals and solvents is inevitable. A great advantage of the present CA-PGS system, however, is that no chemical solvents nor toxic catalysts were used during the synthesis or crosslinking steps which likely has a great contribution to the compatibility of the system.

Overall, this initial cytotoxicity evaluation demonstrated the nontoxicity of CA-PGS system suggesting the biocompatibility of the system which makes it a convenient construct as a cell delivery vehicle and mechanical support device.

3.9. H9C2 Cell Proliferation on the Materials

The cell proliferation analysis was performed by using AlamarBlue analysis on the pre-determined dates of the culture period. To determine the H9C2 cardiac myoblast cell populations on the material, the increase in optic density of the test solution was determined as a function of the proliferation and the results were presented in Figure 21.

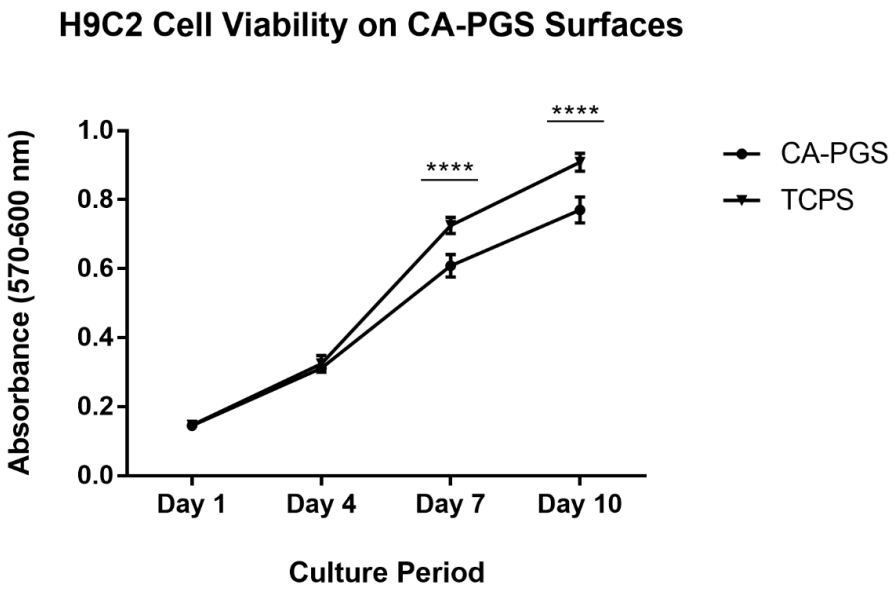

Figure 3.8. H9C2 cell proliferation on materials surface.

On the 1st day of the culture period, the cardiac myoblast cells both seeded to CA-PGS and TCPS were exhibited the same optic density. These results imply that the equal amount of cell seeding was succeeded to either TCPS or CA-PGS. The optic density suggesting the viable cell number was also recorded as the same on the 4th

day of the culture period. The proliferation trend differed from the 4th day of the culture period for the materials. Although cardiac myoblast cells exhibited a high survival and proliferation rate in CA-PGS, those in TCPS were recorded statistically higher than those in CA-PGS ($p<0.0001$). Similar differences were previously reported in the literature and it was linked to the differences between the materials and TCPS such as surface area, long culture period, lack of nutrition and/or space [224]. In our study, these results were specifically linked to the acidic by products degrades slowly from the CA-PGS to the culture medium. In any case, CA-PGS materials are thought to be biocompatible and promote cell adhesion and cell growth.

3.10. Cell-Material Interaction Analysis

The cell-seeded constructs were examined by Scanning Electron Microscopy to interpret the cell distribution, cell proliferation and cell-material interactions and the representative SEM micrographs were presented in Figure 22. In the myocardial tissue engineering, the cells are expected to adhere and proliferate on the patch material before it started to degrade [229]. The H9C2 cardiac myoblast cells normally exhibit different morphology in the culture conditions from spindle shape to ameboid shape regarding several factors such as passage number, oxidative stress, etc. [240]. Moreover, they exhibit elongated spindled shape when exposed to electrical stimulation and they start re-orientation in culture conditions [242]. In our study, cells were observed in a spherical form on the material’s surface on the first day of the culture suggesting the cells' recognition of the material and its adaptation phase.

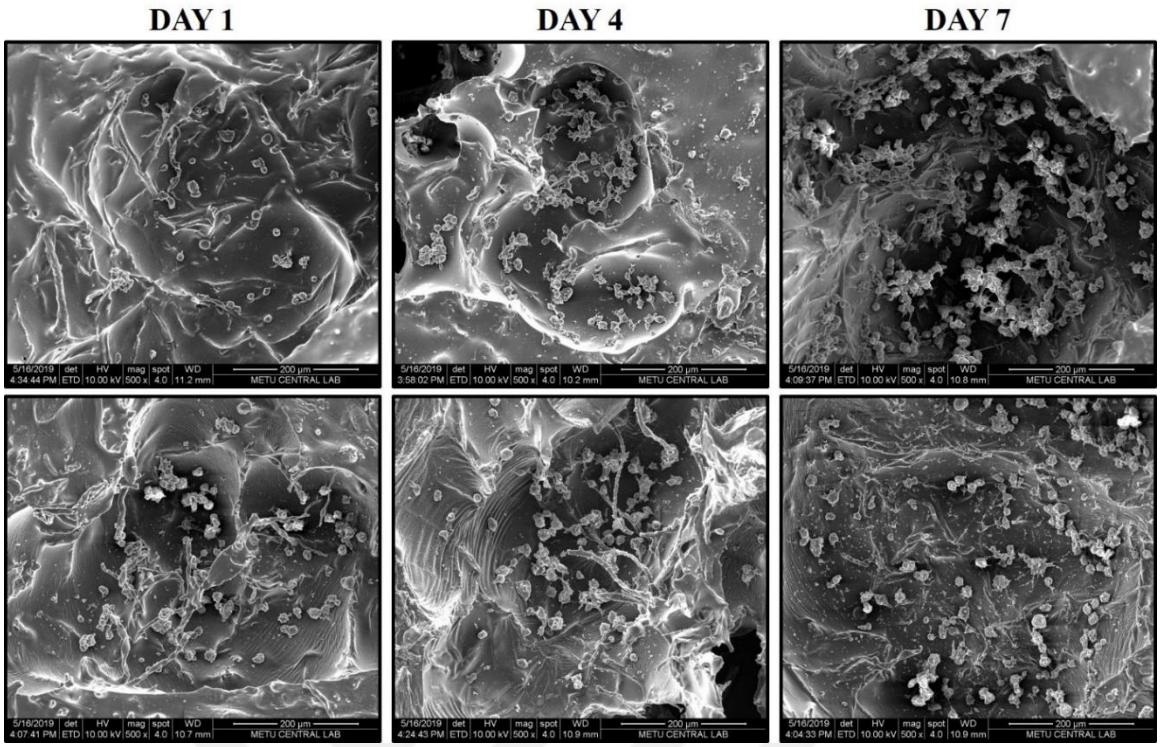

Figure 3.9. SEM micrographs of the cell seeded materials.

The SEM micrographs belonging to the 4th and the 7th day of the culture put forth the increase in the cell number in agreement with the viability assay. These results indicate that the materials support cell adhesion and proliferation.

Moreover, it was understood that most cells were both in spindle and ameboid shape when the cell behaviour was examined closely on 10th day of the culture in higher magnifications (Figure 23). These results showed that the cells remained their original morphologies after 10 days in culture period. Starting from this point of view, it was believed that a better cellular organization will be encountered thanks to the conductive carbon network within the material when electrical stimulation is applied to the materials.

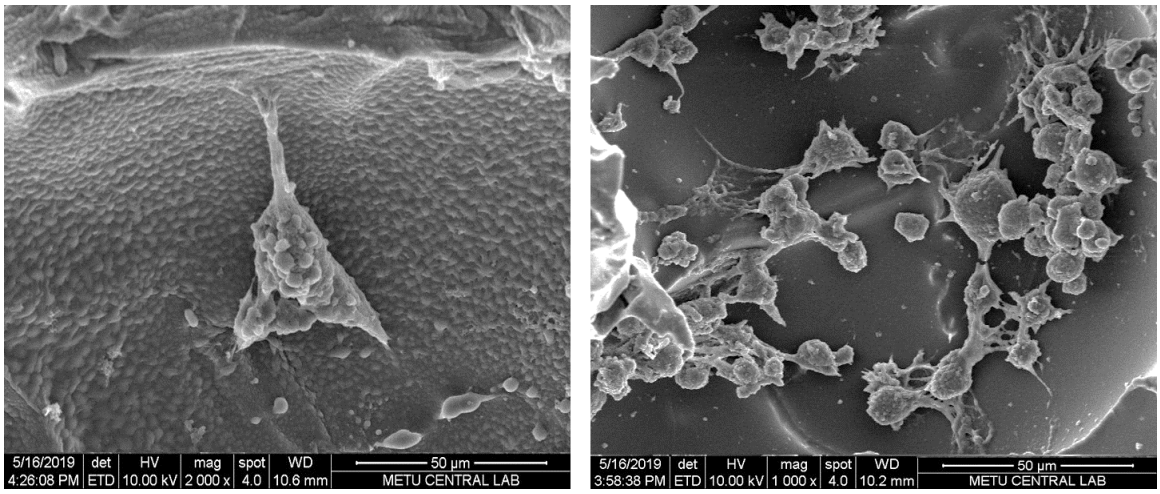

Figure 3.10. H9C2 cell behavior on the CA-PGS constructs.

4. Conclusion

In summary, the aim of this study was to synthesize and characterize a cardiac patch with electrical and mechanical properties matching those of the human myocardium. Another aim of the current study is to investigate, for the first time, the potential applications of Carbon Aerogel in myocardial tissue engineering as one area that has not been explored to date to the best of our knowledge. To this end, a novel, cost-effective and electrically conductive composite of waste paper-derived Carbon Aerogel and elastomeric poly (glycerol sebacate) (CA-PGS) was successfully developed, and the potential of this new Carbon Aerogel-reinforced polymeric composite to be a cardiac patch was explored for the first time. The resulting composite system features a branched distribution and a random orientation of the Carbon Aerogel's microbelts within the polymeric matrix and a rough surface with a random network of dots and interconnected macropores. In addition, the incorporation of CA's microbelts into the elastomer resulted in a significant enhancement in the electrical conductivity and the elasticity of the developed composite compared to the pure PGS. In particular, our developed CA-PGS composite system exhibited an electrical conductivity of $65 \pm 14 \times 10^{-3}$ $S \cdot m^{-1}$ and a Young's modulus of 0.366 ± 0.080 MPa which are well consistent with what reported for the native myocardium. The L929 mouse fibroblast seeded on CA-PGS composite samples confirmed the biocompatibility of our developed composite system. Moreover, cell culture test results showed that CA-PGS composite system supported cell adhesion and proliferation of the H9C2 cardiac myoblast cells. The results of this work, therefore, indicate that this novel composite system might be a promising biomaterial for cardiac repair, and as a proof-of-principle study, the present work provides the opportunity for further studies in the context of cardiac patch applications.

REFERENCES

[1] Marieb, E. and K. Hoehn, *Tissue, the living fabric.* Human Anatomy and Physiology, **2003**: p. 108-141.

[2] McKinley, M.P. and V.D. O'loughlin, *Human anatomy*. Second ed. **2008**: McGraw-Hill Higher Education.

[3. Weinhaus, A.J. and K.P. Roberts, *Anatomy of the human heart*, in *Handbook of cardiac anatomy, physiology, and devices*. **2009**, Springer. p. 59-85.

[4] Marieb, E.N. and K. Hoehn, *The Cardiovascular System: The Heart.* **2006**.

[5] Marieb, E. and K. Hoehn, *Muscles and muscle tissue.* Human anatomy and physiology, **2007**: p. 279-323.

[6] Katz, A., *Cellular and molecular basis of myocardial contraction.* Heart Failure: Pathogenesis and Treatment. London: Martin Dunitz, **2002**: p. 3-20.

[7] World Health Organization. *Cardiovascular Disease*. **2017**; Available from: http://www.who.int/cardiovascular_diseases/en/.

[8] Thompson, A.P.L., *Complications after Myocardial Infarction*, in *Evidence-Based Cardiology*. **2010**. p. 495-515.

[9] DiSalvo, T. and J. Shin, *The clinical syndrome of heart failure*, in *Heart Failure*. **2013**, CRC Press. p. 1-8.

[10] Savinova, O.V. and A.M. Gerdes, *Myocyte changes in heart failure.* Heart failure clinics, **2012**. 8(1): p. 1-6.

[11] Benjamin, E.J., et al., *Heart Disease and Stroke Statistics—2017 Update.* Circulation, 2017. **2017**(135).

[12] Jugdutt, B.I., *Ischemia/infarction.* Heart failure clinics, **2012**. 8(1): p. 43-51.

[13] O'Connor, C.M. and G.W. Stough, *Heart failure*, in *Cardiovascular Clinical Trials: Putting the Evidence into Practice*. **2012**, John Wiley & Sons, Inc. p. 117-142.

[14] Dorn II, G.W., *Molecular signaling networks underlying cardiac hypertrophy and failure*, in *Heart Failure*. **2013**, CRC Press. p. 31-42.

[15] Mendis, S., et al., *Global atlas on cardiovascular disease prevention and control*. **2011**: Geneva: World Health Organization.

[16] Fujita, B., et al., *State-of-the-Art in Tissue-Engineered Heart Repair*, in *Cardiac Regeneration*. **2017**, Springer. p. 219-239.

[17] Association, A.H. *Heart Attack*. **2018**; Available from: https://www.heart.org/.

[18] Baliga, R., Y. Chandrashekhar, and J. Narula, *Apoptosis in congestive heart failure.* Heart Failure. Pathogenesis and Management. London: Martin Dunitz, **2002**: p. 293-314.

[19] Kajstura, J., et al., *Apoptotic and necrotic myocyte cell deaths are independent contributing variables of infarct size in rats.* Laboratory investigation; a journal of technical methods and pathology, **1996**. 74(1): p. 86-107.

[20] Saraste, A., et al., *Apoptosis in human acute myocardial infarction.* Circulation, **1997**. 95(2): p. 320-323.

[21] Liu, Y., et al., *Myocyte nuclear mitotic division and programmed myocyte cell death characterize the cardiac myopathy induced by rapid ventricular pacing in dogs.* Laboratory investigation; a journal of technical methods and pathology, **1995**. 73(6): p. 771-787.

[22] Yared, K. and J. Hung, *Ventricular remodeling and secondary valvular dysfunction in heart failure progression*, in *Heart Failure*. **2013**, CRC Press. p. 95-118.

[23] O'Connor, C.M.S., George W. , *Heart failure*, in *Cardiovascular Clinical Trials: Putting the Evidence into Practice*. **2012**, John Wiley & Sons, Inc. p. 117-142.

[24] Paul J Hauptman, K.S., *Management of Overt Heart Failure*, in *Evidence-Based Cardiology*. **2010**. p. 657-738.

[25] Group*, C.T.S., *Effects of enalapril on mortality in severe congestive heart failure.* New England Journal of Medicine, **1987**. 316(23): p. 1429-1435.
[26] Swedberg, K., J. Kjekshus, and C.T.S. Group, *Effects of enalapril on mortality in severe congestive heart failure: results of the Cooperative North Scandinavian Enalapril Survival Study (CONSENSUS).* The American journal of cardiology, **1988**. 62(2): p. 60A-66A.
[27] Yusuf, S., et al., *Effect of enalapril on survival in patients with reduced left ventricular ejection fractions and congestive heart failure.* The New England journal of medicine, **1991**. 325(5): p. 293-302.
[28] Zannad, F., et al., *Eplerenone in patients with systolic heart failure and mild symptoms.* New England Journal of Medicine, **2011**. 364(1): p. 11-21.
[29] Mark, D.B., et al., *Quality of life with defibrillator therapy or amiodarone in heart failure.* New England Journal of Medicine, **2008**. 359(10): p. 999-1008.
[30] Camm, W.D.T.A.J., *Pacemaker Therapy, Including Cardiac Resynchronization Therapy*, in *Evidence-Based Cardiology*. **2010**. p. 636-672.
[31] Adams, K., Lindenfeld J, Arnold JMO, Baker DW, Barnard DH, Baughman KL, Boehmer JP, Deedwania P, Dunbar SB, Elkayam U, Gheorghiade M, Howlett JG, Konstam MA, Kronenberg MW, Massie BM, Mehra MR, Miller AB, Moser DK, Patterson JH, Rodeheffer RJ, Sackner-Bernstein J, Silver MA, Starling RC, Stevenson LW, Wagoner LE, *Executive Summary: HFSA **2006** Comprehensive Heart Failure Practice Guideline.* J Cardiac Failure, **2006**: p. 10–38.
[32] ROSE, E.A., et al., *Long-Term Use of a Left Ventricular Assist Device for End-Stage Heart Failure.* N Engl J Med, **2001**. 345(20).
[33] Long, J.W., et al., *Long-Term Destination Therapy With the HeartMate XVE Left Ventricular Assist Device: Improved Outcomes Since the REMATCH Study.* Congestive Heart Failure, **2006**. 11(3): p. 133-138.
[34] Serge Gregoire, S.M.W., *A brief primer on the development of the heart*, in *Heart Failure*. **2013**, CRC Press. p. 1-8.
[35] Lars H. Lund, K.K.K., Wida S. Cherikh, Samuel Goldfarb, Anna Y. Kucheryavaya, Bronwyn J. Levvey, Bruno Meiser, Joseph W. Rossano, Daniel C. Chambers, Roger D. Yusen, Josef Stehlik,, *The Registry of the International Society for Heart and Lung Transplantation: Thirty-fourth Adult Heart Transplantation Report—2017; Focus Theme: Allograft ischemic time.* The Journal of Heart and Lung Transplantation, **2017**. 36(10): p. 1037-1046.
[36] Colvin-Adams, M., et al., *OPTN/SRTR **2012** annual data report: heart.* American Journal of Transplantation, **2014**. 14(S1): p. 113-138.
[37] OPTN. *Data about the status of U.S. heart transplantation on a national level*. 26/08/**2019**]; Available from: https://optn.transplant.hrsa.gov/data/.
[38] CHEN, Q.Z., *Myocardial Tissue Engineering*, in *Tissue Engineering Using Ceramics and Polymers*. **2014**, Elsevier Ltd. p. 387-413.
[39] Akhyari, P., et al., *Strategies for Myocardial Tissue Engineering: The Beat Goes On*, in *Myocardial Tissue Engineering*. **2011**, Springer. p. 49-79.
[40] Ye, H., et al., *Polyester elastomers for soft tissue engineering.* Chemical Society Reviews, **2018**.
[41] Pecha, S. and Y. Yildirim, *Myocardial tissue engineering for cardiac repair*, in *Liver, Lung and Heart Regeneration*. **2017**, Springer. p. 153-164.
[42] Zimmermann, W.-H., *Tissue engineered myocardium*, in *Myocardial Tissue Engineering*. **2010**, Springer. p. 111-132.
[43] Dvir, T., J. Leor, and S. Cohen, *Creating unique cell microenvironments for the engineering of a functional cardiac patch*, in *Myocardial Tissue Engineering*. **2010**, Springer. p. 81-94.
[44] Gaetani, R., et al., *Tissue Engineering for Cardiac Regeneration*, in *Myocardial Tissue Engineering*. **2011**, Springer. p. 1-27.
[45] Weinberger, F., I. Mannhardt, and T. Eschenhagen, *Engineering cardiac muscle tissue: a maturating field of research.* Circulation research, **2017**. 120(9): p. 1487-1500.

[46] Hartman, M.E., J.J. Chong, and M.A. Laflamme, *State of the Art in Cardiomyocyte Transplantation*, in *Cardiac Regeneration*. **2017**, Springer. p. 177-218.
[47] Shimizu, T. and K. Matsuura, *Myocardial tissue engineering*. **2015**: CRC Press.
[48] Rosellini, E., et al., *Engineering of multifunctional scaffolds for myocardial repair through nanofunctionalization and microfabrication of novel polymeric biomaterials*, in *Myocardial Tissue Engineering*. **2010**, Springer. p. 187-214.
[49] Yuji Haraguchi, N.Y., Tatsuya Shimizu, Masayuki Yamato, and Teruo Okano, *Cell Sheet–Based Tissue Engineering*, in *Myocardial Tissue Engineering*. **2015**, CRC Press Taylor & Francis Group. p. 107-124.
[50] Giraud, M.-N. and I. Borrego, *Myocardial Tissue Engineering: A 5 Year—Update*, in *Liver, Lung and Heart Regeneration*. **2017**, Springer. p. 197-209.
[51] Robey, T.E., et al., *Systems approaches to preventing transplanted cell death in cardiac repair.* Journal of molecular and cellular cardiology, **2008**. 45(4): p. 567-581.
[52] Zvibel, I., F. Smets, and H. Soriano, *Anoikis: roadblock to cell transplantation?* Cell transplantation, **2002**. 11(7): p. 621-630.
[53] Genovese, J.A., et al., *Electrospun nanocomposites and stem cells in cardiac tissue engineering*, in *Myocardial Tissue Engineering*. **2011**, Springer. p. 215-242.
[54] Sasagawa, T., *Scaffold-Based Myocardial Patches*, in *Myocardial Tissue Engineering*. **2015**, CRC Press Taylor & Francis Group. p. 125-139.
[55] Takagi, S., *Scaffold-Based Tissue Engineering*, in *Myocardial Tissue Engineering*. **2015**, CRC Press Taylor & Francis Group. p. 98-106.
[56] Boccaccini, A.R. and S.E. Harding, *Myocardial tissue engineering*. Vol. 6. **2011**: Springer.
[57] Chen, Q.-Z., et al., *Characterisation of a soft elastomer poly (glycerol sebacate) designed to match the mechanical properties of myocardial tissue.* Biomaterials, **2008**. 29(1): p. 47-57.
[58] Leor, J., Y. Amsalem, and S. Cohen, *Cells, scaffolds, and molecules for myocardial tissue engineering.* Pharmacology & therapeutics, **2006**. 105(2): p. 151-163.
[59] Lee, E.J.H., Pamela *Cardiac Tissue Engineering*, in *Tissue Engineering for Artificial Organs: Regenerative Medicine, Smart Diagnostics and Personalized Medicine*. **2017**. p. 413-443.
[60] Pham, T.L.-B., N.B. Vu, and P. Van Pham, *Stem Cell Therapy for Ischemic Heart Disease*, in *Liver, Lung and Heart Regeneration*. **2017**, Springer. p. 165-195.
[61] Rana, D., et al., *Induced Pluripotent Stem Cells in Scaffold-Based Tissue Engineering.* Tissue Engineering for Artificial Organs: Regenerative Medicine, Smart Diagnostics and Personalized Medicine, **2017**. 1: p. 111-142.
[62] Li, R.-K., et al., *Survival and function of bioengineered cardiac grafts.* Circulation, **1999**. 100(suppl 2): p. II-63-Ii-69.
[63] Leor, J., et al., *Bioengineered cardiac grafts.* Circulation, **2000**. 102(suppl 3): p. Iii-56-Iii-61.
[64] Li, R.-K., et al., *Construction of a bioengineered cardiac graft.* The Journal of thoracic and cardiovascular surgery, **2000**. 119(2): p. 368-375.
[65] Amir, G., et al., *Evaluation of a peritoneal-generated cardiac patch in a rat model of heterotopic heart transplantation.* Cell transplantation, **2009**. 18(3): p. 275-282.
[66] Kamelger, F., et al., *A comparative study of three different biomaterials in the engineering of skeletal muscle using a rat animal model.* Biomaterials, **2004**. 25(9): p. 1649-1655.
[67] Li, R.K., *Cell transplantation to improve heart function: cell or matrix.* Yonsei Medical Journal, **2004**. 45(Suppl): p. S72A3-S73A3.
[68] Siepe, M., et al., *Myoblast-seeded biodegradable scaffolds to prevent post–myocardial infarction evolution toward heart failure.* The Journal of Thoracic and Cardiovascular Surgery, **2006**. 132(1): p. 124-131.
[69] Siepe, M., et al., *Construction of skeletal myoblast-based polyurethane scaffolds for myocardial repair.* Artificial organs, **2007**. 31(6): p. 425-433.
[70] Giraud, M.N., et al., *Long-term evaluation of myoblast seeded patches implanted on infarcted rat hearts.* Artificial organs, **2010**. 34(6): p. E184-E192.

[71] Blumenthal, B., et al., *Polyurethane scaffolds seeded with genetically engineered skeletal myoblasts: a promising tool to regenerate myocardial function.* Artificial organs, **2010**. 34(2): p. E46-E54.
[72] Poppe, A., et al., *Hepatocyte Growth Factor-Transfected Skeletal Myoblasts to Limit the Development of Postinfarction Heart Failure.* Artificial organs, **2012**. 36(3): p. 238-246.
[73] Matsubayashi, K., et al., *Improved left ventricular aneurysm repair with bioengineered vascular smooth muscle grafts.* Circulation, **2003**. 108(10 suppl 1): p. II-219-II-225.
[74] Kellar, R.S., et al., *Scaffold-based three-dimensional human fibroblast culture provides a structural matrix that supports angiogenesis in infarcted heart tissue.* Circulation, **2001**. 104(17): p. 2063-2068.
[75] Lancaster, J., et al., *Viable fibroblast matrix patch induces angiogenesis and increases myocardial blood flow in heart failure after myocardial infarction.* Tissue Engineering Part A, **2010**. 16(10): p. 3065-3073.
[76] Thai, H.M., et al., *Implantation of a three-dimensional fibroblast matrix improves left ventricular function and blood flow after acute myocardial infarction.* Cell transplantation, **2009**. 18(3): p. 283-295.
[77] Fitzpatrick III, J.R., et al., *Tissue-engineered pro-angiogenic fibroblast scaffold improves myocardial perfusion and function and limits ventricular remodeling after infarction.* The Journal of thoracic and cardiovascular surgery, **2010**. 140(3): p. 667-676.
[78] Pok, S., et al., *Biocompatible carbon nanotube-chitosan scaffold matching the electrical conductivity of the heart.* ACS Nano, **2014**. 8(10): p. 9822-32.
[79] Kharaziha, M., et al., *Tough and flexible CNT-polymeric hybrid scaffolds for engineering cardiac constructs.* Biomaterials, **2014**. 35(26): p. 7346-54.
[80] Ahadian, S., et al., *Moldable elastomeric polyester-carbon nanotube scaffolds for cardiac tissue engineering.* Acta Biomater, **2016**.
[81] Martins, A.M., et al., *Electrically conductive chitosan/carbon scaffolds for cardiac tissue engineering.* Biomacromolecules, **2014**. 15(2): p. 635-43.
[82] Park, H., et al., *Biomimetic scaffold combined with electrical stimulation and growth factor promotes tissue engineered cardiac development.* Experimental cell research, **2014**. 321(2): p. 297-306.
[83] Martinelli, V., et al., *Carbon nanotubes promote growth and spontaneous electrical activity in cultured cardiac myocytes.* Nano Lett, **2012**. 12(4): p. 1831-8.
[84] Wu, Y., et al., *Carbon Nanohorns Promote Maturation of Neonatal Rat Ventricular Myocytes and Inhibit Proliferation of Cardiac Fibroblasts: a Promising Scaffold for Cardiac Tissue Engineering.* Nanoscale Res Lett, **2016**. 11(1): p. 284.
[85] Yildirim, Y., et al., *Development of a biological ventricular assist device: preliminary data from a small animal model.* Circulation, **2007**. 116(11 suppl): p. I-16-I-23.
[86] Krupnick, A., et al., *A murine model of left ventricular tissue engineering.* The Journal of Heart and Lung Transplantation, **2001**. 20(2): p. 197-198.
[87] Schaefer, A., et al., *Long-term effects of intracoronary bone marrow cell transfer on diastolic function in patients after acute myocardial infarction: 5-year results from the randomized-controlled BOOST trial—an echocardiographic study.* European Journal of Echocardiography, **2009**. 11(2): p. 165-171.
[88] Nygren, J.M., et al., *Bone marrow–derived hematopoietic cells generate cardiomyocytes at a low frequency through cell fusion, but not transdifferentiation.* Nature medicine, **2004**. 10(5): p. 494.
[89] Alvarez-Dolado, M., et al., *Fusion of bone-marrow-derived cells with Purkinje neurons, cardiomyocytes and hepatocytes.* nature, **2003**. 425(6961): p. 968.
[90] Tian, L., et al., *Emulsion electrospun nanofibers as substrates for cardiomyogenic differentiation of mesenchymal stem cells.* Journal of Materials Science: Materials in Medicine, **2013**. 24(11): p. 2577-2587.

[91] Crowder, S.W., et al., *Poly(epsilon-caprolactone)-carbon nanotube composite scaffolds for enhanced cardiac differentiation of human mesenchymal stem cells.* Nanomedicine (Lond), **2013**. 8(11): p. 1763-76.
[92] Borriello, A., et al., *Optimizing PANi doped electroactive substrates as patches for the regeneration of cardiac muscle.* J Mater Sci Mater Med, **2011**. 22(4): p. 1053-62.
[93] Santiago, J.A., R. Pogemiller, and B.M. Ogle, *Heterogeneous differentiation of human mesenchymal stem cells in response to extended culture in extracellular matrices.* Tissue Engineering Part A, **2009**. 15(12): p. 3911-3922.
[94] Maureira, P., et al., *Repairing chronic myocardial infarction with autologous mesenchymal stem cells engineered tissue in rat promotes angiogenesis and limits ventricular remodeling.* Journal of biomedical science, **2012**. 19(1): p. 93.
[95] Guo, H.-D., et al., *Transplantation of marrow-derived cardiac stem cells carried in fibrin improves cardiac function after myocardial infarction.* Tissue Engineering Part A, **2010**. 17(1-2): p. 45-58.
[96] Fukuhara, S., et al., *Bone marrow cell-seeded biodegradable polymeric scaffold enhances angiogenesis and improves function of the infarcted heart.* Circulation journal: official journal of the Japanese Circulation Society, **2006**. 69(7): p. 850-857.
[97] Jin, J., et al., *Transplantation of mesenchymal stem cells within a poly (lactide-co-ε-caprolactone) scaffold improves cardiac function in a rat myocardial infarction model.* European journal of heart failure, **2009**. 11(2): p. 147-153.
[98] Guan, J., et al., *The stimulation of the cardiac differentiation of mesenchymal stem cells in tissue constructs that mimic myocardium structure and biomechanics.* Biomaterials, **2011**. 32(24): p. 5568-5580.
[99] Simpson, D., et al., *A tissue engineering approach to progenitor cell delivery results in significant cell engraftment and improved myocardial remodeling.* Stem Cells, **2007**. 25(9): p. 2350-2357.
[100] Van Dijk, A., et al., *Differentiation of human adipose-derived stem cells towards cardiomyocytes is facilitated by laminin.* Cell and tissue research, **2008**. 334(3): p. 457-467.
[101] Russo, V., et al., *Porous, Ventricular Extracellular Matrix-Derived Foams as a Platform for Cardiac Cell Culture.* BioResearch open access, **2015**. 4(1): p. 374-388.
[102] Choi, Y.S., et al., *Differentiation of human adipose-derived stem cells into beating cardiomyocytes.* Journal of cellular and molecular medicine, **2010**. 14(4): p. 878-889.
[103] Song, Y.-H., et al., *VEGF is critical for spontaneous differentiation of stem cells into cardiomyocytes.* Biochemical and biophysical research communications, **2007**. 354(4): p. 999-1003.
[104] Araña, M., et al., *Epicardial delivery of collagen patches with adipose-derived stem cells in rat and minipig models of chronic myocardial infarction.* Biomaterials, **2014**. 35(1): p. 143-151.
[105] Sun, C.-K., et al., *Direct implantation versus platelet-rich fibrin-embedded adipose-derived mesenchymal stem cells in treating rat acute myocardial infarction.* International journal of cardiology, **2014**. 173(3): p. 410-423.
[106] Liu, B.-H., et al., *Spheroid formation and enhanced cardiomyogenic potential of adipose-derived stem cells grown on chitosan.* BioResearch open access, **2013**. 2(1): p. 28-39.
[107] Nagata, H., et al., *Cardiac Adipose-Derived Stem Cells Exhibit High Differentiation Potential to Cardiovascular Cells in C57BL/6 Mice.* Stem cells translational medicine, **2016**. 5(2): p. 141-151.
[108] Yang, Y., et al., *MRI studies of cryoinjury infarction in pig hearts: ii. Effects of intrapericardial delivery of adipose-derived stem cells (ADSC) embedded in agarose gel.* NMR in Biomedicine, **2012**. 25(2): p. 227-235.
[109] Wu, X., et al., *Tissue-engineered microvessels on three-dimensional biodegradable scaffolds using human endothelial progenitor cells.* American Journal of Physiology-Heart and Circulatory Physiology, **2004**. 287(2): p. H480-H487.

[110] Ryu, J.H., et al., *Implantation of bone marrow mononuclear cells using injectable fibrin matrix enhances neovascularization in infarcted myocardium.* Biomaterials, **2006**. 26(3): p. 319-326.
[111] Kadner, A., et al., *Human umbilical cord cells for cardiovascular tissue engineering: a comparative study.* European journal of cardio-thoracic surgery, **2004**. 25(4): p. 635-641.
[112] Cortes-Morichetti, M., et al., *Association between a cell-seeded collagen matrix and cellular cardiomyoplasty for myocardial support and regeneration.* Tissue engineering, **2007**. 13(11): p. 2681-2687.
[113] Levenberg, S., et al., *Differentiation of human embryonic stem cells on three-dimensional polymer scaffolds.* Proceedings of the National Academy of Sciences, **2003**. 100(22): p. 12741-12746.
[114] Lee, M.Y., et al., *High density cultures of embryoid bodies enhanced cardiac differentiation of murine embryonic stem cells.* Biochemical and biophysical research communications, **2011**. 416(1): p. 51-57.
[115] Kehat, I., et al., *Human embryonic stem cells can differentiate into myocytes with structural and functional properties of cardiomyocytes.* The Journal of clinical investigation, **2001**. 108(3): p. 407-414.
[116] van Laake, L.W., et al., *Human embryonic stem cell-derived cardiomyocytes survive and mature in the mouse heart and transiently improve function after myocardial infarction.* Stem cell research, **2007**. 1(1): p. 9-24.
[117] Lee, T.J., et al., *Graphene enhances the cardiomyogenic differentiation of human embryonic stem cells.* Biochem Biophys Res Commun, **2014**. 452(1): p. 174-80.
[118] Kofidis, T., et al., *Injectable bioartificial myocardial tissue for large-scale intramural cell transfer and functional recovery of injured heart muscle.* The Journal of thoracic and cardiovascular surgery, **2004**. 128(4): p. 571-578.
[119] Schaaf, S., et al., *Human engineered heart tissue as a versatile tool in basic research and preclinical toxicology.* PloS one, **2011**. 6(10): p. e26397.
[120] Zhang, D., et al., *Tissue-engineered cardiac patch for advanced functional maturation of human ESC-derived cardiomyocytes.* Biomaterials, **2013**. 34(23): p. 5813-5820.
[121] Lü, S., et al., *Both the transplantation of somatic cell nuclear transfer-and fertilization-derived mouse embryonic stem cells with temperature-responsive chitosan hydrogel improve myocardial performance in infarcted rat hearts.* Tissue Engineering Part A, **2010**. 16(4): p. 1303-1315.
[122] Habib, M., et al., *A combined cell therapy and in-situ tissue-engineering approach for myocardial repair.* Biomaterials, **2011**. 32(30): p. 7514-7523.
[123] Gupta, M.K., et al., *Combinatorial polymer electrospun matrices promote physiologically-relevant cardiomyogenic stem cell differentiation.* PloS one, **2011**. 6(12): p. e28935.
[124] Chen, Q.-Z., et al., *An elastomeric patch derived from poly (glycerol sebacate) for delivery of embryonic stem cells to the heart.* Biomaterials, **2010**. 31(14): p. 3885-3893.
[125] Kofidis, T., et al., *Myocardial restoration with embryonic stem cell bioartificial tissue transplantation.* The Journal of heart and lung transplantation, **2006**. 24(6): p. 737-744.
[126] Xiong, Q., et al., *A fibrin patch-based enhanced delivery of human embryonic stem cell-derived vascular cell transplantation in a porcine model of postinfarction left ventricular remodeling.* Stem Cells, **2011**. 29(2): p. 367-375.
[127] Zhang, J., et al., *Functional cardiomyocytes derived from human induced pluripotent stem cells.* Circulation research, **2009**. 104(4): p. e30-e41.
[128] Mummery, C.L., et al., *Differentiation of human embryonic stem cells and induced pluripotent stem cells to cardiomyocytes: a methods overview.* Circulation research, **2012**. 111(3): p. 344-358.
[129] Pawani, H. and D. Bhartiya, *Pluripotent stem cells for cardiac regeneration: overview of recent advances & emerging trends.* The Indian journal of medical research, **2013**. 137(2): p. 270.

[130] Zhang, J., et al., *Extracellular matrix promotes highly efficient cardiac differentiation of human pluripotent stem cells: the matrix sandwich method.* Circulation research, **2012**. 111(9): p. 1125-1136.
[131] Bolli, R., et al., *Cardiac stem cells in patients with ischaemic cardiomyopathy (SCIPIO): initial results of a randomised phase 1 trial.* The Lancet, **2011**. 378(9806): p. 1847-1857.
[132] Barile, L., et al., *Cardiac stem cells: isolation, expansion and experimental use for myocardial regeneration.* Nature Reviews Cardiology, **2007**. 4(S1): p. S9.
[133] Liu, T.C.K., et al., *Encapsulation of cardiac stem cells in superoxide dismutase-loaded alginate prevents doxorubicin-mediated toxicity.* Journal of tissue engineering and regenerative medicine, **2013**. 7(4): p. 302-311.
[134] Di Felice, V., et al., *Silk fibroin scaffolds enhance cell commitment of adult rat cardiac progenitor cells.* Journal of tissue engineering and regenerative medicine, **2015**. 9(11): p. E51-E64.
[135] Zimmermann, W.-H. and R. Cesnjevar, *Cardiac tissue engineering: implications for pediatric heart surgery.* Pediatric cardiology, **2009**. 30(5): p. 716-723.
[136] Shafiee, A. and A. Atala, *Tissue engineering: toward a new era of medicine.* Annual review of medicine, **2017**. 68: p. 29-40.
[137] Ahadian, S., et al., *Biomaterials in Tissue Engineering.* Tissue Engineering for Artificial Organs: Regenerative Medicine, Smart Diagnostics and Personalized Medicine, **2017**. 1: p. 35-83.
[138] Huang, N.F., et al., *Injectable biopolymers enhance angiogenesis after myocardial infarction.* Tissue engineering, **2006**. 11(11-12): p. 1860-1866.
[139] Thompson, C.A., et al., *Percutaneous transvenous cellular cardiomyoplasty: a novel nonsurgical approach for myocardial cell transplantation.* Journal of the American College of Cardiology, **2003**. 41(11): p. 1964-1971.
[140] Dai, W., et al., *Thickening of the infarcted wall by collagen injection improves left ventricular function in rats: a novel approach to preserve cardiac function after myocardial infarction.* Journal of the American College of Cardiology, **2006**. 46(4): p. 714-719.
[141] Zhang, P., et al., *Artificial matrix helps neonatal cardiomyocytes restore injured myocardium in rats.* Artificial organs, **2006**. 30(2): p. 86-93.
[142] Eschenhagen, T., et al., *Three-dimensional reconstitution of embryonic cardiomyocytes in a collagen matrix: a new heart muscle model system.* The FASEB journal, **1997**. 11(8): p. 683-694.
[143] Zimmermann, W.H., et al., *Three-dimensional engineered heart tissue from neonatal rat cardiac myocytes.* Biotechnology and bioengineering, **2000**. 68(1): p. 106-114.
[144] Kofidis, T., et al., *Bioartificial grafts for transmural myocardial restoration: a new cardiovascular tissue culture concept*. **2003**, Elsevier Science BV.
[145] Gonnerman, E.A., et al., *The promotion of HL-1 cardiomyocyte beating using anisotropic collagen-GAG scaffolds.* Biomaterials, **2012**. 33(34): p. 8812-8821.
[146] Chachques, J.C., et al., *Myocardial assistance by grafting a new bioartificial upgraded myocardium (MAGNUM clinical trial): one year follow-up.* Cell transplantation, **2007**. 16(9): p. 927-934.
[147] Prabhakaran, M.P., et al., *Electrospun biocomposite nanofibrous patch for cardiac tissue engineering.* Biomedical materials, **2011**. 6(5): p. 055001.
[148] Ravichandran, R., et al., *Poly (glycerol sebacate)/gelatin core/shell fibrous structure for regeneration of myocardial infarction.* Tissue Engineering Part A, **2011**. 17(9-10): p. 1363-1373.
[149] Shachar, M., et al., *The effect of immobilized RGD peptide in alginate scaffolds on cardiac tissue engineering.* Acta biomaterialia, **2011**. 7(1): p. 152-162.
[150] Dvir, T., et al., *Prevascularization of cardiac patch on the omentum improves its therapeutic outcome.* Proceedings of the National Academy of Sciences, **2009**. 106(35): p. 14990-14995.

[151] Gallina, C., et al., *Development of morphology and function of neonatal mouse ventricular myocytes cultured on a hyaluronan-based polymer scaffold.* Journal of cellular biochemistry, **2012**. 113(3): p. 800-807.
[152] Giraud, M.N., et al., *Hydrogel-based engineered skeletal muscle grafts normalize heart function early after myocardial infarction.* Artificial organs, **2008**. 32(9): p. 692-700.
[153] Christman, K.L., et al., *Injectable fibrin scaffold improves cell transplant survival, reduces infarct expansion, and induces neovasculature formation in ischemic myocardium.* Journal of the American College of Cardiology, **2004**. 44(3): p. 654-660.
[154] Christman, K., et al. *Myoblasts delivered in an injectable fibrin scaffold improve cardiac function and preserve left ventricular geometry in a chronic myocardial infarction model*. in *Circulation*. **2003**. LIPPINCOTT WILLIAMS & WILKINS 530 WALNUT ST, PHILADELPHIA, PA 19106-3621 USA.
[155] Davis, M.E., et al., *Injectable self-assembling peptide nanofibers create intramyocardial microenvironments for endothelial cells.* Circulation, **2006**. 111(4): p. 442-450.
[156] Davis, M.E., et al., *Local myocardial insulin-like growth factor 1 (IGF-1) delivery with biotinylated peptide nanofibers improves cell therapy for myocardial infarction.* Proceedings of the National Academy of Sciences, **2006**. 103(21): p. 8155-8160.
[157] Annabi, N., et al., *Highly elastic micropatterned hydrogel for engineering functional cardiac tissue.* Advanced functional materials, **2013**. 23(39): p. 4950-4959.
[158] Prabhakaran, M.P., et al., *Electrospun composite scaffolds containing poly (octanediol-co-citrate) for cardiac tissue engineering.* Biopolymers, **2012**. 97(7): p. 529-538.
[159] Zong, X., et al., *Electrospun fine-textured scaffolds for heart tissue constructs.* Biomaterials, **2006**. 26(26): p. 5330-5338.
[160] Ke, Q., et al., *Embryonic stem cells cultured in biodegradable scaffold repair infarcted myocardium in mice.* ACTA PHYSIOLOGICA SINICA-CHINESE EDITION-, **2006**. 57(6): p. 673.
[161] Kellar, R.S., et al., *Cardiac patch constructed from human fibroblasts attenuates reduction in cardiac function after acute infarct.* Tissue engineering, **2006**. 11(11-12): p. 1678-1687.
[162] Radisic, M., et al., *Mathematical model of oxygen distribution in engineered cardiac tissue with parallel channel array perfused with culture medium containing oxygen carriers.* American Journal of Physiology-Heart and Circulatory Physiology, **2006**. 288(3): p. H1278-H1289.
[163] Wang, Y., et al., *A tough biodegradable elastomer.* Nature biotechnology, **2002**. 20(6): p. 602.
[164] Ravichandran, R., et al., *Expression of cardiac proteins in neonatal cardiomyocytes on PGS/fibrinogen core/shell substrate for Cardiac tissue engineering.* International journal of cardiology, **2013**. 167(4): p. 1461-1468.
[165] Ravichandran, R., et al., *Minimally invasive injectable short nanofibers of poly (glycerol sebacate) for cardiac tissue engineering.* Nanotechnology, **2012**. 23(38): p. 385102.
[166] Chen, Q., et al., *Elastomeric nanocomposites as cell delivery vehicles and cardiac support devices.* Soft Matter, **2010**. 6(19): p. 4715-4726.
[167] Ishii, O., et al., *In vitro tissue engineering of a cardiac graft using a degradable scaffold with an extracellular matrix–like topography.* The Journal of thoracic and cardiovascular surgery, **2006**. 130(5): p. 1358-1363.
[168] Shin, M., et al., *Contractile cardiac grafts using a novel nanofibrous mesh.* Biomaterials, **2004**. 25(17): p. 3717-3723.
[169] McDevitt, T.C., et al., *Spatially organized layers of cardiomyocytes on biodegradable polyurethane films for myocardial repair.* Journal of Biomedical Materials Research Part A: An Official Journal of The Society for Biomaterials, The Japanese Society for Biomaterials, and The Australian Society for Biomaterials and the Korean Society for Biomaterials, **2003**. 66(3): p. 586-595.

[170] Alperin, C., P. Zandstra, and K. Woodhouse, *Polyurethane films seeded with embryonic stem cell-derived cardiomyocytes for use in cardiac tissue engineering applications.* Biomaterials, **2006**. 26(35): p. 7377-7386.
[171] Shimizu, T., et al., *Cell sheet engineering for myocardial tissue reconstruction.* Biomaterials, **2003**. 24(13): p. 2309-2316.
[172] Piao, H., et al., *Effects of cardiac patches engineered with bone marrow-derived mononuclear cells and PGCL scaffolds in a rat myocardial infarction model.* Biomaterials, **2007**. 28(4): p. 641-649.
[173] Mukherjee, S., et al., *Elastomeric electrospun scaffolds of poly (L-lactide-co-trimethylene carbonate) for myocardial tissue engineering.* Journal of Materials Science: Materials in Medicine, **2011**. 22(7): p. 1689-1699.
[174] Sireesha, M., V.J. Babu, and S. Ramakrishna, *Biocompatible and biodegradable elastomer/fibrinogen composite electrospun scaffolds for cardiac tissue regeneration.* RSC Advances, **2015**. 5(125): p. 103308-103314.
[175] Zhang, B., et al., *Platform technology for scalable assembly of instantaneously functional mosaic tissues.* Science advances, **2015**. 1(7): p. e1500423.
[176] Davenport Huyer, L., et al., *Highly elastic and moldable polyester biomaterial for cardiac tissue engineering applications.* ACS Biomaterials Science & Engineering, **2016**. 2(5): p. 780-788.
[177] Li, Y., G.A. Thouas, and Q.-Z. Chen, *Biodegradable soft elastomers: synthesis/properties of materials and fabrication of scaffolds.* RSC Advances, **2012**. 2(22): p. 8229-8242.
[178] Ye, G. and X. Qiu, *Conductive biomaterials in cardiac tissue engineering.* Biotarget, **2017**. 1(5).
[179] Boccaccini, A.R. and P.X. Ma, *Tissue engineering using ceramics and polymers*. **2014**: Elsevier.
[180] Smith, A.S., et al., *Micro-and nano-patterned conductive graphene–PEG hybrid scaffolds for cardiac tissue engineering.* Chemical Communications, **2017**. 53(53): p. 7412-7415.
[181] Zhou, J., et al., *Engineering the heart: evaluation of conductive nanomaterials for improving implant integration and cardiac function.* Sci Rep, **2014**. 4: p. 3733.
[182] Stout, D.A., B. Basu, and T.J. Webster, *Poly(lactic-co-glycolic acid): carbon nanofiber composites for myocardial tissue engineering applications.* Acta Biomater, **2011**. 7(8): p. 3101-12.
[183] Asiri, A.M., et al., *Greater cardiomyocyte density on aligned compared with random carbon nanofibers in polymer composites.* Int J Nanomedicine, **2014**. 9: p. 5533-9.
[184] Stout, D.A., et al., *Growth characteristics of different heart cells on novel nanopatch substrate during electrical stimulation.* Biomed Mater Eng, **2014**. 24(6): p. 2101-7.
[185] You, J.O., et al., *Nanoengineering the heart: conductive scaffolds enhance connexin 43 expression.* Nano Lett, **2011**. 11(9): p. 3643-8.
[186] Bi, H., et al., *Carbon microbelt aerogel prepared by waste paper: an efficient and recyclable sorbent for oils and organic solvents.* Small, **2014**. 10(17): p. 3544-3550.
[187] Aydin, H., et al., *Microwave-assisted rapid synthesis of poly (glycerol-sebacate) elastomers.* Biomaterials Science, **2013**. 1(5): p. 503-509.
[188] Chen, Q.-Z., et al., *Biomaterials in cardiac tissue engineering: ten years of research survey.* Materials Science and Engineering: R: Reports, **2008**. 59(1-6): p. 1-37.
[189] Qazi, T.H., et al., *Development and characterization of novel electrically conductive PANI–PGS composites for cardiac tissue engineering applications.* Acta biomaterialia, **2014**. 10(6): p. 2434-2445.
[190] Wang, Y., Y.M. Kim, and R. Langer, *In vivo degradation characteristics of poly (glycerol sebacate).* Journal of Biomedical Materials Research Part A: An Official Journal of The Society for Biomaterials, The Japanese Society for Biomaterials, and The Australian Society for Biomaterials and the Korean Society for Biomaterials, **2003**. 66(1): p. 192-197.

[191] Wang, L., et al., *Bioethanol production from various waste papers: economic feasibility and sensitivity analysis.* Applied energy, **2013**. 111: p. 1172-1182.
[192] Xu, D., et al., *A green and facile method toward synthesis of waste paper-derived 3D functional porous graphene via in situ activation of cobalt (II).* Journal of Materials Chemistry A, **2015**. 3(31): p. 16072-16078.
[193] Nguyen, S.T., et al., *Cellulose aerogel from paper waste for crude oil spill cleaning.* Industrial & engineering chemistry research, **2013**. 52(51): p. 18386-18391.
[194] Gao, J., P.M. Crapo, and Y. Wang, *Macroporous elastomeric scaffolds with extensive micropores for soft tissue engineering.* Tissue engineering, **2006**. 12(4): p. 917-925.
[195] Peschel, G., et al., *Growth of keratinocytes on porous films of poly (3-hydroxybutyrate) and poly (4-hydroxybutyrate) blended with hyaluronic acid and chitosan.* Journal of Biomedical Materials Research Part A: An Official Journal of The Society for Biomaterials, The Japanese Society for Biomaterials, and The Australian Society for Biomaterials and the Korean Society for Biomaterials, **2008**. 85(4): p. 1072-1081.
[196] Ventrelli, L., et al., *Influence of nanoparticle-embedded polymeric surfaces on cellular adhesion, proliferation, and differentiation.* Journal of Biomedical Materials Research Part A, **2014**. 102(8): p. 2652-2661.
[197] Wu, Z.Y., et al., *Ultralight, flexible, and fire-resistant carbon nanofiber aerogels from bacterial cellulose.* Angewandte Chemie, **2013**. 125(10): p. 2997-3001.
[198] Scholze, B. and D. Meier, *Characterization of the water-insoluble fraction from pyrolysis oil (pyrolytic lignin). Part I. PY–GC/MS, FTIR, and functional groups.* Journal of Analytical and Applied Pyrolysis, **2001**. 60(1): p. 41-54.
[199] Rai, R., et al., *Synthesis, properties and biomedical applications of poly (glycerol sebacate)(PGS): a review.* Progress in polymer science, **2012**. 37(8): p. 1051-1078.
[200] Jeffries, E.M., et al., *Highly elastic and suturable electrospun poly (glycerol sebacate) fibrous scaffolds.* Acta biomaterialia, **2015**. 18: p. 30-39.
[201] Li, X., et al., *Criteria for quick and consistent synthesis of poly (glycerol sebacate) for tailored mechanical properties.* Biomacromolecules, **2015**. 16(5): p. 1525-1533.
[202] Coates, J., *Interpretation of infrared spectra, a practical approach.* Encyclopedia of analytical chemistry, **2000**.
[203] Nagata, M., et al., *Synthesis, characterization, and enzymatic degradation of network aliphatic copolyesters.* Journal of Polymer Science Part A: Polymer Chemistry, **1999**. 37(13): p. 2006-2011.
[204] Jaafar, I.H., et al., *Spectroscopic evaluation, thermal, and thermomechanical characterization of poly (glycerol-sebacate) with variations in curing temperatures and durations.* Journal of materials science, **2010**. 45(9): p. 2525-2529.
[205] Thakur, S. and N. Karak, *Green reduction of graphene oxide by aqueous phytoextracts.* Carbon, **2012**. 50(14): p. 5331-5339.
[206] Huh, S.H., *Thermal reduction of graphene oxide*, in *Physics and Applications of Graphene-Experiments*. **2011**, IntechOpen.
[207] Shrestha, S., *Chemical, Structural and Elemental Characterization of Biosorbents Using FE-SEM, SEM-EDX, XRD/XRPD and ATR-FTIR Techniques*. Vol. 7. **2016**.
[208] Wang, H., et al., *Functionalized highly porous graphitic carbon fibers for high-rate supercapacitive electrodes.* Nano Energy, **2015**. 13: p. 658-669.
[209] Yan, Y., et al., *Effect of multi-walled carbon nanotubes on the cross-linking density of the poly (glycerol sebacate) elastomeric nanocomposites.* Journal of colloid and interface science, **2018**. 521: p. 24-32.
[210] Liang, S., W.D. Cook, and Q. Chen, *Physical characterization of poly (glycerol sebacate)/Bioglass® composites.* Polymer International, **2012**. 61(1): p. 17-22.
[211] Wang, X., M. Berggren, and O. Inganäs, *Dynamic control of surface energy and topography of microstructured conducting polymer films.* Langmuir, **2008**. 24(11): p. 5942-5948.

[212] Dubey, P., *Development of cardiac patches using medium chain length polyhydroxyalkanoates for cardiac tissue engineering*. **2017**, University of Westminster.
[213] Patel, A., et al., *Highly elastomeric poly (glycerol sebacate)-co-poly (ethylene glycol) amphiphilic block copolymers.* Biomaterials, **2013**. 34(16): p. 3970-3983.
[214] Gaharwar, A.K., et al., *Elastomeric nanocomposite scaffolds made from poly (glycerol sebacate) chemically crosslinked with carbon nanotubes.* Biomaterials science, **2015**. 3(1): p. 46-58.
[215] Asiri, A.M., et al., *Understanding greater cardiomyocyte functions on aligned compared to random carbon nanofibers in PLGA.* Int J Nanomedicine, **2015**. 10: p. 89-96.
[216] Bagdadi, A.V., et al., *Poly (3-hydroxyoctanoate), a promising new material for cardiac tissue engineering.* Journal of tissue engineering and regenerative medicine, **2018**. 12(1): p. e495-e512.
[217] Silvestri, A., et al., *Biomimetic myocardial patches fabricated with poly (ε-caprolactone) and polyethylene glycol-based polyurethanes.* Journal of Biomedical Materials Research Part B: Applied Biomaterials, **2014**. 102(5): p. 1002-1013.
[218] Lozano Picazo, P., et al., *New Semi-Biodegradable Materials from Semi-Interpenetrated Networks of Poly (ϵ-caprolactone) and Poly (ethyl acrylate).* Macromolecular bioscience, **2015**. 15(2): p. 229-240.
[219] Khang, D., et al., *Enhanced fibronectin adsorption on carbon nanotube/poly (carbonate) urethane: independent role of surface nano-roughness and associated surface energy.* Biomaterials, **2007**. 28(32): p. 4756-4768.
[220] Nuttelman, C.R., et al., *Attachment of fibronectin to poly (vinyl alcohol) hydrogels promotes NIH3T3 cell adhesion, proliferation, and migration.* Journal of Biomedical Materials Research: An Official Journal of The Society for Biomaterials, The Japanese Society for Biomaterials, and The Australian Society for Biomaterials and the Korean Society for Biomaterials, **2001**. 57(2): p. 217-223.
[221] Arima, Y. and H. Iwata, *Effect of wettability and surface functional groups on protein adsorption and cell adhesion using well-defined mixed self-assembled monolayers.* Biomaterials, **2007**. 28(20): p. 3074-3082.
[222] Srinivasa Reddy, C., et al., *Polycaprolactone/oligomer compound scaffolds for cardiac tissue engineering.* Journal of Biomedical Materials Research Part A, **2014**. 102(10): p. 3713-3725.
[223] Arima, Y. and H. Iwata, *Effects of surface functional groups on protein adsorption and subsequent cell adhesion using self-assembled monolayers.* Journal of Materials Chemistry, **2007**. 17(38): p. 4079-4087.
[224] Chen, P.-H., et al., *A novel polyurethane/cellulose fibrous scaffold for cardiac tissue engineering.* RSC Advances, **2015**. 5(9): p. 6932-6939.
[225] Kaur, G., et al., *Graphene/polyurethane composites: fabrication and evaluation of electrical conductivity, mechanical properties and cell viability.* Rsc Advances, **2015**. 5(120): p. 98762-98772.
[226] Dvir, T., et al., *Nanowired three-dimensional cardiac patches.* Nature nanotechnology, **2011**. 6(11): p. 720.
[227] Bouten, C., et al., *Substrates for cardiovascular tissue engineering.* Advanced drug delivery reviews, **2011**. 63(4-5): p. 221-241.
[228] Forte, G., et al., *Substrate stiffness modulates gene expression and phenotype in neonatal cardiomyocytes in vitro.* Tissue Engineering Part A, **2012**. 18(17-18): p. 1837-1848.
[229] Ganji, Y., et al., *Cardiomyocyte behavior on biodegradable polyurethane/gold nanocomposite scaffolds under electrical stimulation.* Materials Science and Engineering: C, **2016**. 59: p. 10-18.
[230] Engler, A.J., et al., *Embryonic cardiomyocytes beat best on a matrix with heart-like elasticity: scar-like rigidity inhibits beating.* Journal of cell science, **2008**. 121(22): p. 3794-3802.

[231] Tallawi, M., et al., *Poly (glycerol sebacate)/poly (butylene succinate-butylene dilinoleate) fibrous scaffolds for cardiac tissue engineering.* Tissue Engineering Part C: Methods, **2015**. 21(6): p. 585-596.
[232] Jawad, H., et al., *Nanocomposite elastomeric biomaterials for myocardial tissue engineering using embryonic stem cell-derived cardiomyocytes.* Advanced Engineering Materials, **2010**. 12(12): p. B664-B674.
[233] Stuckey, D.J., et al., *Magnetic resonance imaging evaluation of remodeling by cardiac elastomeric tissue scaffold biomaterials in a rat model of myocardial infarction.* Tissue Engineering Part A, **2010**. 16(11): p. 3395-3402.
[234] Kai, D., et al., *Polypyrrole-contained electrospun conductive nanofibrous membranes for cardiac tissue engineering.* J Biomed Mater Res A, **2011**. 99(3): p. 376-85.
[235] Radisic, M. and M.V. Sefton, *Cardiac Tissue*, in *Principles of Regenerative Medicine*. **2011**. p. 877-909.
[236] Novakovic, G.V., T. Eschenhagen, and C. Mummery, *Myocardial tissue engineering: in vitro models.* Cold Spring Harbor perspectives in medicine, **2014**. 4(3): p. a014076.
[237] Stout, D.A., et al., *Mechanisms of greater cardiomyocyte functions on conductive nanoengineered composites for cardiovascular application.* International journal of nanomedicine, **2012**. 7: p. 5653.
[238] Zhang, L. and T.J. Webster, *Nanotechnology and nanomaterials: promises for improved tissue regeneration.* Nano today, **2009**. 4(1): p. 66-80.
[239] Standardization, I.O.f., *ISO 10993-5: Biological Evaluation of Medical Devices. Part 5: Tests For In Vitro Cytotoxicity*. **2009**, ISO Geneva, Switzerland.
[240] Witek, P., et al., *The effect of a number of H9C2 rat cardiomyocytes passage on repeatability of cytotoxicity study results.* Cytotechnology, **2016**. 68(6): p. 2407-2415.
[241] Li, Y., et al., *Synthesis, characterization and properties of biocompatible poly (glycerol sebacate) pre-polymer and gel.* Polymer international, **2013**. 62(4): p. 534-547.
[242] Chen, C., X. Zhang, and Y. Dai, *Effect of pulsed electrical stimulation on the proliferation and differentiation of H9c2 cells.* Xi bao yu fen zi mian yi xue za zhi= Chinese journal of cellular and molecular immunology, **2013**. 29(4): p. 337-340.

HACETTEPE UNIVERSITY
GRADUATE SCHOOL OF SCIENCE AND ENGINEERING
THESIS ORIGINALITY REPORT

HACETTEPE UNIVERSITY
GRADUATE SCHOOL OF SCIENCE AND ENGINEERING
TO THE DEPARTMENT OF BIOENGINEERING

Date: 27/09/2019

Thesis Title / Topic: INVESTIGATION OF WASTE PAPER-DERIVED CARBON AEROGEL/ELASTOMER SYSTEM AS A CARDIAC PATCH

According to the originality report obtained by ~~myself~~/my thesis advisor by using the *Turnitin* plagiarism detection software and by applying the filtering options stated below on 19/09/2019 for the total of 36 pages including the a) Title Page, b) Introduction, c) Main Chapters, d) Conclusion sections of my thesis entitled as above, the similarity index of my thesis is 9 %.

Filtering options applied:

1. Bibliography/Works Cited excluded
2. Quotes excluded / ~~included~~
3. Match size up to 5 words excluded

I declare that I have carefully read Hacettepe University Graduate School of Sciene and Engineering Guidelines for Obtaining and Using Thesis Originality Reports; that according to the maximum similarity index values specified in the Guidelines, my thesis does not include any form of plagiarism; that in any future detection of possible infringement of the regulations I accept all legal responsibility; and that all the information I have provided is correct to the best of my knowledge.

I respectfully submit this for approval.

27/09/2019
Date and Signature

Name Surname: Abdulraheem Mohammed Najı ATYA
Student No: N14125470
Department: Bioengineering
Program:
Status: ☒ Masters ☐ Ph.D. ☐ Integrated Ph.D.

ADVISOR APPROVAL

APPROVED.

Prof. Dr. Halil M. Aydın
(Title, Name Surname, Signature)

CURRICULUM VITAE

Credentials

Name, Surname: Abdulraheem Atya

Place of Birth: Sana'a, Yemen

Marital Status: Married

E-mail: a.raheem.atya@gmail.com

Address: Kutlu Mahallesi, 454. Sokak, 14/14 Mamak Ankara

Education

B.Sc. : Medical Instrument Engineering (2012), University of Science & Technology) - Sana'a, Yemen.

M.Sc. : Bioengineering (2019), Hacettepe University - Ankara, Turkey.

Foreign Languages

English

Turkish

Work Experience

- October 2017- December 2017:
  Arabic - English Translator, part-time, at Statistical, Economic and Social Research and Training Centre for Islamic Countries (SESRIC) - Ankara, Turkey.
- January 2014 – August 2014:
  Sales Engineer for OLYMPUS endoscopy equipment at NATCO AL-RAZI CO. LTD. Sana'a, Yemen
- September 2013 – January 2014:
  Lecturer at Yemeni Jordanian University. Sana'a, Yemen
- September 2012 – January 2014:
  Lecturer at University of Science and Technology (Microcontroller Lab) Sana'a, Yemen.

- September 2012 – April 2013:
  Lecturer at Yemeni High Institute for Health Sciences.
  Sana'a, Yemen

Areas of Experience

Programming languages (Assembly, C, MATLAB), electrical circuit design, ATMEL 8051 microcontroller programming, Biomaterials, Myocardial Tissue Engineering.

Projects and Scholarships

- B.Sc. Scholarship in biomedical engineering from UST (university of science & technology), Yemen, (2008).
- M.Sc. Scholarship in bioengineering- Hacettpe University, from YTB (Presidency for Turks Aboard and Related Communities), Turkey, (2014).
- Project scholarship from Coordination Unit for Scientific Research Projects (BAP) - Hacettepe University, (2016).